Advances in Nonlinear Model Predictive Control for Large-Scale Chemical Process Systems

SUBMITTED IN PARTIAL FULFILLMENT OF THE REQUIREMENTS FOR

the degree of

DOCTOR OF PHILOSOPHY

in

CHEMICAL ENGINEERING

DEVIN WADE GRIFFITH

B.S., CHEMICAL ENGINEERING, UNIVERSITY OF OKLAHOMA

CARNEGIE MELLON UNIVERSITY

PITTSBURGH, PENNSYLVANIA

August, 2018

Acknowledgments

First of all, I would like to thank my advisor Larry Biegler for everything that he has done for me. Larry is most well known for his contributions to our field, but his biggest impact on the world has surely been made through his skill as an advisor. Thank you, Larry, for giving me both so much guidance and so much freedom.

Next, I would like to thank my committee members, Professors Erik Ydstie, Nick Sahinidis, Marija Illic, and Aaron Johnson, as well as my collaborators over the years Xue Yang, Mingzhao Yu, Victor Zavala of the University of Wisconsin, Sachin Patwardhan, and Sachin's group at IIT Bombay. It has been a privilege to learn from and work with such great people.

I would also like to say thank you to my many other great teachers over the years. To Linda Smith for being kind to me and giving me a reason to enjoy math, to Brenda Hebert for first teaching me how to do proofs, and to my OSSM professors, Donald Murphy and Michelle Miller, for bringing opportunities to a small town. Also many thanks to Robert Shambaugh for giving me my first research experience, Lance Lobban for inspiring me to pursue process control and suggesting that I go to CMU, Miguel Bagajewicz for introducing me to the PSE field, and the rest of my great professors and peers from the University of Oklahoma for giving me a strong foundation.

I would like to gratefully acknowledge support from the National Science Foundation Graduate Research Fellowship Program Grant No. DGE1252522 and DGE1745016, the Pittsburgh Chapter of the ARCS Foundation, ExxonMobil, the Bertucci family, and the Choctaw Nation of Oklahoma. My success would not be possible if not for those that generously invest in the future of research and graduate students.

I also owe a great debt of gratitude to those who have made the last few years much more enjoyable than they otherwise would have been. To Nikos Lappas, Anirudh Subramanyam, John Eason, Wei Wan, Zach Wilson, the rest of Larry's group, and the PSE community at CMU, I am very fortunate to have been able to spend this time here with all of you.

Finally, I would like to dedicate this work to my family. To my grandparents Cloyis and Mary Clay, Charles and Velma Jean Griffith, and Ginger Morgan, thank you for all the love and support you have given me. To my stepmother Joni Griffith and her family for adding so much to mine. To my mother Lisa Clay for always encouraging my success, and to my father Kevin Griffith for instilling in me all of my best qualities. Thank you all, and I hope I will make you proud.

Devin Wade Griffith
Pittsburgh, PA
August, 2018

Abstract

Model predictive control is an optimization based form of control that is commonly used in the chemical industry due to its natural handling of multiple-input-multiple-output systems and inequality constraints. Nonlinear model predictive control takes advantage of fully nonlinear process models in order to provide higher accuracy across a wider range of states. However, linear MPC is still much more common in the chemical industry than nonlinear MPC due to various additional complications in the implementation. This thesis seeks to ease the implementation and increase performance of NMPC for large-scale systems via fundamental developments that leverage both control and optimization theory.

First, we address the issues of NMPC applied with plant-model mismatch. Robust NMPC methods tend to be computationally expensive or lead to conservatism in performance. Therefore, we propose a framework by which NMPC may be given a straightforward robust reformulation in order to ensure nonlinear programming properties that connect to the continuity properties of the Lyapunov function used to show robustness. These reformulations are shown to be easily extended to the more specialized NMPC formulations shown later in the thesis. Also, we show a method by which robustness bounds may be calculated for processes under control by NMPC.

Next, we consider the computation of terminal conditions (regions and costs). Terminal conditions are a critical aspect of NMPC formulations that is closely intertwined with stability of the controller and feasibility of the optimization problem. We formulate terminal conditions via the quasi-infinite horizon methodology, and propose an extension for bounding nonlinear system effects that allows application to large-scale nonlinear systems. We demonstrate these calculations on examples of varying scales from the literature.

Also, we consider the application of economic NMPC (eNMPC) to large-scale systems. We propose an eNMPC scheme which enforces stability though a stabilizing constraint, a method which we deem eNMPC-sc. We show that eNMPC-sc is input-to-state practically stable (ISpS) with a robust reformulation, and we demonstrate on computational examples, including a large-scale distillation system, that eNMPC-ec can provide better economic performance without burdensome offline calculations to ensure stability.

Finally, we consider the selection of the predictive horizon length. In particular, we consider a method for updating horizon lengths online that we call adaptive horizon NMPC (AH-NMPC). We show an algorithm utilizing NLP sensitivity calculations from sIPOPT that provides sufficient horizon lengths in real time, and we leverage the terminal conditions from the quasi-infinite horizon approach in order to show both nominal and robust stability (ISpS) in the case of horizons changing from timepoint to timepoint. We then demonstrate this controller on benchmark examples from the literature, including the large-scale distillation system analyzed earlier, and note significant decreases in the average solve time of the NLP solved online.

Contents

List of Tables

List of Figures

Chapter 1

Introduction

Chemical manufacturing processes are a critical aspect of the modern economy, and have been for at least as long as recorded history, given our propensity for fermentation and distillation. This criticality is only amplified by our current reliance on fossil fuels and petroleum products. Although the most basic of chemical processes, such as home-brewing or cooking, may be operated by hand, today's economically-vital chemical manufacturing processes are comprised of large-scale and vastly complex systems of interacting elements that are controlled, and even optimized, by advanced computer algorithms. Given the apparent importance of the operation of these processes, this thesis seeks to further investigate the intricacies and possibilities of computer control algorithms in the chemical industry.

In this chapter, we discuss the background of process control in the chemical industry. First we give the context of the hierarchical control structure, and then we specifically focus on the role of advanced process control. Furthermore, observations are made on the recent advances and trends in research. Finally, we state the motivation and problem statement for this work, and give an outline of the content contained herein.

1.1 Hierarchical Process Operations

Given the vastly disparate time-scales of the various decisions made in regards to chemical manufacturing processes, these decisions are typically separated into a hierarchy of layers,

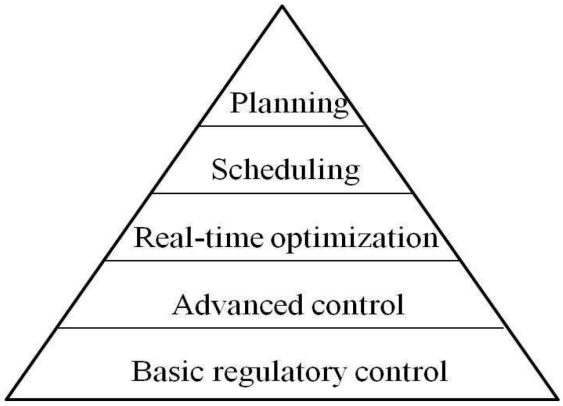

Figure 1.1: Hierarchy of process operations [1]

as shown in Figure 1.1. Although it seems obvious that a simultaneous consideration of all layers would lead to the best enterprise operation, this is generally infeasible due to the computational complexity and modeling difficulties of such a problem. Thus, the layers are treated separately, with decisions being passed from the top down, from slower time scales to faster time scales. The planning layer is concerned with the long-term production goals of the enterprise, and operates on the scale of weeks to months. This layer decides what products to make and what feedstocks to buy based on economic forecasts of the market, with the actual operation of the plant modeled coarsely or not at all. The uncertainty in the planning layer is mostly comprised of price, supply, and demand. The scheduling layer is then concerned with determining an order of tasks that accomplishes the overall production goals, and typically operates on the timescale of days to weeks, using very simplified models of the plant. This layer decides what products to make when, in what order, and on what equipment, with the primary goal of fulfilling demand in a given time frame. The uncertainty in the scheduling layer is largely comprised of equipment breakdoqn and production time. Both the planning and scheduling layers may be operated heuristically,

or by a rigorous optimization problem formulated as a mixed integer program (MIP) that often accounts for uncertainty explicitly [4].

In the real-time optimization (RTO) [5] layer, an economically optimal steady-steady is calculated from a detailed process model. For a given product specification, and current operating plant parameters, RTO determines the most desirable operating conditions for the plant, and operates on the time scale of hours. The uncertainty here is mostly in the process parameters which may range from reaction rate constants, to fouling factors, to real-time energy prices. Thanks to advances in computation power, the RTO problem may be formulated and solved as a nonlinear program (NLP).

In the advanced control layer, which operates on the time scale of minutes, dynamic control trajectories are determined that steer the process to the steady-state determined by the RTO. Until the 1970s, the industrial standard for this layer was proportional-integral-derivative control (PID), however applying PID to such multi-dimensional systems with operating constraints is troublesome. Today, this layer typically takes the form of model predictive control (MPC) [6] which optimizes a linearized dynamic model in order to determine control actions. This optimization usually takes the form of a linearly constrained quadratic program (QP). The model is typically obtained from data-driven input-output response methods, such as in the historically significant dynamic matrix control (DMC) software [7]. However, this linear data-driven model may not be consistent with the RTO model, and furthermore may be inaccurate over wider ranges of operating conditions. Thus the motivation for nonlinear model predictive control (NMPC), which takes advantage of a nonlinear, dynamic, first-principles process model to provide greater accuracy. This comes with many implementation issues, which will be the focus of this thesis and expounded upon throughout. The uncertainties in this layer come from unknown dynamic model parameters as well as noise.

Finally, we have the regulatory control layer, which operates on the time scale of seconds. The regulatory control is purposed to ensure that the control trajectories determined by the advanced control layer are actually realized by the valves. Since the dynamics here are typically concerned with the fast interactions between a given valve and flow rate, for example, PID is still the standard here. The uncertainties in this layer are mostly in valve dynamics.

1.2 Advanced Process Control

Here we further consider the advanced control layer, as well as the other pieces that it directly interacts with, which can be seen in Figure 1.2. The RTO calculates an economically optimal steady-state based on raw material specifications, product specifications, energy prices, etc., that is then sent to the control layer. The control layer then sends control actions to the plant based on the optimization of a dynamic process model. For the remainder of this work, we assume that control actions are implemented accurately and further discussion of the regulatory control layer is omitted. The process, which also receives disturbances that may come in any form of plant-model mismatch, then outputs measurements to parameter and state estimation. Estimators are then used to provide a state estimate as an initial condition for the dynamic process model, as well as parameter estimates to update both the steady-state and dynamic models.

For the purposes of this work, we assume that the estimation tasks are completed accurately, although we later investigate their effects on the dynamics via influencing changes in the steady-state. Common nonlinear estimators include the Extended Kalman Filter (EKF) and the Unscented Kalman Filter (UKF) [8, 9]. More recent applications include moving horizon estimation (MHE), which is the estimation analogue of NMPC and is the

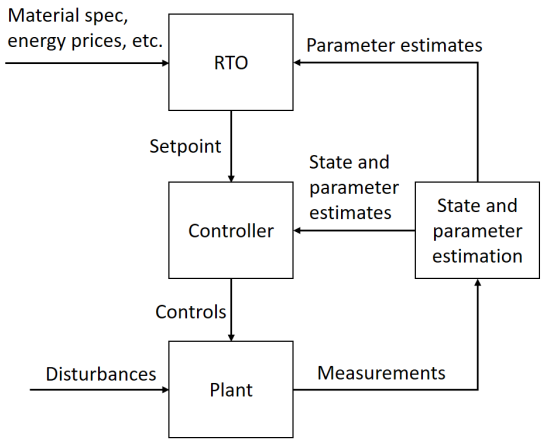

Figure 1.2: Advanced control structure

subject of recent research that allows for fast implementations [10] as well as handling of gross errors [11].

Although the focus of this work will be on the control layer, we would be remiss to ignore interactions with the RTO layer. In recent studies there has been a push to combine the RTO and control layers into one dynamic real-time optimization (DRTO) [12] or economic nonlinear model predictive control (eNMPC) [13] layer. The benefits of this are in the elimination of inconsistencies between the two layers, as well as running an economic optimization at a faster time scale in order to better respond to disturbances. However, setpoint stabilization is still an important characteristic to industrial practitioners, so it seems unlikely that steady-state calculations will be removed completely in the near future. Also, there has been considerable work to integrate other layers of the hierarchy, such as planning and scheduling [14], scheduling and RTO [15], as well as scheduling and control [16, 17]. However, we do not address interactions with planning or scheduling here.

As mentioned previously, a broad spectrum of controllers of varying performance qual-

ities and computational difficulties have been implemented in the chemical industry over the last several decades, from PID, to LQG [18], to more advanced forms of optimization-based control. Model predictive control (MPC) has seen a variety of applications in chemical processes, and its advantages include a natural way of handling inequality constraints and multiple-input-multiple-output systems due to the optimization formulation of the problem. A survey of industrial uses of MPC is given in [19], and a thorough treatment of MPC is given in [20]. The most common forms of MPC currently would be DMC-plus, as well as its various peers, which use linear data-driven models. These softwares are attractive to the practitioner because they include constructive methods for obtaining a process model to use for control, and dynamic optimization problems with linear constraints are generally easier to formulate and solve. Because of this, such applications still greatly outnumber NMPC applications in the industry. However, due to the highly nonlinear nature of thermodynamics and reaction kinetics in chemical processes, NMPC has the potential to provide great benefits in certain applications, such as polymer grade transitions, and NMPC softwares based on nonlinear first-principles models such as NOVA-NLC [21] and PFC [22] have had significant success. An introduction to NMPC is given in [23], and an overview of industrial NMPC applciations is given in [24]. Furthermore, if a sensible initialization strategy is used, an exact solution to the nonlinear programming (NLP) problem is not required, as shown in [25]. Recent work in advanced-step NMPC allows for control regardless of model solution time, as developed in [26] and [27], although these technologies require an online implementation of NLP sensitivity calculations. The applicability of NMPC is sure to grow as control and optimization strategies improve, but there is currently a large gap between academic research and industrial applications. There are many interesting theoretical developments in the literature whose application to or relevance for systems beyond toy problems is not apparent. Therefore, the future of advanced process

control largely depends on the researcher with the motivation of an engineer.

1.3 Research Problem Statement

The main motivation for this thesis is that, due to the complexity of its implementation, NMPC is still relatively uncommon in industrial applications compared to linear MPC, despite the significant benefits that it can provide for highly nonlinear chemical processes. This is true even if a first-principles dynamic process model and enough computational power to optimize it are both available; even in this case, the formulation of an optimization problem that gives desirable control performance is not straightforward for nonlinear systems. We seek to investigate all pieces of the NMPC formulation in order to develop advanced methods that lead to more practical implementations for large-scale systems. Importantly, we see this task through both the lenses of control and optimization theory, and we always keep in mind that the optimization problem we write must provide practical control benefits, be reasonably straightforward to formulate for systems with many states, and be solved online. To that end, we propose extensions to traditional MPC theory as well as recent literature advances that are practical from the engineering point of view, and we then give them a deep analysis from the academic perspective. Finally, any advances we propose should be demonstrable on a system with many (hundreds) of states.

1.4 Thesis Outline

Thesis thesis is organized by chapters that each focus on different aspects of the NMPC problem as shown in Figure 1.3, and is further organized as follows:

Chapter 2 establishes the basic notation and definitions, stability theory, results and optimization properties that we utilize throughout this work. Also, the fundamental formu-

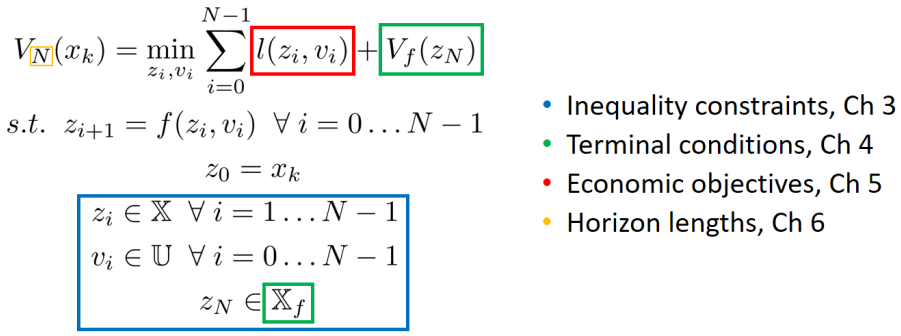

Figure 1.3: Thesis topics

lations of NMPC are introduced.

Chapter 3 deals with the robustness issues that arise with state-dependent inequality constraints, which can be important for safety, performance, or stability. We handle these constraints via a robust reformulation of the NLP that can be shown to have properties that ensure continuity with respect to parametric perturbations and thus continuity of the Lyapunov function. We use this to show that NMPC with a robust reformulation satisfies the input-to-state stability property (ISS), which includes a robustly positive invariant region around the setpoint that scales with the magnitude of plant-model mismatch. Moreover, we show throughout this thesis that this approach may be easily extended to more specialized NMPC formulations. Finally, we show a method by which robustness bounds of ISS may be calculated.

Chapter 4 addresses the calculation of terminal conditions for NMPC. Terminal conditions (regions and costs) are vital components of an NMPC formulation that are used to show stability and recursive feasibility. However, the calculation of terminal conditions for nonlinear systems is not straightforward. We address this through the quasi-infinite horizon framework, by which terminal conditions are chosen to approximate the infinite

horizon problem in a region close to setpoint, so that the NMPC problem sis comprised of a rigorous finite horizon and an approximated infinite horizon. We extend this framework to be more easily applied to large-scale systems through a new method of bounding nonlinear system effects. Furthermore, we show how these calculations may be applied even in the case of steady-states that change online. We demonstrate the calculation of these terminal conditions and the effect of tuning parameters on benchmark examples, including a large-scale distillation system.

Chapter 5 address economic NMPC (eNMPC). This is a popular topic in the literature, especially in regards to integrating NMPC with higher levels in the control hierarchy. In eNMPC, the tracking objective is replaced with an economic objective, so that the economic performance of the system is being optimized online. However, the stability properties of NMPC are typically shown by leveraging properties of the tracking (usually quadratic) objective function. It has been shown that eNMPC may be stabilized by adding sufficiently large tracking terms to regularization the economic objective, however calculating these terms is cumbersome and may lead to conservative performance. Thus, we propose to include a stabilizing constraint to the optimization problem in place of regularization weights, an approach that we deem eNMPC-sc. We show that eNMPC-sc with a robust reformulation is input-to-state practically stable (ISpS) with a stability constant that depends on the bounds on control actions. Furthmore, we show that eNMPC-sc may take advantage of the terminal condition calculations of the previous section in order to eliminate the need for endpoint constraints. We demonstrate the effectiveness of eNMPC-sc on examples from literature, and show significant increases in economic performance over regularized eNMPC without needing cumbersome offline calculations.

Chapter 6 concerns the selection of predictive horizon lengths for NMPC. Horizon lengths directly effect both the robustness and computational cost of NMPC. Furthermore, we note

that there is a significant trade-off in this choice, as a longer horizon is more likely to satisfy reachability assumptions in the face of uncertainty, but leads to larger optimization problems and therefore longer control delay, and vice versa. This motivates the development of a method for adapting horizon lengths online that we deem adaptive horizon NMPC (AH-NMPC). We propose a method utilizing sensitivity calculations from sIPOPT to find sufficient horizon lengths online. Leveraging the quasi-infinite horizon properties established earlier, we then show that AH-NMPC is asymptotically stable in the nominal case, as well as ISpS in the robust case with a stability constant that depends on the level of uncertainty in the terminal region. We then demonstrate AH-NMPC on literature examples, including the distillation system introduced earlier, and show significant decreases in average computational time with adaptive horizons.

Chapter 7 provides the concluding remarks for this thesis and enumerates the main contributions contained herein. Also, recommendations are made for future work, both from the perspective of direct extensions to this thesis, as well as more general directions of the field.

Chapter 2

Nonlinear Model Predictive Control

2.1 Introduction

This section presents the basic notation, definitions, and standard results that will be referred to for the remainder of this thesis. This includes the state-space representations of the plant and the model used for the controller, Lyapunov stability theory, nonlinear programming properties, and the general tracking formulation of NMPC.

2.2 Notation and Definitions

We note that chemical processes are typically modeled as a system of dynamic and algebraic equations (DAEs). Many methods are available for the solution of DAEs [28], and in particular collocation methods have been shown to be very effective for the simultaneous optimization of DAEs [29, 30]. Thus, for the purposes of this work, we directly consider the discrete time system:

$$x_{k+1} = f_p(x_k, u_k, w_k) \tag{2.1}$$

with the model:

$$x_{k+1} = f(x_k, u_k) := f_p(x_k, u_k, 0) \tag{2.2}$$

where $x_k \in \mathcal{X} \subset \mathbb{R}^{n_x}$ is a vector of states that fully defines the model at time k, $u_k \in \mathbb{U} \subseteq \mathbb{R}^{n_u}$ is the vector of control actions implemented at time k, and $w_k \in \mathbb{W} \subset \mathbb{R}^{n_w}$ is the vector of disturbances that are realized at time k. Note that $\mathcal{X}$ is not a state constraint set to be added to the optimization problem, but rather the set on which the system is defined and ultimately the region of attraction of the controller. We use $|\cdot|$ as the Euclidean vector norm and $\|\cdot\|$ as the corresponding induced matrix norm. $\mathbb{R}$ is the set of real numbers, $\mathbb{Z}$ is the set of integers, and the subscript $+$ indicates their nonnegative counterparts. We define the truncated disturbance sequence at time $k \in \mathbb{Z}_+$ as $\mathbf{w}_k = [w_0, \dots, w_{k-1}, 0, \dots]$, and the full disturbance sequence $\mathbf{w} = [w_0, w_1, w_2, \dots]$. We also define the set $\mathcal{W} := \{\mathbf{w} : w_k \in \mathbb{W} \text{ for all } k = 0, 1, 2, \dots\}$. We note that the state at time k, x_k, is an implicit function of x_0 and $\mathbf{w}_k$ for a given control scheme, but these arguments are not shown for simplicity. We also make the following basic assumptions on the model and the plant.

Assumption 1. *(Plant properties) (A) $f_p(x, u, w) : \mathbb{R}^{n_x} \times \mathbb{R}^{n_u} \times \mathbb{R}^{n_w} \to \mathbb{R}^{n_x}$ is uniformly continuous with respect to w (B) The set $\mathcal{X} \subset \mathbb{R}^{n_x}$ is control robustly positive invariant for $f_p(\cdot, \cdot, \cdot)$. That is, there exists $u \in \mathbb{U}$ such that $f_p(x, u, w) \in \mathcal{X}$ holds for all $x \in \mathcal{X},\ w \in \mathbb{W}$. (C) The set $\mathcal{X}$ is closed and bounded, and contains the origin in its interior (D) The set $\mathbb{U}$ is closed and bounded, and contains the origin in its interior. (E) The set $\mathbb{W}$ is bounded and $||\mathbf{w}|| := \sup_{k \in \mathbb{Z}_+} |w_k|$.*

Assumption 2. *(Model properties) (A) $f : \mathbb{R}^{n_x} \times \mathbb{R}^{n_u} \to \mathbb{R}^{n_x}$ is twice differentiable in x and u with Lipschitz continuous second derivatives (B) The set $\mathcal{X} \subset \mathbb{R}^{n_x}$ is control positive invariant for $f(\cdot, \cdot)$ That is, there exists $u \in \mathbb{U}$ such that $f(x, u) \in \mathcal{X}$ holds for all $x \in \mathcal{X}$. (C) The setpoint $(x_s, u_s) = (0, 0)$ satisfies $0 = f(0, 0)$.*

2.3 Lyapunov Stability Theory

This section presents the basics of Lyapunov stability theory, named for Russian mathematician Aleksandr Lyapunov [31], that will be used to analyze differing NMPC formulations for the remainder of this thesis. Note that a detailed handling of nonlinear systems and stability theory is given in [32] and [33].

2.3.1 Nominal Stability

Definition 3. *(Comparison Functions) A function $\alpha : \mathbb{R}_+ \to \mathbb{R}_+$ is of class $\mathcal{K}$ if it is continuous, strictly increasing, and $\alpha(0) = 0$. A function $\alpha : \mathbb{R}_+ \to \mathbb{R}_+$ is of class $\mathcal{K}_\infty$ if it is a $\mathcal{K}$ function and $\lim_{s\to\infty} \alpha(s) = \infty$. A function $\beta : \mathbb{R}_+ \times \mathbb{Z}_+ \to \mathbb{R}_+$ is of class $\mathcal{KL}$ if, for each $t \geq 0$, $\beta(\cdot, t)$ is a $\mathcal{K}$ function, and, for each $s \geq 0$, $\beta(s, \cdot)$ is nonincreasing and $\lim_{t\to\infty} \beta(s, t) = 0$.*

Definition 4. *(Attractivity). The system* (2.2) *is attractive on $\mathcal{X}$ if $\lim_{k\to\infty} x_k = 0$ for all $x_0 \in \mathcal{X}$.*

Definition 5. *(Stable Equilibrium Point) The point $x = 0$ is called a stable equilibrium point of* (2.2) *if, for all $k_0 \in \mathbb{Z}_+$ and $\epsilon_1 > 0$, there exists $\epsilon_2 > 0$ such that $|x_{k_0}| < \epsilon_2 \;\Rightarrow\; |x_k| < \epsilon_1$ for all $k \geq k_0$.*

Definition 6. *(Asymptotic Stability) The system* (2.2) *is asymptotically stable on $\mathcal{X}$ if $\lim_{k\to\infty} x_k = 0$ for all $x_0 \in \mathcal{X}$ and $x = 0$ is a stable equilibrium point.*

Definition 7. *(Lyapunov Function) A function $V : \mathcal{X} \to \mathbb{R}_+$ that satisfies the following:*

$$\alpha_1(|x|) \leq V(x) \leq \alpha_2(|x|) \tag{2.3a}$$

$$V(x_{k+1}) - V(x_k) \leq -\alpha_3(|x_k|) \tag{2.3b}$$

where $\alpha_1, \alpha_2, \alpha_3 \in \mathcal{K}_\infty$ is said to be a Lyapunov Function for (2.2).

Theorem 8. *Under Assumption 2, if system* (2.2) *admits a Lyapunov function for some $\alpha_1, \alpha_2, \alpha_3 \in \mathcal{K}_\infty$, then* (2.2) *is asymptotically stable on $\mathcal{X}$.*

See Appendix B of [20] for the proof of the preceding.

2.3.2 Robust Stability

The idea of input-to-state stability (ISS) is used to extend stability analysis to systems with uncertainty. The property was originally described for continuous time (CT) systems in [34] and was extended to discrete time (DT) systems in [35]. Furthermore, ISS has been proposed as a framework for NMPC [36], and it provides a very convenient and natural way of thinking about robust stability.

Definition 9. *(ISS). The system* (2.2) *is input-to-state stable (ISS) on* $\mathcal{X}$ *if* $|x_k| \leq \beta(|x_0|, k) + \gamma(||\mathbf{w}||)$ *holds for all* $x_0 \in \mathcal{X}$ *and* $k \geq 0$*, where* $\beta \in \mathcal{KL}$ *and* $\gamma \in \mathcal{K}$*.*

Definition 10. *(ISS Lyapunov function) A function* $V : \mathcal{X} \to \mathbb{R}_+$ *that satisfies the following:*

$$\alpha_1(|x_k|) \leq V(x_k) \leq \alpha_2(|x_k|) \tag{2.4a}$$

$$V(x_{k+1}) - V(x_k) \leq -\alpha_3(|x_k|) + \sigma(|w_k|) \tag{2.4b}$$

$$\forall \ x_0 \in \mathcal{X}, \ w_k \in \mathbb{W}, \ k \in \mathbb{Z}_+$$

where $\alpha_1, \alpha_2, \alpha_3 \in \mathcal{K}_\infty$*,* $\sigma \in \mathcal{K}$*, is said to be an ISS Lyapunov Function for* (2.1)*.*

Theorem 11. *Under Assumption 1, if system* (2.1) *admits an ISS Lyapunov function for some* $\alpha_1, \alpha_2, \alpha_3 \in \mathcal{K}_\infty$*,* $\sigma \in \mathcal{K}$*, then* (2.1) *is ISS on* $\mathcal{X}$*.*

We note that, in the nominal case (with no disturbances), ISS reduces to asymptotic stability. The following is a useful variant of ISS.

Definition 12. *(ISpS): Under Assumption 1, the system* (2.1) *is input-to-state practically stable (ISpS) on* $\mathcal{X}$ *if* $|x_k| \leq \beta(|x_0|, k) + \gamma(||\mathbf{w}||) + c$ *holds for all* $x_0 \in \mathcal{X}$ *and* $k \geq 0$*, where* $\beta \in \mathcal{KL}$*,* $\gamma \in \mathcal{K}$*, and* $c \in \mathbb{R}_+$*.*

We note that Definition 12 is only useful given a reasonable bound on c. In the case that $c = 0$, Definition 12 simplifies to Input-to-State Stability (ISS).

Definition 13. *(ISpS Lyapunov function) A function $V : \mathcal{X} \to \mathbb{R}_+$ that satisfies the following:*

$$\alpha_1(|x_k|) \leq V(x_k) \leq \alpha_2(|x_k|) + c_1 \tag{2.5a}$$

$$V(x_{k+1}) - V(x_k) \leq -\alpha_3(|x_k|) + \sigma(|w_k|) + c_2 \tag{2.5b}$$

$$\forall \ x_0 \in \mathcal{X}, \ w_k \in \mathbb{W}, \ k \in \mathbb{Z}_+$$

where $\alpha_1, \alpha_2, \alpha_3 \in \mathcal{K}_\infty$, $\sigma \in \mathcal{K}$, and $c_1, c_2 \in \mathbb{R}_+$, is said to be an ISpS Lyapunov Function for (2.1).

Theorem 14. *Under Assumption 1, if system* (2.1) *admits an ISpS Lyapunov function for some $\alpha_1, \alpha_2, \alpha_3 \in \mathcal{K}_\infty$, $\sigma \in \mathcal{K}$, and $c_1, c_2 \in \mathbb{R}_+$, then* (2.1) *is ISpS on $\mathcal{X}$.*

The reader is referred to [36] for more details on these definitions.

2.4 Nonlinear Programming Properties

In this section, we define NLP properties for the generic problem:

$$\min_{\mathbf{y}} \ \Phi(\mathbf{y}, p) \tag{2.6a}$$

$$\text{s.t. } c(\mathbf{y}, p) = 0 \tag{2.6b}$$

$$h(\mathbf{y}, p) \leq 0, \tag{2.6c}$$

where p is a parameter.

Definition 15. *The Lagrange function of* (2.6) *is:*

$$L(\mathbf{y}, \nu, \eta, p) = \Phi(\mathbf{y}, p) + \nu^T c(\mathbf{y}, p) + \eta^T h(\mathbf{y}, p) \tag{2.7}$$

where ν and η are multipliers of appropriate dimension. A point $\mathbf{y}^*$ is called a KKT-point if there exist multipliers ν and η which satisfy

$$\nabla_{\mathbf{y}} L(\mathbf{y}^*, \nu, \eta, p) = 0 \tag{2.8a}$$

$$c(\mathbf{y}^*, p) = 0 \tag{2.8b}$$

$$h(\mathbf{y}^*, p) \leq 0 \tag{2.8c}$$

$$\eta^T h(\mathbf{y}^*, p) = 0 \tag{2.8d}$$

$$\eta \geq 0 \tag{2.8e}$$

The set of all multipliers ν and η which satisfy the KKT conditions (2.8) *for a parameter p is $\mathcal{M}(p)$. The active constraint set is $J = \{j | h_j(\mathbf{y}^*, p) = 0\}$.*

Definition 16. *(LICQ, [37]) The linear independence constraint qualification (LICQ) holds at $\mathbf{y}^*$ when the gradient vectors*

$$\nabla c(\mathbf{y}^*, p); \nabla h_j(\mathbf{y}^*, p) \quad \forall\ j \in J \tag{2.9}$$

are linearly independent. LICQ also implies that the multipliers ν, η are unique.

Definition 17. *(SSOSC, [38]) The strong second order sufficient condition (SSOSC) holds at $\mathbf{y}^*$ with multipliers ν and η if*

$$q^T \nabla_{\mathbf{yy}} L(\mathbf{y}^*, \nu, \eta, p) q > 0 \quad \textit{for all } q \neq 0 \tag{2.10}$$

such that

$$\begin{aligned} \nabla c_i(\mathbf{y}^*, p)^T q = 0, \quad i = 1, .., n_c \\ \nabla h_j(\mathbf{y}^*, p)^T q = 0, \quad \textit{for } \eta_j > 0, j \in J. \end{aligned} \tag{2.11}$$

Definition 18. *(SC, [38]) At $\mathbf{y}^*$ of* (2.6) *with multipliers (ν, η), the strict complementarity condition (SC) holds if $\eta_j - h_j(\mathbf{y}^*, p) > 0$ for each $j \in J$.*

Definition 19. *(MFCQ,[37]) For problem* (2.6)*, the Mangasarian-Fromovitz Constraint Qualification (MFCQ) holds at the optimal point* $\mathbf{y}^*$ *if and only if:*

- *The rows of* $\nabla c(\mathbf{y}^*, p)$ *are linearly independent.*
- *There exists a vector* $\mathbf{q}$ *such that*

$$\nabla_{\mathbf{y}} c(\mathbf{y}^*, p)^T \mathbf{q} = 0 \tag{2.12a}$$

$$\nabla_{\mathbf{y}} h_j(\mathbf{y}^*, p)^T \mathbf{q} < 0 \quad \forall\ j \in J \tag{2.12b}$$

As shown in [39], the MFCQ implies that the set of Lagrange multipliers $\mathcal{M}(p)$ remains bounded in a polyhedron.

Definition 20. *(CRCQ, [40]) For Problem (2.6), the constant rank constraint qualification (CRCQ) holds at* $(\mathbf{y}^*, p_0)$*, when for any subset* $\bar{J} \subset J$*, the gradients:*

$$\nabla h_j(\mathbf{x}, p)\ j \in \bar{J}, \quad \nabla c(\mathbf{x}, p) \tag{2.13}$$

retain constant rank near the point $(\mathbf{y}^*, p_0)$*.*

Definition 21. *(GSSOSC, [41]) The General Strong Second Order Sufficient Condition (GSSOSC) holds at a KKT point* $\mathbf{y}^*$ *if*

$$\mathbf{q}^T \nabla_{\mathbf{yy}} L(\mathbf{y}^*, \nu, \eta, p)\mathbf{q} > 0\ \ \forall\ \mathbf{q} \neq 0 \tag{2.14}$$

such that

$$\nabla_{\mathbf{y}} c(\mathbf{y}^*, p)^T \mathbf{q} = 0, \nabla_{\mathbf{y}} h_j(\mathbf{y}^*, p)^T \mathbf{q} = 0 \tag{2.15}$$

for all $j \in \{j \mid j \in J, \eta_j > 0\}$

holds for all $\nu, \eta \in \mathcal{M}(p)$*.*

2.5 Nonlinear Model Predictive Control Formulations

This section presents the most basic and standard NMPC formulations. First, consider the infinite horizon NMPC formulation [42]:

$$\min_{v_i} \quad \sum_{i=0}^{\infty} L(z_i, v_i) \tag{2.16a}$$

$$\text{s.t.} \quad z_{i+1} = f(z_i, v_i) \;\; \forall \; i = 0 \dots \infty \tag{2.16b}$$

$$z_0 = x_k \tag{2.16c}$$

$$v_i \in \mathbb{U} \;\; \forall \; i = 0 \dots \infty \tag{2.16d}$$

With a controllability assumption, i.e. existence of some solution to (2.16) that limits to the origin, then (2.16) automatically ensures asymptotic stability when $w_k = 0 \; \forall k \in \mathbb{I}_+$. This is because *recursive feasibility* holds for (2.16) due to the principle of optimality, since the solution at time $k+1$ is the same as the solution to the problem at time k, excluding the first time point. However, this formulation is obviously not practical for real applications, since (2.16) cannot be solved for nonlinear systems in general. Therefore, consider a finite horizon formulation:

$$\min_{v_i} \quad \sum_{i=0}^{N} L(z_i, v_i) \tag{2.17a}$$

$$\text{s.t.} \quad z_{i+1} = f(z_i, v_i) \;\; \forall \; i = 0 \dots N-1 \tag{2.17b}$$

$$z_0 = x_k \tag{2.17c}$$

$$v_i \in \mathbb{U} \;\; \forall \; i = 0 \dots N-1 \tag{2.17d}$$

$$\tag{2.17e}$$

Although this formulation is immediately more attractive due to computational tractability, it comes with the additional assumption that the horizon N is "long enough". This can be analyzed, e.g., via the so-called "turnpike property" [43], however this is difficult to quantify for general nonlinear systems. Instead, consider the traditional terminal cost / terminal region NMPC formulation [44]:

$$\mathcal{P}(x) : V_N(x) = \min_{v_i} \quad \sum_{i=0}^{N-1} L(z_i, v_i) + \psi(z_N) \tag{2.18a}$$

$$\text{s.t.} \;\; z_{i+1} = f(z_i, v_i) \;\; \forall \, i = 0 \dots N-1 \tag{2.18b}$$

$$z_0 = x_k \tag{2.18c}$$

$$v_i \in \mathbb{U} \;\; \forall \, i = 0 \dots N-1 \tag{2.18d}$$

$$z_N \in \mathcal{X}_f \tag{2.18e}$$

where $z \in \mathbb{R}^{n_x}$ and $v \in \mathbb{R}^{n_u}$ are the predicted states and controls, respectively. The mapping $L : \mathcal{X} \times \mathbb{U} \to \mathbb{R}_+$ is the tracking stage cost penalizing deviations from the setpoint, and $\psi : \mathcal{X}_f \to \mathbb{R}_+$ is the terminal cost. At each time k, the NLP is solved for x_k, and the first control is implemented to the system, that is $u_k := v_{0|_k}$. The principle idea of this formulation is that the terminal cost ψ and terminal region $\mathcal{X}$ should somehow account for what happens after the finite horizon N.

Note that it is also possible to formulate NMPC without a terminal region and only a terminal cost [25, 45], however the construction of such a problem is not straightforward. Furthermore, it is also possible to formulate NMPC with only a terminal region and no terminal cost, however this assumes that a different stabilizing controller is implemented once a region close to the setpoint is entered. This is known as dual-mode control [46, 47].

The following assumption imposes a basic requirement on the nature of the tracking stage cost and other basic assumptions for tracking NMPC formulations.

Assumption 22. *(A) There exist* $\alpha_U, \alpha_L, \alpha_{U,\psi}, \alpha_{L,\psi} \in \mathcal{K}_\infty$ *such that* $\alpha_U(|x|) \geq L(x,u) \geq \alpha_L(|x|)\ \forall\ x \in \mathcal{X},\ u \in \mathbb{U}$ *and* $\alpha_{U,\psi}(|x|) \geq \psi(x) \geq \alpha_{L,\psi}(|x|)\ \forall\ x \in \mathcal{X}_f$*. (B) A solution to (3.1) exists for all* $x_k \in \mathcal{X}$*. (C) The functions* $L(x,u)$*,* $f(x,u)$*, and* $\psi(x)$ *are twice uniform continuously differentiable with respect to* x *and* u*. (D) There exists* $\alpha_\psi \in \mathcal{K}_\infty$ *and a control law* $u_f(x)$ *such that* $\psi(f(x,u_f(x))) - \psi(x) \leq -\alpha_\psi(|x|)\ \ \forall\ x \in \mathcal{X}_f$*. (E) At the solution of* (3.1)*, the control input* $u_k := v_{0|_k}$ *satisfies Assumptions 2(B) and 1(B).*

Definition 23. *Weak controllability [48] is satisfied for a given NMPC formulation if there exists a control trajectory* $v_i, i = 0 \ldots N-1$ *satisfying*

$$\sum_{i=0}^{N-1} |v_i| \leq \alpha_{wc}(|x|) \tag{2.19}$$

for some $\alpha_{wc} \in \mathcal{K}_\infty$*.*

The upper bound $\alpha_U(|x|) \geq L(x,u)$ holds if weak controllability holds, since $|v_i| \leq \alpha(|x|)$ holds $\forall\ i$.

The tracking stage cost usually has the form

$$L(z,v) = z^T Q z + v^T R v \tag{2.20}$$

where Q, R are positive semidefinite matrices but other norms can also be used to satisfy Assumption 22A [49, 50]. The following result is standard.

Theorem 24. *Under Assumption 2 and weak controllability,* $V_N(x)$ *satisfies the conditions of a Lyapunov function* (2.3b)*, and thus system* (2.2) *under control by NMPC* (3.1) *is asymptotically stable for all* $x_0 \in \mathcal{X}$*.*

The proof of Theorem 24 follows along the same lines as that of linear MPC in [25]. The lower bound $\alpha_1(|x|) \leq V_N(x)$ holds because of the quadratic tracking objective. The upper bound $V_N(x) \leq \alpha_2(|x|)$ holds because of weak controllability. The descent inequality

$V_N(x_{k+1}) - V_N(x_k) \leq -\alpha_3(|x_k|)$ holds because the terminal cost and region are chosen to ensure recursive feasibility by Assumption 22 (D).

Finally, we also note that NMPC with an endpoint constraint:

$$\min_{v_i} \quad \sum_{i=0}^{N-1} L(z_i, v_i) \tag{2.21a}$$

$$\text{s.t.} \quad z_{i+1} = f(z_i, v_i) \;\; \forall\, i = 0 \dots N-1 \tag{2.21b}$$

$$z_0 = x_k \tag{2.21c}$$

$$v_i \in \mathbb{U} \;\; \forall\, i = 0 \dots N-1 \tag{2.21d}$$

$$z_N = 0 \tag{2.21e}$$

is a special case of the terminal region / terminal cost formulation with $\mathcal{X}_f = 0$ and $\psi(z_N) = 0$. This formulation avoids the difficult choice of ψ and $\mathcal{X}$, but tightens the feasibility assumption (22 (B)) in that the setpoint must be exactly reachable in N steps. This can lead to a tightly constrained problem that may be difficult for a solver to provide a solution for, and ultimately leads to larger N and therefore larger problem size.

Note that, since ψ and $\mathcal{X}_f$ have traditionally been considered difficult to calculate for nonlinear systems, and the endpoint constraint can be quite restrictive, formulation (2.17) is actually the most common in real-world applications. However, a conservatively long N must typically be chosen, leading to large optimization problems, long computational times, and therefore limited applicability of NMPC in general.

Chapter 3

Robustness of NMPC

3.1 Introduction

Although the starting point for the analysis of any control scheme is to consider the nominal case, i.e. $w_k = 0 \ \forall \ k \in \mathbb{I}_+$ and the process model is perfect, it is a natural requirement of any controller that it be able to operate in the presence of uncertainty. Although stability properties hold nicely for the case of NMPC with a perfect model, there are examples where NMPC may not converge close to the setpoint for arbitrarily small plant-model mismatch [51]. There have been many approaches in the literature to extending NMPC to better handle uncertainty, including Tube-based NMPC [52, 53], Min-max NMPC [54, 55], back-off constraints [56, 57], contracting constraints [58], and multi-stage NMPC [59]. However, all of these methods suffer from greatly increased computational costs or conservativeness. Research on these so-called "robust NMPC" schemes is still ongoing and has important applications, however we desire an easy and effective method of ensuring that an NMPC formulation that is stable in the nominal case at least behaves in a bounded fashion in the presence of plant-model mismatch. To that end, we introduce the idea of a robust reformulation of the NMPC problem in order to ensure the continuity properties that lead to the desired robust stability properties. Moreover, this method is often easily extended to apply to new NMPC formulations that are nominally stable, which will be leveraged multiple times in the remainder of this thesis.

3.2 Robust Stability via NLP Reformulations

Robustness issues with NMPC tend to arise with the addition of state constraints, which include the terminal constraint mentioned previously, but may also account for operating constraints along the path to the terminal constraint. In this case, the NMPC problem takes the following form:

$$\min_{v_i} \quad \sum_{i=0}^{N-1} L(z_i, v_i) + \psi(z_N) \tag{3.1a}$$

$$\text{s.t.} \quad z_{i+1} = f(z_i, v_i) \;\; \forall\, i = 0 \dots N-1 \tag{3.1b}$$

$$z_0 = x_k \tag{3.1c}$$

$$v_i \in \mathbb{U} \;\; \forall\, i = 0 \dots N-1 \tag{3.1d}$$

$$z_i \in \mathbb{X} \;\; \forall\, i = 0 \dots N-1 \tag{3.1e}$$

$$z_N \in \mathcal{X}_f \tag{3.1f}$$

We introduce a robust reformulation of this problem, where these constraints are softened with a slack variable penalized in the objective, and the problem solved online becomes:

$$\begin{aligned} V_N^r(x) = \min & \sum_{i=0}^{N-1} L(z_i, v_i) + \psi(z_N) \\ & + \rho \left(\sum_{i=0}^{N-1} \left(\epsilon_i^{up} + \epsilon_i^{lo} \right) + \epsilon_f \right) \end{aligned} \tag{3.2a}$$

$$s.t. \; z_{i+1} = f(z_i, v_i) \;\; \forall\, i = 0 \dots N-1 \tag{3.2b}$$

$$z_i \leq z^{up} + \epsilon_i^{up} \;\; \forall\, i = 0 \dots N-1 \tag{3.2c}$$

$$z_i \geq z^{lo} - \epsilon_i^{lo} \;\; \forall \, i = 0 \ldots N-1 \tag{3.2d}$$

$$v_i \in \mathbb{U} \;\; \forall \, i = 0 \ldots N-1 \tag{3.2e}$$

$$z_0 = x \tag{3.2f}$$

$$|z_N| \leq c_f + \epsilon_f \tag{3.2g}$$

$$\epsilon_i^{up}, \epsilon_i^{lo}, \epsilon_f \geq 0 \tag{3.2h}$$

This reformulation is constructed to ensure that the NLP solved online satisfies MFCQ (Definition 19), and therefore the objective function V_N^r, i.e. the Lyapunov function used to show stability, is uniformly continuous in x. Also note that this formulation fits into the framework of zone-tracking MPC [60]. Then we make use of the following result, from Theorem 2 in [36], to show that V_N^r is an ISS Lyapunov function.

Theorem 25. *Suppose that Assumptions 1 and 2 hold, $V(x)$ is a Lyapunov function for* (2.2)*, and $V(x)$ is uniformly continuous in x. Then $V(x)$ is also an ISS Lyapunov function for* (2.1)*.*

Thus, since NMPC admits a Lyapunov function, we need only to show the continuity property, which we show the the properties of the NLP. In the following section it is explicitly shown that (6.24) satisfies MFCQ.

3.3 NLP Properties of NMPC

In order to show robust stability properties, we first show that the Lyapunov function is uniformly continuous with respect to disturbances. To this end, we recognize that MPC is a parametric programming problem with respect to x_0. We then make use of Lemma 26 which is a consequence of Theorem 3.1 in [61].

Lemma 26. *If* (6.24) *satisfies the GSSOSC (Definition 21) and the MFCQ (Definition 19), then there exists* $\sigma_V \in \mathcal{K}$ *such that*

$$|V_N^r(x_1) - V_N^r(x_2)| \leq \sigma_V(|x_1 - x_2|)$$

We now show that the MFCQ holds.

Lemma 27. *Under Assumption 2, the NLP (6.24) satisfies the MFCQ.*

Proof. Consider the constraints of (3.1) rewritten as the following:

$$z_0 = x_k \tag{3.3a}$$

$$z_{i+1} = f(z_i, v_i) \quad i = 0, \ldots, N-1 \tag{3.3b}$$

$$g_u(v_i) \leq 0 \quad i = 0, \ldots, N-1 \tag{3.3c}$$

$$g_x(z_i) \leq 0 \quad i = 0, \ldots, N \tag{3.3d}$$

Linearizing the equality constraints and the *active* inequality constraints of (3.3) at the solution leads to:

$$F_z d_z + F_v d_v = 0 \tag{3.4a}$$

$$G_{x,z}^J d_z \leq 0 \tag{3.4b}$$

$$G_{u,v}^J d_v \leq 0 \tag{3.4c}$$

where d_z and d_v are search directions in the states and controls, respectively, and we define the matrices:

$$F_z = \begin{bmatrix} I & & & & \\ -F_z^0 & I & & & \\ & -F_z^1 & I & & \\ & & \ddots & \ddots & \\ & & & -F_z^{N-1} & I \end{bmatrix} \tag{3.5a}$$

$$F_v = \begin{bmatrix} 0 & & & & \\ -F_v^0 & & & & \\ & -F_v^1 & & & \\ & & \ddots & & \\ & & & -F_v^{N-1} \end{bmatrix} \tag{3.5b}$$

$$G_{x,z}^J = diag\{G_{x,z}^{j_0}, G_{x,z}^{j_1}, \ldots, G_{x,z}^{j_{N-1}}, G_{x,z}^{j_N}\} \tag{3.5c}$$

$$G_{u,v}^J = diag\{G_{u,v}^{j_0}, G_{u,v}^{j_1}, \ldots, G_{u,v}^{j_{N-1}}, 0\} \tag{3.5d}$$

where F_z^i and F_v^i are the Jacobians of $f(z_i, v_i)$ with respect to variables z_i and v_i, $G_{x,z}^{J_i}$ is the Jacobian of the active constraints of g_x at time i, and $G_{u,v}^{J_i}$ is the Jacobian of the active constraints of g_u at time i. We see that F_z is square and nonsingular and that the matrix $\nabla c^T = [F_z \mid F_v \mid 0]$ is full row rank. Hence, the equality constraint gradients are linearly independent. Also, the submatrices $G_{x,z}^{j_i}$ and $G_{u,v}^{j_i}$ may be of variable dimension and even be empty. Furthermore, the relaxation of the active state constraints of (3.3) at the optimum leads to:

$$G_{x,z}^J d_z - E_{J,x} d_{\xi,x} \leq 0 \tag{3.6a}$$

$$d_\xi \geq 0 \tag{3.6b}$$

$$G_{u,v}^J d_v \leq 0 \tag{3.6c}$$

$$\tag{3.6d}$$

where ξ is the concatenation of the ℓ_1 penalty relaxation variables and

$$\nabla g_J^T = \begin{bmatrix} G_{x,z}^J & 0 & -E_J \\ 0 & 0 & -I \\ 0 & G_{u,v}^J & 0 \end{bmatrix} \tag{3.7}$$

where E_J is composed of the rows of the identity matrix that correspond to the active inequalities.

Since the set $\mathbb{U}$ is convex and has an interior, we can find some d_v^0 such that $g_u^j(v^* + d_v^0) < 0 \; \forall j \in J$. Applying Taylor's Theorem gives:

$$\begin{aligned} g_u^j(v^* + d_v^0) &= g_u^j(v^*) + \nabla g_u^j(v^*)^T d_v^0 \\ &+ \frac{1}{2}(d_v^0)^T \nabla^2 g_u^j(v^* + t d_v^0) d_v^0 < 0 \end{aligned} \tag{3.8}$$

for $j \in J$ and some $t \in [0, 1]$. Since $g_u^j(v^*) = 0$ and by convexity $\frac{1}{2}(d_v^0)^T \nabla^2 g_u^j(v^* + t d_v^0) d_v^0 \geq 0$, we have

$$\begin{aligned} \nabla g_u^j(v^*)^T d_v^0 &= g_u^j(v^* + d_v^0) \\ &- \frac{1}{2}(d_v^0)^T \nabla^2 g_u^j(v^* + t d_v^0) d_v^0 < 0 \end{aligned} \tag{3.9}$$

so we have $G_{u,v}^J d_v^0 < 0$.

Now define the concatenated variables and set $q^T = [d_z^T \mid d_v^T \mid d_\xi^T]$ with $d_z = -F_z^{-1} F_v d_v^0$, $d_v = d_v^0$. Then given d_v^0 choose d_ξ as follows:

$$E_J d_\xi > -G_{x,z}^J F_z^{-1} F_v d_v^0 \tag{3.10a}$$

and we see that $\nabla g_J^T q < 0$ and $\nabla c^T q = 0$ in Definition 19. Hence MFCQ is satisfied for system (3.3). □

3.4 Computation of ISS Bounds for NMPC

The goal of this section is to explicitly calculate the values of ISS bounds for NMPC. The chief difficulty for this problem lies in finding rigorous bounds that are small enough to

be useful. To aid in this, the ISS theorem is extended to allow for an uncertain term that depends on the state of the system as well as the realization of uncertainty. Also, general forms of the comparison functions are proposed to be used for the case of NMPC. Then, these comparison functions are used to formulate predictive ISS bounds through the ISS Lyapunov theorem for DT systems. A method of finding the parameters of the comparison functions is described, and computational examples include a scalar linear system and a nonlinear CSTR. Note that the notation introduced in this section should be considered as only being defined locally.

3.4.1 The ISS Lyapunov Theorem with a Modified Uncertain Term

Since, for NMPC, the controls u_k are determined as some function $u_k = \kappa(x_k)$ by the optimizer, we will consider the system written as $x_{k+1} = f_u(x_k, w_k)$, $x_k \in \mathcal{X}, w_k \in \mathbb{W}$, with initial state x_0. Recall that if the system is ISS, then:

$$|x_k| \leq \beta(|x_0|, k) + \gamma(||\mathbf{w}_k||) \;\; \forall k \in \mathbb{I}^+ \tag{3.11}$$
$$\forall\, x_0 \in \mathcal{X},\; \mathbf{w}_k \in \mathcal{W}$$

where $\beta(\cdot,\cdot)$ is of class $\mathcal{KL}$, and $\gamma(\cdot)$ is of class $\mathcal{K}$.

Furthermore, this property can be decomposed into two time periods: $|x_k| \leq \beta(|x_0|, k) \;\; \forall\, k \in \{0, \dots, k_0 - 1\}$, and $|x_k| \leq \gamma(||\mathbf{w}_k||) \;\; \forall\, k \in \{k_0, k_0 + 1, \dots\}$, where k_0 is the first time that $|x_k| \leq \gamma(||\mathbf{w}_k||)$. That is, the system trajectory has an asymptotic bound $\beta(|x_0|, k)$, until the first time that the trajectory crosses the boundary of the ball of radius $\gamma(||\mathbf{w}_k||)$. This ball is then positive invariant, meaning the system trajectory never leaves it, although the state value of the trajectory may take any value inside the ball.

Here we state a version of the Lyapunov-based ISS theorem from [35] that is extended to allow for a uncertain term that is a function of the state as well as the realization of

uncertainty, which leads to a tighter bound since one value need not hold for all states. The proof is also summarized, so that the functional forms of the bounds are apparent. Note that we only show where the proof deviates from [35]. We also rely on the extension to systems with state constraints shown in Appendix B of [20]. Assume that there exists a Lyapunov function $V(x)$ that admits the following comparison functions:

$$\alpha_1(|x|) \leq V(x) \leq \alpha_2(|x|) \;\; \forall \, x \in X, \tag{3.12a}$$

$$V(f(x,w)) - V(x) \leq -\alpha_3(|x|) + \sigma(|x|,|w|) \tag{3.12b}$$

$$\forall \, x \in X, \, w \in \mathbb{W}$$

where $\alpha_1(\cdot)$, $\alpha_2(\cdot)$, and $\alpha_3(\cdot) \in \mathcal{K}_\infty$, $\sigma(|x|,0) = 0$ and $\sigma(|x|,|w|)$ is continuous and strictly increasing with respect to either argument for nonzero $|w|$. Now define the functions $\alpha_4(\cdot)$, $\rho(\cdot)$, and $\hat{\alpha}_4(\cdot)$ to have the following properties: $\alpha_4(\cdot) = \alpha_3 \circ \alpha_2^{-1}(\cdot)$, $\hat{\alpha}_4(s) \leq \alpha_4(s) \;\; \forall \; s$, $id - \hat{\alpha}_4(\cdot) \in \mathcal{K}_\infty$, $\rho(\cdot) \in \mathcal{K}_\infty$, and $id - \rho(\cdot) \in \mathcal{K}_\infty$, where id denotes the identity function. See lemma B.1 of [35] for proof that $\hat{\alpha}_4(\cdot)$ exists. Now, assume that we have a solution to the following auxiliary optimization problem:

$$min \;\; b \tag{3.13a}$$

$$s.t. \quad \rho \circ \hat{\alpha}_4 \circ b \geq \sigma(|x|, ||\mathbf{w}||) \quad \forall \, x : V(x) \leq b \tag{3.13b}$$

$$\rho \circ \hat{\alpha}_4 \circ V(x) \geq \sigma(|x|, ||\mathbf{w}||) \quad \forall \, x : V(x) > b \tag{3.13c}$$

$$b \geq 0 \tag{3.13d}$$

where $||\mathbf{w}||$ is an upper bound on $|w_k|$. Assuming a solution to (3.13) is the key point that allows σ to be a function of $|x|$. In words, this problem is to determine the smallest Lyapunov function value, b, that defines a sublevel set in the state space that is positive invariant for f and a superlevel set that has an asymptotic descent property. Note that the two constraints above can be simplified to solvable forms for specific cases (see Section

3.4.5). We can now say that the system is ISS, and we can construct β and γ by following the proof of Lemma 3.5 in [35]. Consider the set $D = \{x : V(x) \leq b\}$. If $x \in D$, then we have:

$$V(f_u(x,w)) \leq V(x) - \alpha_3(|x|) + \sigma(|x|, ||\mathbf{w}||) \tag{3.14a}$$

$$\leq V(x) - \alpha_4 \circ V(x) + \sigma(|x|, ||\mathbf{w}||) \tag{3.14b}$$

$$\leq V(x) - \hat{\alpha}_4 \circ V(x) + \sigma(|x|, ||\mathbf{w}||) \tag{3.14c}$$

$$= (id - \hat{\alpha}_4) \circ V(x) + \sigma(|x|, ||\mathbf{w}||) \tag{3.14d}$$

$$\leq (id - \hat{\alpha}_4) \circ b + \sigma(|x|, ||\mathbf{w}||) \tag{3.14e}$$

$$= (id - \hat{\alpha}_4) \circ b + \sigma(|x|, ||\mathbf{w}||)$$

$$+\rho \circ \hat{\alpha}_4 \circ b - \rho \circ \hat{\alpha}_4 \circ b \tag{3.14f}$$

$$\leq (id - \hat{\alpha}_4)(b) + \rho \circ \hat{\alpha}_4(b) \tag{3.14g}$$

$$= -(id - \rho) \circ \hat{\alpha}_4(b) + b \quad \leq b \tag{3.14h}$$

$$\forall\, x \in D,\ x \in \mathcal{X},\ \mathbf{w} \in \mathcal{W}$$

Note that step (3.14f) to (3.14g) holds due to satisfaction of (3.13b). Thus, the constant b is the Lyapunov function value that corresponds to the invariant ball, so set $\gamma(||\mathbf{w}_k||) = \alpha_1^{-1}(b)$. Now consider $x \notin D$:

$$V(f_u(x,w)) - V(x) \leq -\alpha_3(|x|) + \sigma(|x|, ||\mathbf{w}||) \tag{3.15a}$$

$$\leq -\alpha_4 \circ V(x) + \sigma(|x|, ||\mathbf{w}||) \tag{3.15b}$$

$$\leq -\hat{\alpha}_4 \circ V(x) + \sigma(|x|, ||\mathbf{w}||) \tag{3.15c}$$

$$= -\hat{\alpha}_4 \circ V(x) + \rho \circ \hat{\alpha}_4 \circ V(x) + \sigma(|x|, ||\mathbf{w}||)$$

$$-\rho \circ \hat{\alpha}_4 \circ V(x) \tag{3.15d}$$

$$\leq -\hat{\alpha}_4 \circ V(x) + \rho \circ \hat{\alpha}_4 \circ V(x) \tag{3.15e}$$

$$= -(id - \rho) \circ \hat{\alpha}_4 \circ V(x) \tag{3.15f}$$

$$\forall\ x \notin D,\ x \in \mathcal{X},\ \mathbf{w} \in \mathcal{W}$$

Note that step (3.15d) to (3.15e) holds due to satisfaction of (3.13c). Furthermore, following from (3.15f), we have that:

$$V(x_{k+1}) \leq (id - (id - \rho) \circ \hat{\alpha}_4) \circ V(x_k) \tag{3.16a}$$

$$V(x_{k+1}) \leq (id - (id - \rho) \circ \hat{\alpha}_4) \circ \alpha_2(|x_k|) \tag{3.16b}$$

$$x_{k+1} \leq \alpha_1^{-1}((id - (id - \rho) \circ \hat{\alpha}_4) \circ \alpha_2(|x_k|)) \tag{3.16c}$$

$$|x_k| \leq (\alpha_1^{-1}((id - (id - \rho) \circ \hat{\alpha}_4) \circ \alpha_2(|x_0|)))^k$$

$$=: \beta(|x_0|, k) \tag{3.16d}$$

$$\forall\ x \notin D,\ x \in \mathcal{X},\ \mathbf{w} \in \mathcal{W}$$

where the superscript k denotes the function of a function, k times (the result of the expression is plugged back in, in place of $|x_0|$, k times). Note that the right-hand side of (3.16b) is of class $\mathcal{K}_\infty$. The final expression holds true $\forall\ k \in \{0, \ldots, k_0 - 1\}$, where k_0 is the first time such that $|x_k| \leq \gamma(||\mathbf{w}_k||)$.

3.4.2 A Degree of Freedom in the Bounds

Notice that $\rho(\cdot)$ can be any function that fulfills $\rho(\cdot) \in \mathcal{K}_\infty$, and $id - \rho(\cdot) \in \mathcal{K}_\infty$. To see the effect of $\rho(\cdot)$, inspect (3.13) and (3.16d). The choice of $\rho(\cdot)$ affects the magnitude of b and therefore affects $\gamma(||\mathbf{w}_k||)$ as it appears in (3.11). If we choose $\rho(s)$ to be close to s, then we are effectively choosing a smaller value b and a smaller $\gamma(||\mathbf{w}_k||)$. This means that j_0 becomes a point further forward in time, and $\gamma(||\mathbf{w}_k||)$ only has to bound x_k after some larger fraction of the initial state has decayed. This gives tighter bounding of $|x_k|$ as

$k \to \infty$. On the other hand, $\beta(|x_0|, k)$ becomes larger. The opposite holds if we make $\rho(s)$ close to 0. Thus, varying $\rho(\cdot)$ will lead to different functions $\beta(\cdot, \cdot)$ and $\gamma(\cdot)$, and they will correspond to different b, $\gamma(||\mathbf{w}_k||)$, $\beta(|x_0|, k)$, and j_0.

For ease of use, we will define $\rho(s) = \epsilon_1 s, \ \epsilon_1 \in (0, 1)$, so that ϵ_1 close to 1 gives the tightest $\gamma(||\mathbf{w}_k||)$, and ϵ_1 close to 0 gives the tightest $\beta(|x_0|, k)$.

3.4.3 Application to NMPC

The goal of this section is to describe simple but useful forms for the functions α_1, α_2, α_3, and σ that can be put to use in the context of NMPC to calculate $\gamma(||\mathbf{w}_k||)$ and $\beta(|x_0|, k)$. Previous work, for example [62, 63], has shown that functions exist, but derived them in terms of Lipschitz constants and a controllability function that would be difficult to find and would provide loose bounds. So instead, we propose a general form for these functions with parameters that can be calculated.

Suppose that we let the Lyapunov function bounds have a power law form, $\alpha_i(|x|) = N_i|x|^{\mu_i}$, where N_i and μ_i are positive parameters that can be found from open loop calculations. The function σ will be addressed in detail in the next section. Note that $\alpha_1(|x|)$ and $\alpha_2(|x|)$ must provide strict lower and upper bounds on $V_N(x)$, respectively, and $N_3|x|^{\mu_3}$ must provide a strict lower bound to $l(x_0, u_0)$. Also, we require that $\mu_1 \geq \mu_2$, so that $\alpha_2(|x|) \geq \alpha_1(|x|)$ holds true near the origin.

Now we need to define $\hat{\alpha}_4(\cdot)$ so that $\hat{\alpha}_4(s) \leq \alpha_4(s) \quad \forall \ s$ and $id - \hat{\alpha}_4(\cdot) \in \mathcal{K}_\infty$ are satisfied. The function $\hat{\alpha}_4(\cdot)$ can be constructed piecewise from combinations of $\alpha_4(\cdot)$ and the identity function. First, for convenience, define $\theta = N_3 N_2^{-\mu_3/\mu_2}$ and $B = \mu_3/\mu_2$, so that $\alpha_4(\cdot) = \theta(\cdot)^B$. Now, we must consider three possible cases: $B < 1$, $B > 1$, or $B = 1$.

If $B < 1$, then:

$$\hat{\alpha}_4(s) := \begin{cases} \epsilon_2 s \ , & s \in \left[0, \left(\frac{\epsilon_2}{\theta}\right)^{\frac{1}{B-1}}\right) \\ \theta s^B \ , & s \in \left[\left(\frac{\epsilon_2}{\theta}\right)^{\frac{1}{B-1}}, \infty\right) \end{cases} \tag{3.17}$$

If $B > 1$, then:

$$\hat{\alpha}_4(s) := \begin{cases} \theta s^B \ , & s \in \left[0, \left(\frac{1}{B\theta}\right)^{\frac{1}{B-1}}\right) \\ \epsilon_2 s + \theta \left(\frac{1}{B\theta}\right)^{\frac{B}{B-1}} & \\ -\epsilon_2 \left(\frac{1}{B\theta}\right)^{\frac{1}{B-1}} \ , & s \in \left[\left(\frac{1}{B\theta}\right)^{\frac{1}{B-1}}, \infty\right) \end{cases} \tag{3.18}$$

If $B = 1$, then:

$$\hat{\alpha}_4(s) := \epsilon_2 \theta s \ , \quad \epsilon_2 < 1/\theta \tag{3.19}$$

In all cases, ϵ_2 is user determined, $\epsilon_2 \in (0, 1)$, and a larger ϵ_2 gives a tighter bound. It is easily verifiable that these particular forms of $\hat{\alpha}_4(\cdot)$ have the necessary properties.

3.4.4 Expressions for the Uncertain Term

Guaranteed form

First consider the expression for the uncertain term in [62], $\sigma(\cdot) = l_V l_w(\cdot)$, where l_V is the Lipschitz constant of the Lyapunov function, and l_w is the Lipschitz constant of f with respect to w. Instead of treating l_V as a constant, let $l_V(|x|) = c|x| + t$ with constants $c > 0$ and $t > 0$, and define it to be an upper bound on $|dV_n(x)/d|x||$. As we will see in the examples section, this form for l_V works well for bounding real data. Note that this will be referred to as the "guaranteed" form of σ.

Approximate form

Now, consider a form for $\sigma(\cdot)$ that includes a further assumption. Suppose that the system $x_{k+1} = f_u(x_k, 0)$ exhibits nominal stability, so that there exists a Lyapunov function

with the following properties:

$$\alpha_1(|x|) \leq V(x) \leq \alpha_2(|x|) \tag{3.20a}$$

$$V(f(x,0)) - V(x) \leq -\alpha_3(|x|) \tag{3.20b}$$

$$\forall\ x \in X$$

With the assumption that that $f_u(\cdot,\cdot)$ is Lipschitz continuous with respect to its second argument so that $|f_u(x,w)| \leq |f_u(x,0)| + l_w|w|$, and that $|f_u(x,0)| << l_w||\mathbf{w}||$, then:

$$V(f_u(x,w)) - V(f(x,0))$$

$$\leq \alpha_2(|f_u(x,w)|) - \alpha_1(|f_u(x,0)|) \tag{3.21a}$$

$$\Rightarrow V(f_u(x,w)) - V(x)$$

$$\leq -\alpha_3(|x|) + \alpha_2(|f_u(x,w)|) - \alpha_1(|f_u(x,0)|) \tag{3.21b}$$

$$\leq -\alpha_3(|x|) + \alpha_2(|f_u(x,0)| + l_w||\mathbf{w}||)$$

$$-\alpha_1(|f_u(x,0)|) \tag{3.21c}$$

$$\leq -\alpha_3(|x|) + \alpha_2(|f_u(x,0)| + l_w||\mathbf{w}||) \tag{3.21d}$$

$$\approx -\alpha_3(|x|) + \alpha_2(l_w||\mathbf{w}||) \tag{3.21e}$$

$$\forall\ x \in \mathcal{X},\ \mathbf{w} \in \mathcal{W}$$

This implies that $\sigma(|w|) = \alpha_2(l_w||\mathbf{w}_k||)$, which removes dependence on $|x|$. Notice that this form may no longer be a strict bound due to the assumption mentioned above. A way of stating this assumption in practical terms is that, after control is applied, any deviation from the setpoint is much more due to the uncertainty than the control action. This assumption seems to work well when the uncertainty is only due to memoryless noise. This will be referred to as the "approximate" form of σ.

3.4.5 Reformulation of Auxiliary Problem

We now find a way to solve (3.13). The constraints as written are not usable, since we do not have an analytical expression for $V(x)$. However, they may be reformulated into usable constraints. For the first constraint we have:

$$\rho \circ \hat{\alpha}_4 \circ b \geq \sigma(|x|, ||\mathbf{w}_k||) \quad \forall\, x : V(x) \leq b \tag{3.22a}$$

$$\Leftarrow \quad \rho \circ \hat{\alpha}_4 \circ b \geq \sigma(|x|, ||\mathbf{w}_k||) \quad \forall\, x : \alpha_1(|x|) \leq b \tag{3.22b}$$

$$\Leftrightarrow \quad \rho \circ \hat{\alpha}_4 \circ b \geq \sigma(|x|, ||\mathbf{w}_k||) \quad \forall\, x : |x| \leq \alpha_1^{-1}(b) \tag{3.22c}$$

$$\Leftarrow \quad \rho \circ \hat{\alpha}_4 \circ b \geq \sigma(\alpha_1^{-1}(b), ||\mathbf{w}_k||) \tag{3.22d}$$

Then for the second constraint we have:

$$\rho \circ \hat{\alpha}_4 \circ V(x) \geq \sigma(|x|, ||\mathbf{w}_k||) \quad \forall\, x : V(x) > b \tag{3.23a}$$

$$\Leftarrow \rho \circ \hat{\alpha}_4 \circ \alpha_1(|x|) \geq \sigma(|x|, ||\mathbf{w}_k||) \quad \forall\, x : V(x) > b \tag{3.23b}$$

$$\Leftarrow \rho \circ \hat{\alpha}_4 \circ \alpha_1(|x|) \geq \sigma(|x|, ||\mathbf{w}_k||) \quad \forall\, x : \alpha_2(|x|) > b \tag{3.23c}$$

$$\Leftarrow \rho \circ \hat{\alpha}_4 \circ \alpha_1(|x|) \geq \sigma(|x|, ||\mathbf{w}_k||) \quad \forall\, x : |x| \geq \alpha_2^{-1}(b) \tag{3.23d}$$

Substitute $|x| = \alpha_1^{-1}(b)$ to see that (3.23d) satisfies (3.22d). Thus, once specific functional forms are chosen, solving this problem simplifies to solving a nonlinear equation ((3.23d) as an equality) and checking derivatives (that is, verifying that the derivative w.r.t. $|x|$ of the LHS of (3.23d) is greater than or equal to that of the RHS in the necessary range). Note that, although this reformulation leads to (3.13) being solvable, the resulting value of b will be larger than the optimal value of the original problem.

3.5 Case Studies

3.5.1 Scalar LQR Example

Consider the scalar example: $f(x,u,w) = Ax + Bu + w = .75x + .25\,u + w$, $l(x,u) = x^2 + u^2$. Also, let $\mathbb{X}_f$ be the steady state. To solve this problem, we will use infinite horizon discrete-time linear quadratic regulator (LQR), and the Lyapunov function bounds may be found analytically. In this case, the Lyapunov function has the form $V_\infty(x) = \sum_{k=0}^{\infty}(x_k^T Q x + u_k^T R u_k) = x^T J x$ where x is the initial condition and J solves a discrete time Riccati equation. This gives $J = 2$, so set $N_1 = N_2 = 2$. We also have $u_k = Kx_k$, where $K = -(B^T JB + R)^{-1}B^T JA$. So, to find N_3, we calculate $Q + K^T RK$, which gives $N_3 = 1.11$. Also, since we have $V_\infty(x) = 2x^2 = 2|x|^2$, we can use $l_V = 4|x|$.

We will consider the case where the guaranteed form of the uncertain term is used. Consider uniform noise with $w \in [-1,1]$ and $x_0 = 10$. Now, we must make a choice for ϵ_1, since many are possible and will provide different information. Consider $\epsilon_1 = 0.6$ and $\epsilon_1 = 0.8$, with results in Figure 3.1. Recall that the trajectory of the system is bounded, as shown in (3.11), by $\beta(|x_0, k)$ until the trajectory crosses $\gamma(||\mathbf{w}_k||)$, after which time the trajectory will always be bounded by $\gamma(||\mathbf{w}_k||)$.

Notice that this gives a rather loose bound, but it is an absolute guarantee. We can also compute $\gamma(||\mathbf{w}_k||)$ for $\epsilon_1 \approx 1$, which gives $\gamma(||\mathbf{w}_k||) = 3.6$, still a rather loose bound. However, it is a guarantee no matter the realization of the noise. Now, consider the case where $w_k = 1 \ \forall\, k$. See Figure 3.2, with $\epsilon_1 \approx 1$. Now, with a much "worse" case realization of the uncertainty,$\gamma(||\mathbf{w}_k||)$ gives a much tighter bound. Notice that since we chose $\epsilon_1 \approx 1$, $\beta(|x_0|, k)$ is nearly constant, so we have no guarantee of when $|x|$ will be bounded by $\gamma(||\mathbf{w}_k||)$.

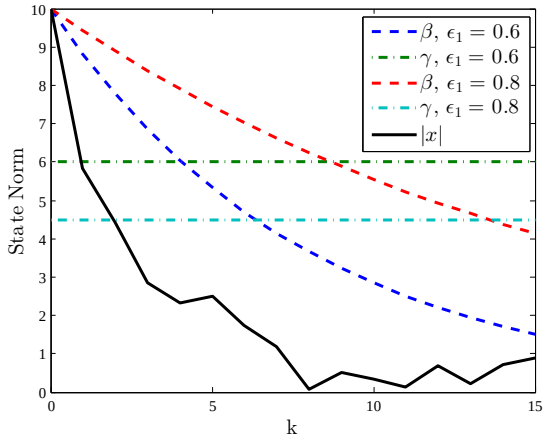

Figure 3.1: Scalar system, uniform noise

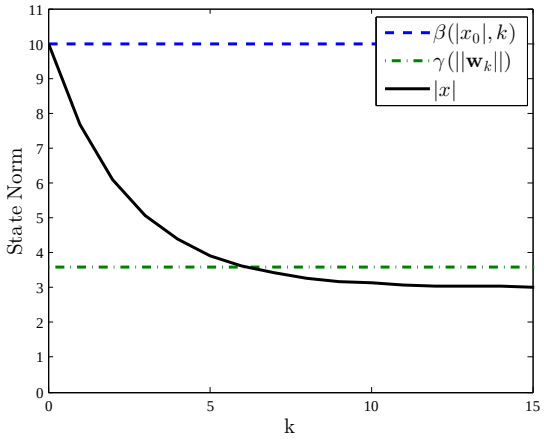

Figure 3.2: Scalar system, $w_k = 1$, $\epsilon_1 = 1$

3.5.2 CSTR Example

Consider a CSTR with the consecutive competitive reactions $A+B \xrightarrow{k1} C$ and $B+C \xrightarrow{k2} D$. The CSTR has three feeds with volumetric flow rates F_A and F_B and concentrations C_{F_A} and C_{F_B}. Each reactant feed only contains one component, and the volumetric flow rates are the control variables. Flow of pure water, F_W, is also available as a control variable. All three have an upper limit of 20. The CSTR has exiting concentrations C_A, C_B, C_C, & C_D. These are the state variables. The exiting volumetric flow rate is $F_T = F_A + F_B + F_W$. The problem will be considered with parameters shown in Table 3.1. The steady state objective is $min\ F_A P_{F_A} + F_B P_{F_B} + F_W P_{F_W} - F_T C_C P_C$ where P_{F_i} is the purchase price of feed i, and P_C is the sales price per mole of the product. The solution to the steady state problem is shown in Table 3.2.

We use a quadratic stage cost with $Q = I_4$ and $R = I_3$, as well as additive state noise. As in the last example, let $\mathbb{X}_f$ be the steady state. Now we need to find estimates for N_1, N_2, and N_3 from open loop tests, since this is not an LQR problem. To do this, we choose a sample space of the states. The bounds on the sample space are $0.5\,C_{i,ss} \leq C_i \leq 1.5\,C_{i,ss}\ \forall\, i$, where i denotes the reaction component. A uniform distribution of initial points is taken

Table 3.1: Nonlinear CSTR Parameters

$k_1 = 10$	$k_2 = 4$	$C_{FA} = 5$
$C_{FB} = 5$	$V = 10$	$P_{F_A} = 1$
$P_{F_B} = 1$	$P_{F_W} = 0.5$	$P_C = 1$

Table 3.2: Nonlinear CSTR steady state values

$C_{Ass} = 1.665$	$C_{Bss} = 0.200$	$C_{Css} = 1.044$	$C_{Dss} = 0.349$
$F_{Ass} = 14.650$	$F_{Bss} = 9.305$	$F_{Wss} = 0$	$l_{ss} = -1.044$

across the sample space, and 100,000 points are chosen. An open loop control problem is solved with the initial state at each one of these points. We use a step size of 0.1 and a controller horizon time of 50. Three point Radau collocation is used to discretize the differential equations, and IPOPT [64] is used to solve the optimization problems. We found that, for $\alpha_i(|x|) = N_i|x|^{\mu_i}$, $N_1 = 1.4$, $N_2 = 2.9$, $\mu_1 = 2.2$, and $\mu_2 = 1.85$ provide valid bounds within this range. The bounds are shown in Figure 3.3. Note that the bound parameters are chosen to give the tightest possible bounds that are true.

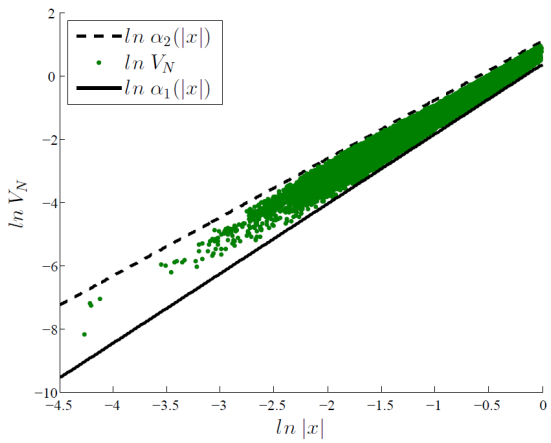

Figure 3.3: CSTR Lyapunov function bounds

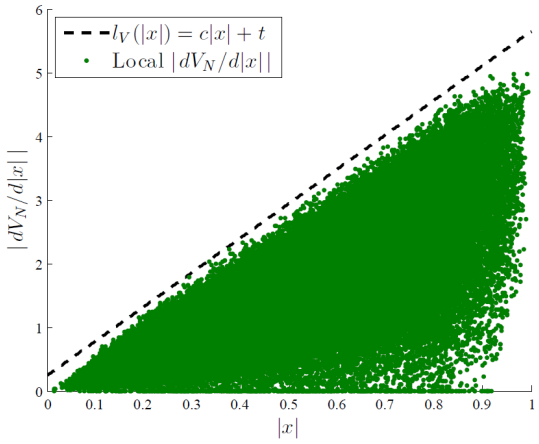

Figure 3.4: Overestimation of $|dV_N(x)/d|x||$

Also, since the stage cost is quadratic, $N_3 = 1$ and $\mu_3 = 2$ provide a valid lower bound for the first stage cost. Finally, to approximate l_V, we compute, for a given initial point x_g, $|V(x_g) - V(x_{a,i})|/|x_g - x_{a,i}|$ for the eight points $x_{a,i},\ i = 1 \dots 8$ closest to x_g. We then take the maximum value of these eight numbers, and use that as the local $|dV_N/d|x||$ associated to x_g. These values are then plotted against the norm, and a linear over-estimator $l_V(|x|) = c|x| + t$ with $c = 5.4$ and $t = 0.24$ is chosen. This is shown in Figure 3.4.

So now everything needed is available to provide predictive trajectory bounds. Note that for a dynamic simulation, the initialization for the first NLP will be linear with time, and the subsequent NLPs will be initialized with the solution from the previous NLP moved one time step backward. This aligns with the theory in [25] to allow for stability even without an exact solution to a given NLP.

Consider the case with $C_{i,0} = 1.5\, C_{i,ss}$ and $w_{ki} \in [-0.1\, C_{i,ss}, 0.1\, C_{i,ss}]\ \forall\, k, i$. First use the approximate form of σ from (3.21e). The trajectory of the system and ISS bounds for the cases that $\epsilon_1 = 0.7$ and $\epsilon_1 = 0.9$ are shown in Figure 3.5. Again, although the bound appears to work well here, it is not a guarantee for all realizations of the noise.

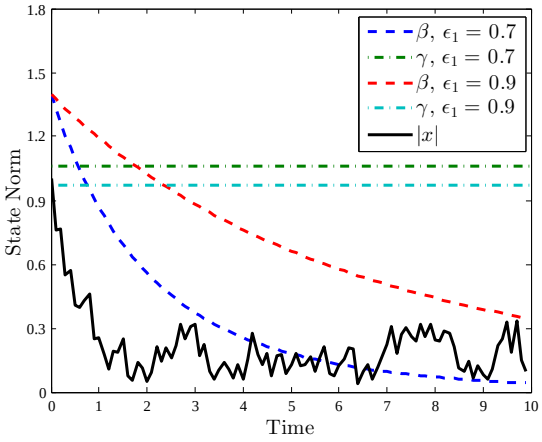

Figure 3.5: CSTR with approximate γ and uniform noise

The guaranteed sensitivity expression is very conservative for this system. If we set $\epsilon_1 = 1$ and calculate the size of the invariant ball, then we see $\gamma(||\mathbf{w}_k||) = 0.937$ for the approximate expression and $\gamma(||\mathbf{w}_k||) = 6.326$ for the guaranteed expression. Although the guaranteed bound is true, it is not particularly useful. This shows the limitations with an increasing number of states.

3.6 Conclusions

This chapter has discussed the robustness issues that arise with NMPC. Instead of other robust NMPC formulations that may be computationally cumbersome or conservative in performance, we propose a straightforward method for reformulating the NLPs solved online so that they satisfy the NLP properties that ensure the continuity of the objective, which can be used to show robustness. This is easily extended to other, more specialized NMPC formulations that will be shown later in the thesis.

Furthermore, wextend the ISS results for NMPC to calculate predictive state trajectory bounds. The ISS theorem for discrete time systems is extended to allow for an uncertain

term that depends on the state as well as the realization of uncertainty. Functional forms for the Lyapunov function bounds are proposed, and a method for calculating their parameters is shown. Example calculations are shown for a linear scalar system and a nonlinear CSTR. The difficulty of scaling this method to larger systems highlights a weakness of the ISS framework, in that proving the existence of ISS bounds does not take the place of simulations or tuning.

Chapter 4

Terminal Constraints

4.1 Introduction

Terminal conditions are an important aspect of ensuring the stability of NMPC. However, calculating terminal constraints and costs for the nonlinear case is not straightforward. In [65], terminal conditions are calculated via the construction of a linear differential inclusion (LDI) and the solution of a linear matrix inequality. However, the construction of the LDI can be prohibitively difficult for large-scale systems.

In [44], a quasi-infinite horizon approach is proposed in which the terminal cost is computed based on a controller for the linearized system, and the terminal region represents a region of attraction for the linear controller applied to the nonlinear system. This method was applied to an experimental quad-tank system in [3] and further extended in [66]. This method was developed for discrete time models in [67] and [68], which eliminates the need for a small discretization step upon implementation. These methods require finding a Lipschitz constant for the nonlinear part of the system or solving a series nonconvex optimization problems to global optimality, either of which makes application to a large system cumbersome. Instead, we propose a method of bounding only the higher order nonlinear effects of the system via simulations under LQR control. This appears more practical and leads to a method of calculating terminal conditions that is scalable. We demonstrate this method on three systems from the literature, including a large-scale distillation system.

4.2 Quasi-Infinite Horizon NMPC

Establishing Assumption 22 (D) is a key difficulty in ensuring the stability of (3.1). This assumption is satisfied if there exists a stabilizing controller in the terminal region with $\psi(x)$ as a control Lyapunov function.

In [44], it is proposed to use an infinite-horizon LQR applied to the linearized system as the stabilizing controller in the terminal region. Finding the size of the terminal region is then a question of finding the largest region around the setpoint in which the LQR is stabilizing for the nonlinear system. This is done in previous works by finding a Lipschitz constant for the nonlinear system and analyzing the descent of the Lyapunov function, or by solving a sequence of global optimization problems. The terminal cost is then the cost function of the LQR, $\psi(x) = x^T P x$.

The main issue with this method is that finding the terminal region via a Lipschitz constant bound or by solving a sequence of global optimization problems can be cumbersome when applied to a large system. In the next section we propose a more practical method of finding the size of the terminal region via a bound on the higher order nonlinear effects of the system that applies more easily to large systems. We also do the analysis in discrete time, as in [67] and [68].

4.2.1 Extension for Large-Scale Systems

Consider (2.2) broken down into linear and nonlinear parts with the terminal control law $u_f(x) = -Kx$ applied, so that

$$x_{k+1} = f(x_k, -Kx_k) = A_K x_k + \phi(x_k, -Kx_k) \tag{4.1}$$

where $A = \frac{\partial f(0,0)^T}{\partial x}$, $B = \frac{\partial f(0,0)^T}{\partial u}$, $A_K = A - BK$, the pair (A, B) is assumed to be stabilizable, and $\phi : \mathcal{X} \times \mathbb{U} \to \mathcal{X}$ is the nonlinear part of the system dynamics. For the

terminal control law u_f we choose infinite horizon LQR applied to the linearized system, so that

$$\psi(x) = x^T P x = \min \sum_{i=0}^{\infty} z_i^T \widetilde{Q} z_i + v_i^T \widetilde{R} v_i \tag{4.2a}$$

$$s.t.\ z_{i+1} = A z_i + B v_i \ \ \forall\ i = 0 \dots \infty \tag{4.2b}$$

$$z_0 = x. \tag{4.2c}$$

where $\widetilde{Q} := Q + \Delta Q$, $\Delta Q \succ 0$, $\widetilde{R} := R + \Delta R$, and $\Delta R \succeq 0$. Define $W := Q + K^T R K$, $\Delta W := \Delta Q + K^T \Delta R K$, and $\widetilde{W} := \widetilde{Q} + K^T \widetilde{R} K$. In order to show a stability region of the linear controller for the nonlinear system, it is necessary to show a bound on the nonlinear system effects. To that end, we show the existence of a bound of the following form.

Theorem 28. *There exists $M, q \in \mathbb{R}_+$ such that*

$$|\bar{\phi}(x)| \leq M|x|^q \ \ \forall\ x \in \mathcal{X} \tag{4.3}$$

where $\bar{\phi}(x) = \phi(x, -Kx)$.

Proof. Define $\bar{f}(x) := f(x, -Kx)$. Then the nonlinear part of the system is $\bar{\phi}(x) := \bar{f}(x) - A_K x$. By Taylor's Theorem we have

$$\begin{aligned} \bar{\phi}_j(x) &= \bar{\phi}_j(0) + \nabla \bar{\phi}_j(0)^T x \\ &+ \frac{1}{2} \int_0^1 x^T \nabla^2 \bar{\phi}_j(x\tau) x \ d\tau \ \ \forall\ i = 1 \dots n_x \end{aligned} \tag{4.4}$$

where j is indexed over each state. Note that, at $x = 0$, $\bar{\phi}_j(x) = 0$ and $\nabla \bar{\phi}_j(x)^T = \nabla \bar{f}_j(x)^T - \nabla(A_{K,j}, x_j) = A_{K,j} - A_{K,j} = 0$. Then

$$\bar{\phi}_j(x) = \frac{1}{2} \int_0^1 x^T \nabla^2 \phi_j(x\tau) x \ d\tau \tag{4.5}$$

Since f is twice continuously differentiable, we define:

$$\lambda_m := \max_{x \in \mathcal{X}, j \in \{1 \ldots n_x\}} \| \nabla^2 \bar{\phi}_j(x) \| \tag{4.6}$$

and thus

$$|\bar{\phi}_j(x)| \leq \frac{\lambda_m}{2} |x|^2 \ \ \forall \ j = 1 \ldots n_x \tag{4.7}$$

which gives

$$|\bar{\phi}(x)|^2 = \sum_{j=1}^{n_x} |\bar{\phi}(x)|^2 \leq n_x \left(\frac{\lambda_m}{2} |x|^2 \right)^2 \tag{4.8}$$

therefore

$$|\bar{\phi}(x)| \leq \sqrt{n_x} \frac{\lambda_m}{2} |x|^2 \tag{4.9}$$

Thus (4.3) is satisfied with $M = \sqrt{n_x} \frac{\lambda_m}{2}$ and $q = 2$. $\square$

Note that, in general, (4.1) represents an implicit discretization of a set of differential and algebraic equations (DAEs) so that ϕ cannot be obtained explicitly, and actually quantifying (4.3) may be tedious. Instead, for practical purposes we will find M and q in (4.3) explicitly via simulations from a sampling of initial conditions in the state space, as will be shown in Section 4.3. Here the key advantages of this method are apparent, in that we only need to solve a series of one step simulations using the linear control, and do not need to iterate on regions for which a Lipschitz constant is valid. It is also possible, however, to obtain larger terminal regions, since a power law bound on a nonlinear term is expected to be a better fit than a linear bound. Although we recognize that it is not possible to guarantee that Theorem 4.3 is satisfied by parameters found through simulations, the kinds of examples that we consider tend to be well-behaved so that overestimating M and q to ensure that Theorem 4.3 can easily be done with practical certainty.

To find the terminal region, we consider the LQR controller (4.2) applied to the fully nonlinear system (2.2). From the optimality conditions for (4.2) the infinite horizon cost matrix $P \in \mathbb{R}^{n\times n}$ satisfies the discrete-time Riccati equation

$$A^T P A - P - (A^T P B)(B^T P B + \widetilde{R})^{-1}(B^T P A) + \widetilde{Q} = 0 \tag{4.10}$$

This also gives the gain matrix $K = (\widetilde{R} + B^T P B)^{-1} B^T P A$ such that $u_f(x) = -Kx$. Then, this satisfies the Lyapunov equation:

$$A_K^T P A_K - P + \widetilde{W} = 0 \tag{4.11}$$

Since $P = \sum_{k=0}^{\infty} (A_K^T)^k \widetilde{W} (A_K)^k$ solves this equation, we can write

$$\|P\| \leq \sum_{k=0}^{\infty} \|(A_K^T)^k \widetilde{W} (A_K)^k\| \leq \frac{\lambda_{\widetilde{W}}^{max}}{1-\hat{\sigma}^2} \tag{4.12}$$

where $\lambda_{\widetilde{W}}^{max}$ is the maximum eigenvalue of $\widetilde{W}$ and we assume the maximum singular value of A_K, $\hat{\sigma} \in [0, 1)$. Similarly, we have:

$$\|A_K^T P\| \leq \|A_K\| \sum_{k=0}^{\infty} \|(A_K^T)^k \widetilde{W} (A_K)^k\| \leq \frac{\hat{\sigma}\lambda_{\widetilde{W}}^{max}}{1-\hat{\sigma}^2} \tag{4.13}$$

To show the descent of the Lyapunov function under evolution of (4.1) in the terminal region we have:

$$\psi(x_{k+1}) - \psi(x_k) \tag{4.14a}$$

$$= x_{k+1}^T P x_{k+1} - x_k^T P x_k \tag{4.14b}$$

$$= (A_K x_k + \bar{\phi}(x_k))^T P (A_K x_k + \bar{\phi}(x_k)) - x_k^T P x_k \tag{4.14c}$$

$$= x_k^T (A_K^T P A_K - P) x_k + 2 x_k^T A_K^T P \bar{\phi}(x_k) + \bar{\phi}(x_k)^T P \bar{\phi}(x_k) \tag{4.14d}$$

$$= -x_k^T \widetilde{W} x_k + 2 x_k^T A_K^T P \bar{\phi}(x_k) + \bar{\phi}(x_k)^T P \bar{\phi}(x_k) \tag{4.14e}$$

$$= -x_k^T W x_k - x_k^T \Delta W x_k + 2 x_k^T A_K^T P \bar{\phi}(x_k) + \bar{\phi}(x_k)^T P \bar{\phi}(x_k) \tag{4.14f}$$

$$\leq -\lambda_{\Delta W}^{min}|x_k|^2 + 2\hat{\sigma}\frac{\lambda_{\widetilde{W}}^{max}}{1-\hat{\sigma}^2}M|x_k|^{q+1} + \frac{\lambda_{\widetilde{W}}^{max}}{1-\hat{\sigma}^2}M^2|x_k|^{2q} \quad \forall\, x_k \in \mathcal{X}_f \tag{4.14g}$$

where $\lambda_{\Delta W}^{min}$ is the minimum eigenvalue of ΔW, which gives the stability condition

$$-\lambda_{\Delta W}^{min} + 2\hat{\sigma}\Lambda_P M|x_k|^{q-1} + \Lambda_P M^2|x_k|^{2(q-1)} \leq 0 \tag{4.15}$$

where $\Lambda_P = \frac{\lambda_{\widetilde{W}}^{max}}{1-\hat{\sigma}^2}$. Then by the quadratic formula:

$$\begin{aligned} &|x| \leq c_f \\ &:= \left(\frac{-\hat{\sigma}\Lambda_P + \sqrt{(\hat{\sigma}\Lambda_P)^2 + \lambda_{\Delta W}^{min}\Lambda_P}}{\Lambda_P M} \right)^{\frac{1}{q-1}} \end{aligned} \tag{4.16}$$

which will be used to define $\mathcal{X}_f = \{x \mid |x| \leq c_f\}$.

Note that it must also be verified that control constraints are satisfied in the terminal region, that is $-Kx \in \mathbb{U} \;\; \forall\, x \in \mathcal{X}_f$. If this does not hold then $\mathcal{X}_f$ must be decreased in size until control constraints are satisfied.

Also note that we have increased the stage costs of the LQR (4.2) relative to Q and R so as to enforce $\psi(x_{k+1}) - \psi(x_k) \leq -x^T W x$ under evolution of the nonlinear dynamics $x_{k+1} = f(x_k, u_k)$, as in [67] and [68].

The procedure for finding the nonlinearity bound and calculating the terminal region is summarized as follows, assuming that the user is starting with a continuous time DAE model:

- Choose a steady state $(x_s s, u_s s)$, e.g. via RTO
- Choose NMPC cost matrices Q and R and LQR cost matrices $\widetilde{Q} \succ Q$ and $\widetilde{R} \succeq R$
- Linearize the DAE model at (x_{ss}, u_{ss})
- Discretize the linearizion of the DAE model with sampling time h to obtain A and B
- Calculate the discrete-time LQR cost-to-go P and gain K from the discrete time linearization (A, B) and LQR cost matrices $(\widetilde{Q}, \widetilde{R})$

- Sample many initial conditions x in the region of interest in the state-space
- Simulate the DAE system forward one sampling time h under constant control $u = -Kx$ from every initial condition x to obtain $f(x, -Kx)$
- Calculate $\bar{\phi}(x) = f(x, -Kx) - (A - BK)x$ for every initial condition x
- Create a scatter plot of $ln|\bar{\phi}(x)|$ vs. $ln|x|$
- Choose slope q and intercept $ln\, M$ to create a valid upper bound for $ln|\bar{\phi}(x)|$
- Calculate c_f from (4.16) using M, q, A, B, Q, R, $\widetilde{Q}$, $\widetilde{R}$, and K

4.3 Case Studies

4.3.1 Two State Example

Here we consider the two-state example from [44].

$$\dot{x}_1 = x_2 + u(\mu + (1-\mu)x_1) \tag{4.17a}$$

$$\dot{x}_2 = x_1 + u(\mu - 4(1-\mu)x_2) \tag{4.17b}$$

$$\mathbb{U} = \{u \in \mathbb{R} - 2.0 \leq u \leq 2.0\} \tag{4.17c}$$

$$Q = 10TI_2 \tag{4.17d}$$

$$R = 0.05/T \tag{4.17e}$$

The steady state is $x_{ss} = (0, 0)$, $u_{ss} = 0$. Also, we define parameters $\rho_x > 0$ and $\rho_u \geq 0$ such that $\Delta Q := \rho_x Q$ and $\Delta R := \rho_u R$. We consider terminal region calculations for system (4.17) using a nonlinearity bound (4.3) found via simulations and terminal region calculated via (4.16). We hold $\rho_u = 1$ constant, and so the nonlinearity bound must be found for each combination of sampling time T and ρ_x. We show this in detail for one

case, $T = 0.1s$ and $\rho_x = 1.1$, in Table 4.1. This is done by simulating the system one step forward under LQR control from a random sampling of $10,000$ initial conditions, and then choosing M and q to bound the data. After this is completed for each case, the terminal region area may be found as πc_f^2, with results shown in Figure 4.2. The nonlinearity bound parameters M and q as well as c_f are summarized in Table 4.1 for each case.

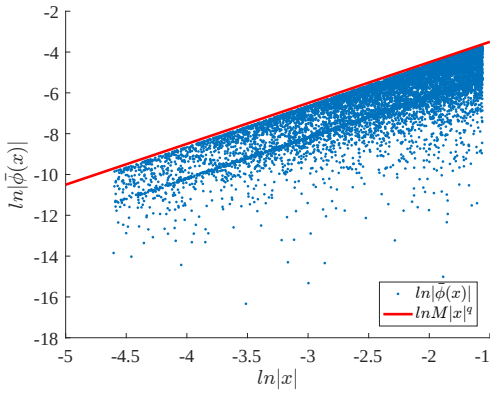

Figure 4.1: Chen and Allgöwer Example, Nonlinear Bound for $T = 0.1s$, $\rho_x = 1.1$

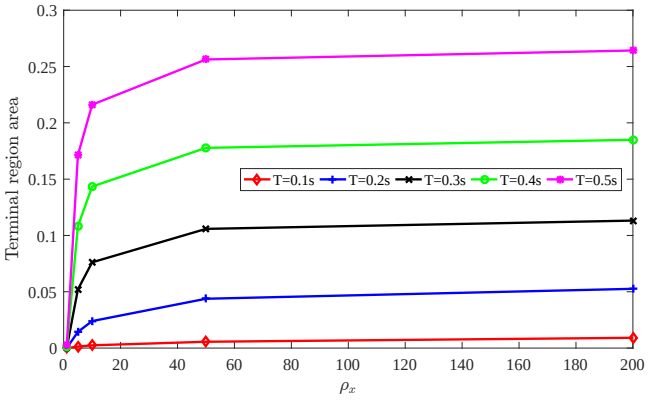

Figure 4.2: Chen and Allgöwer Example, Terminal region calculations with nonlinearity bound

4.3.2 Hicks Reactor

Here we consider the CSTR system [69], which has been used as a benchmark problem in the control literature [70], with model given in (4.18):

$$\frac{z_c}{dt} = (1 - z_c)/(U_{2sf}u_2) - k_0 z_c exp(-E_a/z_T) \tag{4.18a}$$

$$\frac{z_T}{dt} = (z_T^f - z_T)/(U_{2sf}u_2) + k_0 z_c exp(-E_a/z_T) - \nu U_{1sf}u_1(z_T - z_T^{cw}) \tag{4.18b}$$

$$x_{ss} = [0.6416, 0.5387]^T \tag{4.18c}$$

$$u_{ss} = [0.5833, .5]^T \tag{4.18d}$$

Table 4.1: Chen and Allgöwer example, Terminal Region Results with Nonlinearity Bound (M, q, c_f)

T	$\rho_x = 1.1$	$\rho_x = 5$	$\rho_x = 10$	$\rho_x = 50$	$\rho_x = 200$
0.1	-0.5,2,1.18e-3	-0.3,2,2.03e-2	-0.1,2,2.78e-2	0.3, 2,4.22e-2	0.6,2,5.39e-2
0.2	0.4,2.05,5.15e-3	0.7,2.05,6.77e-2	0.8,2.05,8.73e-2	0.9,2.05,0.118	1,2.05,0.129
0.3	0.9,2.1,1.15e-2	1,2.1,0.129	1.1,2.1,0.156	1.15, 2.1,0.184	1.2,2.1,0.190
0.4	1.2,2.15,0.020	1.3,2.15,0.186	1.35,2.15,0.214	1.4,2.15,0.238	1.45,2.15,0.243
0.5	1.4,2.15,2.82e-2	1.45,2.15,0.233	1.5,2.15,0.262	1.55,2.15,0.286	1.6,2.15,0.290

$$\mathbb{U} = \{u_1, u_2 \in \mathbb{R} | -0.4167 \leq u_1 \leq 0.4167; -0.4750 \leq u_2 \leq 0.5\} \tag{4.18e}$$

$$Q = \begin{bmatrix} 10 & 0 \\ 0 & 2 \end{bmatrix} \tag{4.18f}$$

$$R = \begin{bmatrix} 1 & 0 \\ 0 & 0.5 \end{bmatrix} \tag{4.18g}$$

where the states are dimensional concentration z_c and dimensionless temperature z_T. The controls are u_1 cooling water flow, and u_2 inverse of the dilution rate, also dimensionless. The model parameters and scaling factors are given in Table 4.2.

Let the time step $h = 1\,min$. First, we consider that $\rho_x = 50$ is held constant In this case, the nonlinearity bound is changing with ρ_u since the controller gain K is changing. One example of data used to find the nonlinearity bound is shown in Figure 4.4 for the case that $\rho_u = 0.1$. Values of the bound parameters as well as c_f are summarized in Table 4.3. Terminal region area is shown as a function of ρ_u in Figure 4.4.

Table 4.2: Hicks Reactor Parameters

Parameter	Value
z_T^{cw}	0.38
z_T^f	0.395
E_a	5
ν	1.95×10^{-4}
k_0	300
U_{1sf}	600
U_{2sf}	40

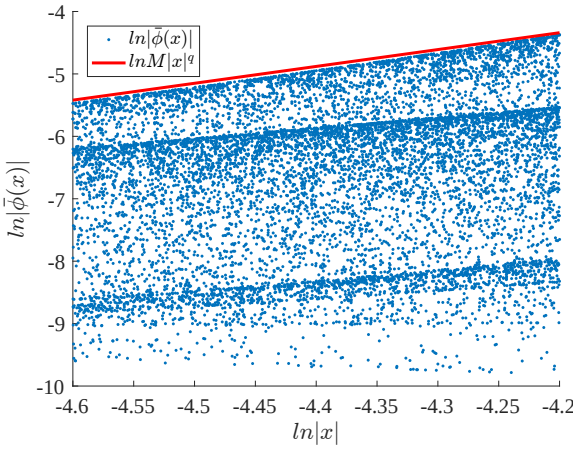

Figure 4.3: LQR, Nonlinearity Bound with $\rho_x = 50$

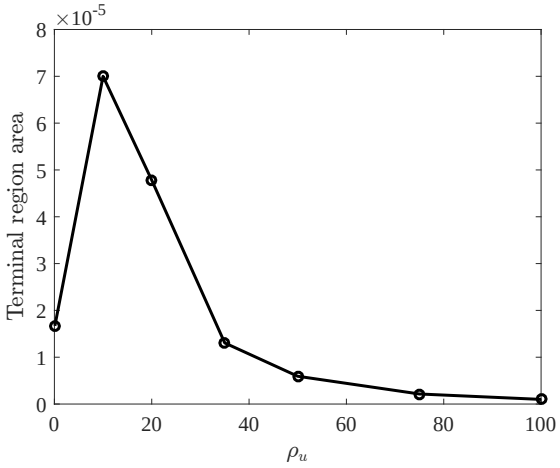

Figure 4.4: LQR, Terminal Region Area with $\rho_x = 50$

Now, we consider the case that $\rho_\psi = \rho_x = \rho_u$. Results for the parameter c_f are summarized in Table 4.4, and results for the terminal region area are shown in Figure 4.5.

Here we show QIH-NMPC simulations for the Hicks reactor, with terminal region and constraint determined via the LQR based approach with $\rho_x = 50$ and $\rho_u = 35$ and non-

Table 4.3: Terminal Region Results with LQR and Nonlinearity Bound, $\rho_x = 50$

ρ_u	M	q	c_f
0.1	1.097e3	2.7	0.00231
10	54.5982	2.3	0.00472
20	28.50	2.25	0.00390
35	25.79	2.2	0.00204
50	23.34	2.18	0.00137
75	21.11	2.16	0.00083
100	20.09	2.15	0.00056

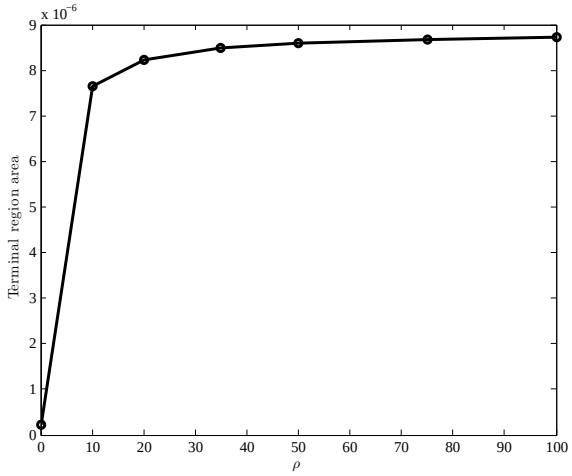

Figure 4.5: LQR, Terminal Region Area with $\rho_\psi = \rho_x = \rho_u$

Table 4.4: Terminal Region Results with LQR and Nonlinearity Bound, $\rho_\psi = \rho_x = \rho_u$

ρ_ψ	.1	10	20	35	50	75	100
c_f	0.00027	0.00156	0.00162	0.00164	0.00165	0.00166	0.00167

linearity bound method. The horizon length is again chosen to be $N = 10$. The state trajectories are shown in Figure 4.6, and the control trajectories are shown in Figures 4.7 and 4.8. As can be seen in the figures, each case shows asymptotic stability.

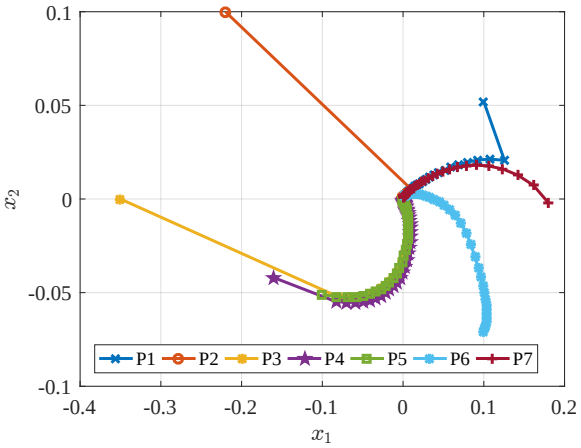

Figure 4.6: Phase portrait of states under discrete time QIH-NMPC

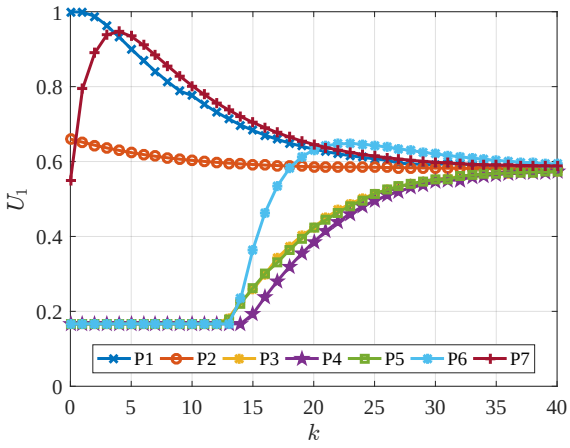

Figure 4.7: First manipulated variable trajectory

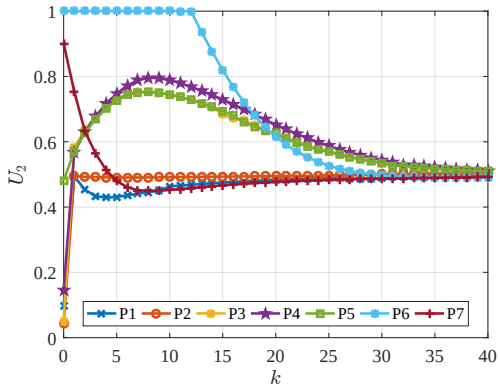

Figure 4.8: Second manipulated variable trajectory

4.3.3 Distillation Example

We consider the challenging nonlinear system shown in Figure 4.9 with two distillation columns in series [2]. Each column is based on the model described in [71], with the main difference that we consider three components, A, B, and C. The bottoms of the first column are the feed to the second column. The flowsheet is shown in Figure 4.9. The distillate of the first column is to be 95% A, the distillate of the second column is to be 95% B, and the bottoms of the second column is to be 95% C. The thermodynamics assume constant relative volatility, and for tray hydraulics, we use the Francis weir formula, with constant $K_{uf} = 21.65$ above the feed and constant $K_{bf} = 29.65$ below the feed. The weir height is 0.25, and the nominal liquid holdup is 0.5. Each column has 41 equilibrium stages including the reboiler, giving a total of 246 states and 8 controls. The model for each column is given below, with variable and parameter definitions in Table 4.5. Note that the subscript denoting which column a variable pertains to is ignored in (4.19)-(4.26) and Table 4.5 for concision.

Vapor Liquid Equilibria

$$a_{i,j} = x_{i,j}\alpha_j$$
$$\forall\, i \in \{0, .., NT-1\}, j \in \{A, B\} \tag{4.19a}$$
$$b_i = x_{i,1}(\alpha_A - 1) + x_{i,2}(\alpha_B - 1) + 1$$
$$\forall\, i \in \{0, .., NT-1\} \tag{4.19b}$$
$$y_{i,j} * b_i = a_{i,j} \tag{4.19c}$$
$$\forall\, i \in \{0, .., NT-1\}, j \in \{A, B\}$$

Vapor Flows

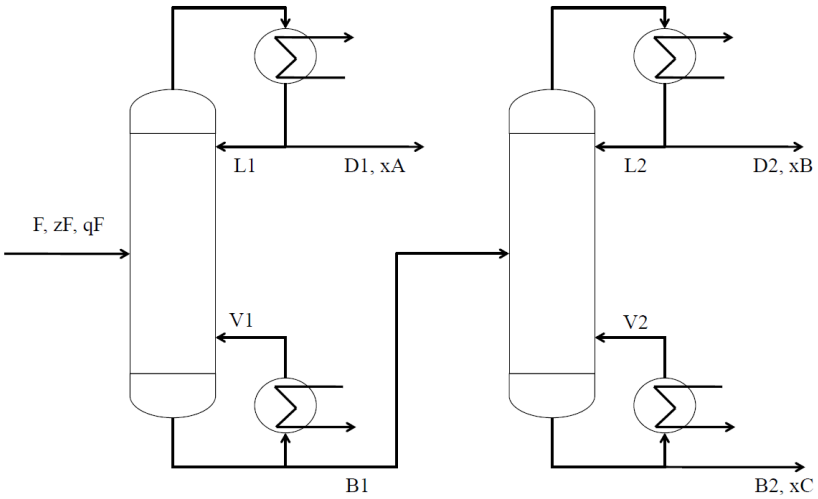

Figure 4.9: Distillation Flowsheet [2]

$$V_i = V_{\bar{B}} \quad \forall\, i \in 1..NF-1 \tag{4.20a}$$

$$V_i = V_{\bar{B}} + (1-q_F)F \quad \forall\, i \in NF..NT-1 \tag{4.20b}$$

Liquid Flows

$$L_i = K_{bf}\left(\frac{(M_i - M_{uw}) + \sqrt{(M_i - M_{uw})^2}}{2}\right)^{1.5}$$

$$\forall\, i \in \{2,..,NF\} \tag{4.21a}$$

$$L_i = K_{uf}\left(\frac{(M_i - M_{uw}) + \sqrt{(M_i - M_{uw})^2}}{2}\right)^{1.5}$$

$$\forall\, i \in \{NF+1,..,NT-1\} \tag{4.21b}$$

$$L_{NT} = L_{\bar{D}} \tag{4.21c}$$

Holdup Balances

$$dM_i/dt = L_{i+1} - L_i + V_{i-1} - V_i$$

$$\forall i \in \{2, .., NT-1\}/\{NF\} \tag{4.22a}$$

$$d(M_i x_{i,j})/dt = L_{i+1}x_{i+1,j} - L_i x_{i,j} + V_{i-1}y_{i-1,j}$$

$$-V_i y_{i,j} \;\; \forall\, i \in \{2, .., NT-1\}/\{NF\}, j \in \{A, B\} \tag{4.22b}$$

Feed Balance

$$dM_{NF}/dt = L_{NF+1} - L_{NF} + V_{NF-1} - V_{NF} + F$$

$$\forall\, j \in \{A, B\} \tag{4.23a}$$

$$d(M_{NF}x_{NF,j})/dt = L_{NF+1}x_{NF+1,j} - L_{NF}x_{NF,j}$$

$$+V_{NF-1}y_{NF-1,j} - V_{NF}y_{NF,j} + Fz_{Fj} \;\; \forall\, j \in \{A, B\} \tag{4.23b}$$

Reboiler Balance (equilibrium stage)

$$dM_1/dt = L_2 - V_{\bar{B}} - \bar{B} \tag{4.24a}$$

$$d(M_1 x_{1,j})/dt = L_2 x_{2,j} - V_{\bar{B}}y_{1,j} - \bar{B}x_{1,j} \;\; \forall\, j \in \{A, B\} \tag{4.24b}$$

Condenser Balance

$$dM_{NT}/dt = V_{NT-1} - L_{\bar{D}} - \bar{D} \tag{4.25a}$$

$$d(M_{NT}x_{NT,j})/dt = V_{NT-1}y_{NT-1,j} - L_{\bar{D}}x_{NT,j}$$

$$-\bar{D}x_{NT,j} \;\; \forall\, j \in \{A, B\} \tag{4.25b}$$

Concentrations

$$M_i\, dx_{i,j}/dt = d(M_i x_{i,j})/dt - x_{i,j}\, dM_i/dt$$

$$\forall i \in \{1, .., NT\}, j \in \{A, B\} \tag{4.26}$$

Table 4.5: Distillation model definitions, i is indexed over trays, j is indexed over components

Variable/Parameter	Definition
$a_{i,j}$,b_i	thermodynamic parameters
$y_{i,j}$	vapor mol fraction
$\alpha_{i,j}$	thermodynamic parameters
V_i	vapor flow
$V_{\bar{B}}$	vapor boilup
NT	number of trays
NF	tray number of feed
M_{uw}	weir height
F	feed flow
L_i	liquid flow
q_F	fraction of lquid in feed
$L_{\bar{D}}$	reflux flow
$x_{i,j}$	liquid mol fraction
M_i	tray holdup
z_F	feed mol fraction
$\bar{D}$	distillate flow
$\bar{B}$	bottoms flow
K_{uf}, K_{bf}	weir constants

We set $\alpha_A = 2$ and $\alpha_B = 1.5$. The economic cost is the cost of feed and energy to the reboilers minus the cost of the products, that is $L^{ec} = p_F \cdot F_1 + pV(V_{\bar{B},1} + V_{\bar{B},2}) - p_A \cdot D_1 - p_B \cdot D_2 - p_C \cdot B_2$, where $p_F = \$1/mol$ is the price of feed, p_i for $i = A, B, C$ is the price

of component i with $p_A = \$1/mol$, $p_B = \$2/mol$, and $p_C = \$1/mol$, $p_V = \$0.008/mol$ is the price per mole vaporized in the reboilers, and the indices represent the first or second column. The feed is saturated liquid, and the composition of the feed is 0.4 mole fraction A, 0.2 mole fraction B, and 0.4 mole fraction C. The setpoint considered here is the economic minimum steady state corresponding to a feed composition of $z_F = (0.4, 0.2, 0.4)$. The purities are implemented as inequality constraints. We discretize the DAE system using three point Radau collocation.

Again, we define parameters $\rho_x > 0$ and $\rho_u \geq 0$ such that $\Delta Q := \rho_x Q$ and $\Delta R := \rho_u R$.For the stage costs we set $Q = 10 I_{246}$ and $R = I_8$, and for the discretization step we set $h = 1min$. For this method we will utilize the extension for large-scale systems with nonlinearity bound (4.3) and terminal regions characterized by (4.16). Furthermore, we consider tuning the terminal regions via $\rho_\psi = \rho_x = \rho_u$, so that K does not change, and therefore the nonlinearity bound does not that to be recomputed. The results of $10,000$ one-step simulations (performed in Matlab with ode45) are shown in Figure 4.10, and the nonlinearity bound parameters are found to be $q = 1.8$ and $M = 0.0743$. Then, c_f is shown as a function of ρ_ψ in Figure 4.11, and numerical values are shown in Table 4.6. As can be seen, there is little benefit in terminal region size to increasing ρ_ψ beyond 100.

Finally, we show close-loop simulations of the distillation system under QIH-NMPC for varying values of ρ_ψ with $N = 10$. To accommodate the optimal control problem, we discretize the DAE system using three point Radau collocation. The models are implemented in AMPL and solved with IPOPT on an Intel i7-4770 3.4 GHz CPU. The simulation results can be seen in Figure 4.12. All cases are convergent to the setpoint, however setting very high values for ρ_ψ leads to degradation in the dynamic performance. This, combined with the observation that high values of ρ_ψ do not significantly increase the terminal region size, leads to the conclusion that moderate values of ρ_ψ are the most practical.

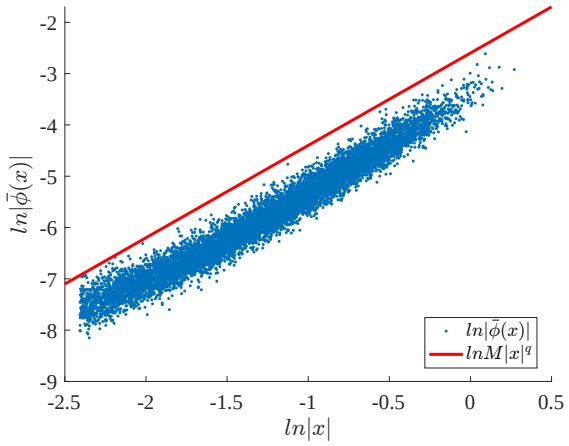

Figure 4.10: Distillation example, nonlinearity bound

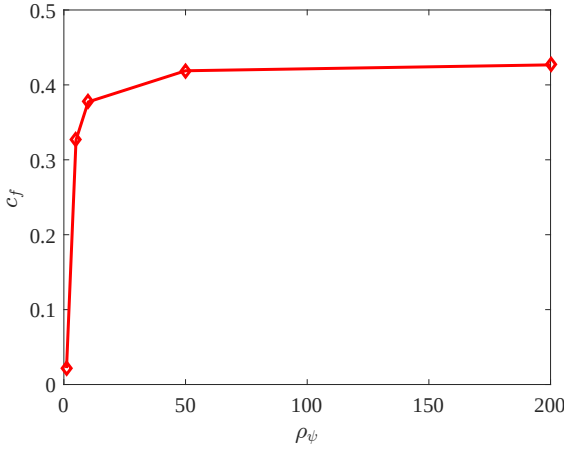

Figure 4.11: Distillation example, terminal regions with $\rho_\psi = \rho_x = \rho_u$

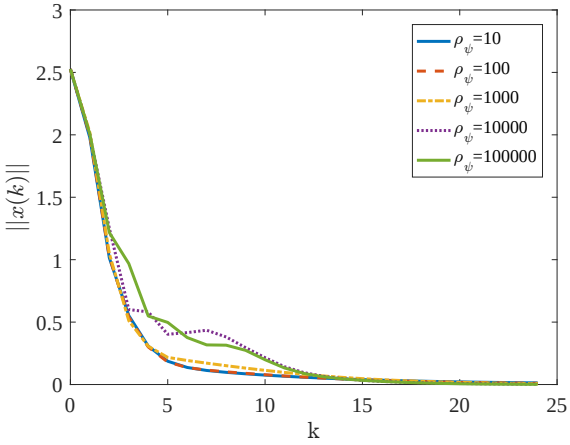

Figure 4.12: Distillation example, dynamic trajectories

4.4 Changing Steady-States

The calculation of terminal conditions may also be considered in the context of offset-free MPC or steady-state updates [59, 72, 73]. In the case that some model parameter is being estimated in real time, it may be desirable to update the steady-state based on real time optimization (RTO) calculations [74]. Furthermore, the steady-state may change for other

Table 4.6: Distillation Example, Terminal Region Results

ρ_ψ	c_f
10	0.3773
100	0.4241
1000	0.4288
10000	0.4293
100000	0.4293

reasons as well, such as predetermined production scheduling. Suppose that the steady-state and control are functions of the system uncertainty, $x_{ss}(w)$ and $u_{ss}(w)$. Now the terminal control gain $K(w)$ system linearization $A_K(w)$ become functions of the steady state and therefore the uncertainty, and the nonlinear part of the system becomes:

$$\phi(w, x, -K(w)(x-x_{ss}(w))) := f(x, -K(w)(x-x_{ss}(w)))-A_K(w)(x-x_{ss}(w)) \ \forall\, w \in \mathbb{W},\ x \in \mathcal{X} \tag{4.27}$$

Assumption 29. *(A)* $x_{ss} : \mathbb{W} \to \mathcal{X}_{ss}$ *and* $u_{ss} : \mathbb{W} \to \mathcal{U}_{ss}$ *are uniformly continuous (B)* $x_{ss}(0) = 0$ *is contained in the interior of* $\mathcal{X}_{ss}$ *and* $u_{ss}(0) = 0$ *is contained in the interior of* $\mathcal{U}_{ss}$ *(C)* $\mathcal{X}_{ss}$ *and* $\mathcal{U}_{ss}$ *are closed and bounded (D)* $f(x_{ss}(w), u_{ss}(w)) = 0\ \forall\ w \in \mathbb{W}$ *(E)* $|\phi(w, x, -K(w)(x - x_{ss}(w))| \leq M|x - x_{ss}(w)|^q\ \ \forall\, w \in \mathbb{W},\ x \in \mathcal{X}$*(F)* ψ *and* c_f *are calculated as in Section 4.2.1 (G)* $\mathbb{W}$ *is bounded and contains* 0 *(H)* $V_N(x_k, 0)$ *admits a control Lyapunov function (Definition 7) (I)* $V_N(x, w)$ *is uniformly continuous w.r.t.* x *and* w

Notice that in Assumption 29(E) the nonlinearity bound is found to hold for all possible steady states. The terminal cost matrix is again defined by (4.10), and the terminal region

is defined as in (4.16), but with all terms becoming dependent on the steady state. So, if the steady-state is updated in real time, then the terminal conditions P and c_f must be as well. However, if the nonlinearity bound is defined as in Assumption 29(E), with M and q not dependent on w, then all of the necessary calculations to update the terminal conditions (system linearization, Riccati equation solution, eigenvalue and singular value calculations) are fast compared to the simulations necessary to find M and q. With changing steady-states, the NLP solved online becomes:

$$V_N(x_k, w_{k-1}) = \min_{v_i} \quad \sum_{i=0}^{N-1} (z_i - x_{ss}(w_{k-1}))^T Q (z_i - x_{ss}(w_{k-1})) \tag{4.28a}$$

$$+ (v_i - u_{ss}(w_{k-1}))^T R (v_i - u_{ss}(w_{k-1})) + \psi(w_{k-1}, z_N) \tag{4.28b}$$

$$\text{s.t. } z_{i+1} = f(z_i, v_i) \ \ \forall\, i = 0 \dots N-1 \tag{4.28c}$$

$$z_0 = x_k \tag{4.28d}$$

$$v_i \in \mathbb{U} \ \ \forall\, i = 0 \dots N-1 \tag{4.28e}$$

$$|z_N - x_{ss}(w)| \leq c_f(w_{k-1}) \tag{4.28f}$$

Theorem 30. *Under Assumption 29, Quasi-infinite horizon NMPC with a changing steady state* (4.28) *is ISS w.r.t.* $x_{ss}(0) = 0$.

Proof.

$$V_N(x_{k+1}, w_k) - V_N(x_k, w_{k-1}) \tag{4.29a}$$

$$= V_N(f_p(x_k, u_k, w_k), w_k) - V_N(x_k, w_{k-1})$$

$$+ V_N(f_p(x_k, u_k, w_k), 0) - V_N(f_p(x_k, u_k, w_k), 0)$$

$$V_N(x_k, 0) - V_N(x_k, 0)$$

$$+V_N(f_p(x_k,u_k,0),0) - V_N(f_p(x_k,u_k,0),0) \tag{4.29b}$$

$$\leq |V_N(f_p(x_k,u_k,w_k),w_k) - V_N(f_p(x_k,u_k,w_k),0)|$$

$$+|V_N(x_k,0) - V_N(x_k,w_{k-1})|$$

$$+|V_N(f_p(x_k,u_k,w_k),0) - V_N(f_p(x_k,u_k,0),0)|$$

$$+V_N(f_p(x_k,u_k,0),0) - V_N(x_k,0) \tag{4.29c}$$

$$\leq -\alpha_3(x_k) + \sigma(||\mathbf{w}_k||) \tag{4.29d}$$

for some $\sigma \in \mathcal{K}$. Thus V_N satisfies Theorem 5.7 with $c_1 = c_2 = 0$, and Quasi-infinite horizon NMPC with a changing steady state is ISS. □

Note that it would also be possible to simply choose the minimum c_f over all steady states, in order to have one terminal region that is always valid, however this may lead to conservative performance.

4.5 Distillation example with changing steady states

Here we consider the simulation of the distillation system from Section 4.3.3 under multiple setpoint changes. As described in Section 4.4, we find the nonlinear bounds parameters M and q such that they hold for all steady states considered.

4.5.1 Terminal Region Calculations

We simulate multiple setpoint transitions, with setpoints calculated from the economic steady state problem for differing nominal feed compositions. The nonlinearity bound, terminal cost, and terminal region must then be calculated for each setpoint at minimum economic cost. To weight the terminal cost we set $\rho_\psi = 100$. The nonlinearity bound in all cases is nearly identical to that found in Figure 4.10, which gives $q = 1.8$ and $M = 0.0743$

Table 4.7: Terminal Region Results

Setpt #	Feed Comp	$\sigma_{A_K}^{max}$	λ_W^{max}	λ_W^{min}	c_f	c_u
1	0.4, 0.2, 0.4	0.910	24.62	10	0.43	0.41
2	0.4, 0.4, 0.2	0.913	27.94	10	0.36	0.37
3	0.2, 0.4, 0.4	0.898	24.38	10	0.51	0.38

as holding for all steady states. The differences are in the LQR control computed from the linearization at each setpoint, and the region which satisfies control constraints $|z_N| \leq c_u$, where c_u is chosen to be the largest value that ensures ensure $-Kz_N \in \mathbb{U}$. For this example, we only consider the lower bounds of zero for each control. The parameter c_f is calculated as in (4.16), and smaller of c_f and c_u is chosen to define the terminal region, so that $c_f := min\ \{c_f, c_u\}$. A summary of the terminal region calculations for each setpoint for different feed compositions is shown in Table 4.7.

4.5.2 Simulations

The distillation column is simulation with setpoints given at $k = 0, 50, 100$ in the order shown in Table 4.7. Since M and q are held constant, the computations to update terminal conditions are trivial. We compare the cases of $N = 25$ with an endpoint constraint (2.21), $N = 15$ with a terminal region and cost (3.1), and $N = 10$ with a terminal region and cost. In Figure 4.13, results are shown for the nominal case (no uncertainty). In Figure 4.14, results are shown for the case with 10% variance in the feed flow and composition. As can be seen, the tracking performances are similar in all cases. There is slight degradation in the tracking performance at around $k = 30$ for $N = 10$, which corresponds to a nonzero slack on the terminal constraint (10^{-4}), which indicates that the feasibility assumption

Table 4.8: Average solve times for distillation system (s)

Case	Nominal	w/ uncertainty
N=25, endpt	154.7	157.3
N=15, term con	74.9	72.4
N=10, term con	40.2	35.7

does not hold, and $N = 10$ is too short. However, the case with $N = 15$ behaves nearly identically to the case with $N = 25$, which shows the value of terminal conditions. Note that the problem with an endpoint and a shorter horizon ($N = 15$ or $N = 10$) is infeasible. Average solve times for each case are shown in Table 4.8. As can be seen, shorter horizons lead to much faster solve times.

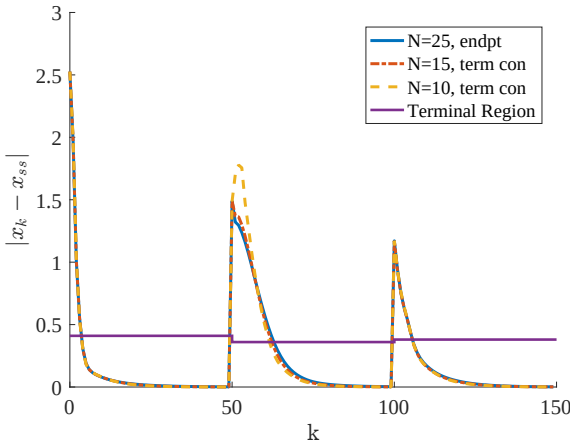

Figure 4.13: Distillation system with changing steady states, nominal

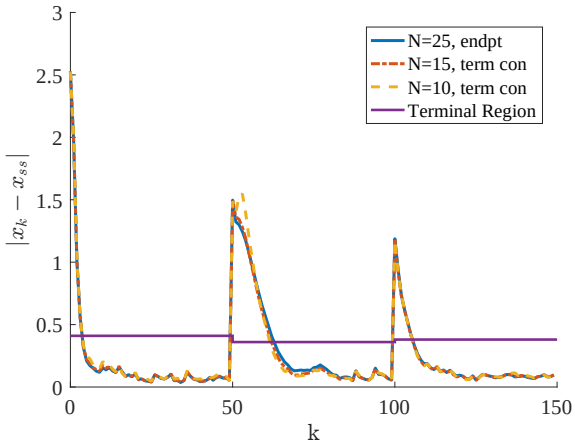

Figure 4.14: Distillation system with changing steady states, noise in feed

4.6 Conclusions

This section has shown a quasi-infinite horizon approach to calculating terminal costs and regions for NMPC that scales to systems with many states. Applications to particular systems were shown with a focus on the effects of tuning parameters. With this, it is possible to formulate valid terminal conditions for practical applications that will allow for reachability analysis and potentially shorter horizons. This is a significant advance in NMPC technology, since formulations with no terminal constraints (2.17) are used in real applications. Further, considerations were shown for the case with changing steady-states and online updates of terminal conditions. In Chapter 6, the properties of the terminal conditions derived from the quasi-infinite horizon framework will be leveraged in order to adaptively update horizon lengths online.

Chapter 5

Economic NMPC for Non-dissipative Systems

5.1 Introduction

Standard stability and robustness analysis tools need to be modified when general (economic) cost functions are used in MPC formulations. Asymptotic stability for economic MPC (eMPC) can be established for systems that satisfy strict dissipativity [13, 48, 75]. In such formulations, strict dissipativity requires the existence of a storage function which can be naturally obtained in certain types of physical systems (e.g., mechanical or energy systems) or that can be obtained if strong duality of the equilibrium point holds. Stability of economic MPC can also be guaranteed if the system satisfies the so-called turnpike property [76, 77], even in the absence of terminal constraints [43, 78]. Furthermore, it has been shown that dissipativity and turnpike properties are closely related [79]. We highlight that dissipativity and turnpike properties currently used in economic MPC are system-specific properties. Consequently, they cannot be guaranteed in general applications and can be difficult to check in practice. This is the case, for instance, in large-scale chemical processes such as polymer plants, separation systems, and pulp and paper plants [80, 81, 82, 83]. To enable asymptotic stability in a more general setting, it is possible to regularize the economic cost function to make it strongly convex (e.g., by adding a tracking cost term) [84, 85], including in cases with a cyclic steady state [86]. Regularization terms, however,

are difficult to tune and can be conservative, limiting economic gains [87].

In [88] it is proposed to replace the regularization term with a stabilizing inequality constraint. The stabilizing constraint is derived by exploiting the inherent robustness margin of an auxiliary and asymptotically stable MPC controller. It is demonstrated that this approach (that which we call eMPC-sc) provides high flexibility to optimize economic performance while retaining stability. Moreover, it is shown that this approach is a special type of regularization-based and Lyapunov-based MPC approaches. In particular, eNMPC-sc provides adaptive regularization through the constraint (as in trust-region schemes used in optimization). The eNMPC-sc controller also differs from the Lyapunov-based approach (see [89]) in that feasibility of the stabilizing constraint can be guaranteed directly, while in the Lyapunov approach the feasible set for the states needs to be adjusted to ensure feasibility. A formulation for the tracking NMPC case with uncertainty with a similar stabilizing constraint is provided in [90]. A closely related formulation is shown in [91], with the main difference being that we avoid explicitly deriving a weighting function. In this work, we analyze the robustness properties of eNMPC-sc, and show that the resulting closed-loop system is (ISpS). We present small and large-scale studies to demonstrate the applicability of the approach.

5.2 Regularized eNMPC Formulations

We now proceed to describe economic NMPC formulations. We define (x_{ss}, u_{ss}) as the solution of the steady-state problem:

$$(x_{ss}, u_{ss}) := \underset{x,u}{\text{argmin}} \;\; L^{ec}(x,u) \tag{5.1a}$$

$$\text{s.t.} \;\; x = f(x,u) \tag{5.1b}$$

$$x \in \mathbb{X}, \; u \in \mathbb{U} \tag{5.1c}$$

where the mapping $L^{ec} : \mathbb{R}^{n_x} \times \mathbb{R}^{n_u} \to \mathbb{R}$ is the economic stage cost. We assume, without loss of generality, that $(x_{ss}, u_{ss}) = (0, 0)$. The NLP solved by a standard economic NMPC (eNMPC) controller is:

$$\min_{z_i, v_i} \sum_{i \in \mathcal{N}} L^{ec}(z_i, v_i) \tag{5.2a}$$

$$\text{s.t. } z_{i+1} = f(z_i, v_i) \ \ \forall\, i \in \mathcal{N} \tag{5.2b}$$

$$z_0 = x_k \tag{5.2c}$$

$$z_i \in \mathbb{X},\ v_i \in \mathbb{U} \ \ \forall\, i \in \mathcal{N} \tag{5.2d}$$

$$z_N = 0 \tag{5.2e}$$

which includes an endpoint constraint for simplicity. Of course we expect better economic performance from this formulation compared to tracking NMPC but asymptotic stability of eNMPC is not guaranteed in general. This is because Assumption 22 (A) is not fulfilled for general $L^{ec}(\cdot, \cdot)$. Stability of eNMPC can be enforced by appending a tracking term that regularizes the economic objective. Under this approach, the regularized eNMPC problem is:

$$\min_{z_i, v_i} \sum_{i \in \mathcal{N}} (L^{ec}(z_i, v_i) + \omega L^{tr}(z_i, v_i)) \tag{5.3a}$$

$$\text{s.t. } z_{i+1} = f(z_i, v_i) \ \ \forall\, i \in \mathcal{N} \tag{5.3b}$$

$$z_0 = x_k \tag{5.3c}$$

$$z_i \in \mathbb{X},\ v_i \in \mathbb{U} \ \ \forall\, i \in \mathcal{N} \tag{5.3d}$$

$$z_N = 0 \tag{5.3e}$$

where $\omega \in \mathbb{R}_+$. We define the rotated stage cost $L^{rot}(x, u) := L^{ec}(x, u) + \omega L^{tr}(x, u) + \lambda(x) - \lambda(f(x, u)))$, where $\lambda : \mathbb{R}^{n_x} \to \mathbb{R}$ is a storage function. One choice for λ is to use the Lagrange multipliers of (5.1), so that $\lambda(x) - \lambda(f(x, u)) = \nu^T(x - f(x, u))$ is locally

nonnegative. We denote this approach as eNMPC-reg.

Definition 31. *The system* (2.2) *is strictly dissipative with respect to supply rate* $L^{ec}(z_i, v_i) + \omega L^{tr}(z_i, v_i)$ *if there exists some* $\alpha \in \mathcal{K}_\infty$ *such that* $L^{rot}(x, u) \geq \alpha(|x|) \; \forall \; x \in \mathbb{R}^{n_x}$

As shown in [13, 48], if strict dissipativity holds, then eNMPC-reg is asymptotically stable. In the case of [48], it is shown that strict dissipativity holds if the steady-state problem (5.1) satisfies strong duality. When $L^{tr}(\cdot)$ is quadratic, weighting matrices Q and R in (2.20) can be found by applying the Gershgorin circle theorem to the Hessian of the rotated stage cost $\nabla^2 L^r(x, u)$, as is done in [84, 87]. Unfortunately, finding and tuning weighting matrices is cumbersome for large problems. In particular, for a general NLP, $\nabla^2 L^r(x, u)$ must be checked at every $x \in \mathcal{X}$ and $u \in \mathbb{U}$ of (5.1) in order to ensure that the Hessian is always positive definite. Furthermore, the end result is often conservative in the sense that the regularization term may dominate the economic stage cost, thus limiting economic performance.

Note that the robustness analysis shown in Section 3.2 extends trivially to eNMPC-reg.

5.3 eNMPC-sc Formulation

It has been recently suggested to replace the tracking regularization terms in the objective with a stabilizing constraint [88]. This controller solves the NLP:

$$\min_{z_i, v_i} \quad \sum_{i \in \mathcal{N}} L^{ec}(z_i, v_i) \tag{5.4a}$$

$$\text{s.t.} \;\; z_{i+1} = f(z_i, v_i) \;\; \forall \; i \in \mathcal{N} \tag{5.4b}$$

$$z_0 = x_k \tag{5.4c}$$

$$z_i \in \mathbb{X}, \; v_i \in \mathbb{U} \;\; \forall \; i \in \mathcal{N} \tag{5.4d}$$

$$z_N = 0 \tag{5.4e}$$

$$\sum_{i\in\mathcal{N}} L^{tr}(z_i, v_i) - V(k-1, \mathbf{w}_{k-1}, x_0)$$
$$\leq -\delta\, L^{tr}(x_{k-1}, u_{k-1}) \tag{5.4f}$$

where $\delta \in (0, 1]$ is a scalar parameter. After the NLP is solved, we inject the control law $u(x_k) = v_0$ into the system and set

$$V(k, \mathbf{w}_k, x_0) := \sum_{i\in\mathcal{N}} L^{tr}(z_i^k, v_i^k), \tag{5.5}$$

where z_i^k, v_i^k is the solution of (5.4) at time k. We thus note that $V(k-1, \mathbf{w}_{k-1}, x_0)$ is the value function at time $k-1$.

Once the control is injected into the system we wait for it to evolve to x_{k+1} and use the value function $V(k, \mathbf{w}_k, x_0)$ in (5.4f) to solve (5.4) at x_{k+1}, and repeat the procedure. Note that, for the problem solved at time $k = 0$, the constraint (5.4f) may simply be excluded. Also, the formulation of the stabilizing constraint (5.4f) is slightly different from that used in [88]. The advantages of this formulation are that we do not require a solution to the tracking problem, and this formulation provides a looser constraint with the same stability properties.

We will prove that under this recursion the constraint (5.4f) forces the descent of $V(k, \mathbf{w}_k, x_0)$ explicitly. We also note that the value function $V(k, \mathbf{w}_k, x_0)$ is a function of the path since the solution of (5.4) depends on the previous value function. In Section 5.4.2 we will prove that, despite this, the value function is a Lyapunov function satisfying the properties of Theorem 32 and thus the system under eNMPC-sc is ISpS. We also note that $\delta = 1$ in (5.4f) corresponds to the most constrained Lyapunov function, and δ approaching zero corresponds to the least constrained. The parameter δ is thus a tuning parameter that shapes closed-loop behavior. A large δ forces a faster approach to the steady state, and small δ allows for more economic flexibility.

We highlight that $V(k-1, \mathbf{w}_{k-1}, x_0)$ and $L^{tr}(x_{k-1}, u_{k-1})$ are fixed quantities in the NLP and thus the stabilizing constraint (5.4f) can be written as $\sum_{i\in\mathcal{N}} L^{tr}(z_i, v_i) \leq \Delta_k$ with $\Delta_k := V(k-1, \mathbf{w}_{k-1}, x_0) - \delta\, L^{tr}(x_{k-1}, u_{k-1})$. If we consider positive definite matrices Q and R, we have that $L^{tr}(z, v) = z^T Q z + v^T R v$ and the stabilizing constraint satisfies $\sum_{i\in\mathcal{N}}(z_i^T Q z_i + v_i^T R v_i) \leq \Delta_k$ and thus defines a trust-region constraint with radius Δ_k around the origin $(0, 0)$. This trust region defines a space that the controller can explore at time instant k to improve economic performance while preserving stability. Moreover, by dualizing the stabilizing constraint we can obtain formulation (5.3). Consequently, we can see that the stabilizing constraint acts as a regularization term. The weight ω, however, is determined by the optimal Lagrange multiplier of (5.4f) and thus changes at each time instant k (i.e., the weight is adaptive). The Lagrange multiplier can be interpreted as the *price of stability*. We highlight that this approach does not require dissipativity with respect to stage costs appearing in the objective (i.e. Definition 31 with $\omega = 0$) or turnpike properties, which contrasts with existing economic NMPC formulations [48, 76]. Because of this, the approach has wider applicability. For instance, because this approach does not require strong duality, any equilibrium point (x_{ss}, u_{ss}) can be used. For more details, see [88].

To establish ISpS for the proposed economic NMPC controller we must ensure uniform continuity of the value function. This property is not guaranteed for the formulation (5.4). This can be achieved by softening the state constraints, as is done in [92]. To do this, we assume that $\mathbb{X}$ and $\mathbb{U}$ are expressed as constraints of the form $\mathbb{X} = \{x : g_x(x) \leq 0\}$ and $\mathbb{U} = \{u : g_u(u) \leq 0\}$. The eNMPC-sc problem is thus:

$$\min_{z_i, v_i} \quad \sum_{i\in\mathcal{N}} L^{ec}(z_i, v_i) + \rho\left(\sum_{i\in\mathcal{N}} \xi_i^x + \xi^S + \xi^{ss,L} + \xi^{ss,U}\right) \tag{5.6a}$$

$$\text{s.t.} \quad z_{i+1} = f(z_i, v_i) \;\; \forall\, i \in \mathcal{N} \tag{5.6b}$$

$$z_0 = x_k \tag{5.6c}$$

$$g_x(z_i) \leq \xi_i^x \ \ \forall\, i \in \mathcal{N} \tag{5.6d}$$

$$g_u(v_i) \leq 0 \ \ \forall\, i \in \mathcal{N} \tag{5.6e}$$

$$-\xi^{ss,L} \leq z_N \leq \xi^{ss,U} \tag{5.6f}$$

$$\sum_{i \in \mathcal{N}} L^{tr}(z_i, v_i) - V(k-1, \mathbf{w}_{k-1}, x_0) \leq -\delta\, L^{tr}(x_{k-1}, u_{k-1}) + \xi^S \tag{5.6g}$$

$$\xi_i^x, \xi^S, \xi^{ss,L}, \xi^{ss,U} \geq 0 \tag{5.6h}$$

where $\xi_i^x, \xi^S, \xi^{ss,L}, \xi^{ss,U}$ are slack variables and $\rho \in \mathbb{R}_+$ is a penalty parameter. Finding a value for ρ for the formulations used in this paper is discussed in Remark 56. Constraint softening allows us to leverage the following properties.

5.4 Stability Analysis

5.4.1 ISpS with a Modified Lyapunov Function

We use the ISpS Lyapunov theorem of [36] with a modified Lyapunov function. Traditionally, the Lyapunov function is a function of the current state, $V : \mathbb{R}^n \to \mathbb{R}$. In this work, we analyze our proposed eNMPC-sc controller using a modified Lyapunov function that is a function of the path, $V : \mathbb{Z}_{\geq 0, \leq K} \times \mathbb{R}^{n_w \times K} \times \mathbb{R}^{n_x} \to \mathbb{R}$ where the first argument is the time step, the second argument is the series of disturbances, and the third argument is the initial state. We first show that the modified Lyapunov function satisfies the ISpS properties established in [36]. This is formalized in the following result.

Theorem 32. *Let Assumption 1 hold. If the system* (2.2) *admits a function* $V(k, \mathbf{w}_k, x_0)$ *satisfy-*

ing:

$$\alpha_1(|x_k|) \leq V(k, \mathbf{w}_k, x_0) \leq \alpha_2(|x_k|) + c_1 \tag{5.7a}$$

$$\begin{aligned} &V(k+1, \mathbf{w}_{k+1}, x_0) - V(k, \mathbf{w}_k, x_0) \\ &\leq -\alpha_3(|x_k|) + \sigma(|w_k|) + c_2 \end{aligned} \tag{5.7b}$$

$$\forall \ x_0 \in \mathcal{X}, \ \mathbf{w} \in \mathcal{W}, \ k \in \mathbb{Z}_+$$

where $\alpha_1, \alpha_2, \alpha_3 \in \mathcal{K}_\infty$, $\sigma \in \mathcal{K}$, and $c_1, c_2 \in \mathbb{R}_+$ then the system is ISpS.

Lemma 33. *For a function $V(k, \mathbf{w}_k, x_0)$ satisfying (5.7), there exists $\alpha_4(\cdot) \in \mathcal{K}_\infty$ such that*

$$\alpha_3(|x_k|) \geq \alpha_4(V(k, \mathbf{w}_k, x_0)) - \bar{c} \tag{5.8}$$

$$\forall \ x_0 \in \mathcal{X}, \ \mathbf{w} \in \mathcal{W}, \ k \in \mathbb{Z}_+$$

for some $\bar{c} \in \mathbb{R}_+$.

Given $V(k, \mathbf{w}_k, x_0)$ and its upper bound, we can find a lower bound of $|x_k|$:

$$|x_k| \geq \begin{cases} \alpha_2^{-1}(V(k, \mathbf{w}_k, x_0) - c_1) \\ \qquad \forall \ V(k, \mathbf{w}_k, x_0) \geq c_1 \\ 0 \ \ \forall \ V(k, \mathbf{w}_k, x_0) < c_1 \end{cases} \tag{5.9a}$$

$$\Rightarrow \alpha_3(|x_k|) \geq \begin{cases} \alpha_3 \circ \alpha_2^{-1}(V(k, \mathbf{w}_k, x_0) - c_1) \\ \qquad \forall \ V(k, \mathbf{w}_k, x_0) \geq c_1 \\ 0 \ \ \forall \ V(k, \mathbf{w}_k, x_0) < c_1 \end{cases} \tag{5.9b}$$

$$\geq \begin{cases} \alpha_3 \circ \alpha_2^{-1}(V(k, \mathbf{w}_k, x_0) - c_1) \\ \qquad \forall \ V(k, \mathbf{w}_k, x_0) \geq c_1 \\ (\alpha_3 \circ \alpha_2^{-1}(c_1)/c_1) V(k, \mathbf{w}_k, x_0) - \alpha_3 \circ \alpha_2^{-1}(c_1) \\ \qquad \forall \ V(k, \mathbf{w}_k, x_0) < c_1 \end{cases} \tag{5.9c}$$

$$=: \alpha_4(V(k, \mathbf{w}_k, x_0)) - \alpha_3 \circ \alpha_2^{-1}(c_1) \tag{5.9d}$$

Then set

$$\alpha_4(V(k,\mathbf{w}_k,x_0)) := \begin{cases} \alpha_3\circ\alpha_2^{-1}(V(k,\mathbf{w}_k,x_0)-c_1)+\alpha_3\circ\alpha_2^{-1}(c_1) \\ \qquad\qquad \forall\, V(k,\mathbf{w}_k,x_0)\geq c_1 \\ (\alpha_3\circ\alpha_2^{-1}(c_1)/c_1)V(k,\mathbf{w}_k,x_0) \\ \qquad\qquad \forall\, V(k,\mathbf{w}_k,x_0)< c_1 \end{cases} \tag{5.10}$$

and set

$$\bar{c} := \alpha_3\circ\alpha_2^{-1}(c_1) \tag{5.11}$$

□

Lemma 34. *For every $\hat{\beta}\in\mathcal{KL}$ and $\hat{c}\in\mathbb{R}_+$, there exists some $\beta\in\mathcal{KL}$ and $\tilde{c}\in\mathbb{R}_+$ such that:*

$$\hat{\beta}(s+\hat{c},k)\leq\beta(s,k)+\tilde{c}\ \ \forall\, s\in\mathbb{R}_+,\ k\in\mathbb{Z}_+ \tag{5.12}$$

Proof. Consider $\tilde{c}=\hat{\beta}(\hat{c},0)$ and any $\bar{\beta}\in\mathcal{KL}$. Then let:

$$\beta(s,k) = \begin{cases} \hat{\beta}(s+\hat{c},k)-\tilde{c}+\bar{\beta}(s,k) \\ \qquad \forall\, s\in\mathbb{R}_+,\ k\in\mathbb{Z}_+ \text{ s.t. } \hat{\beta}(s+\hat{c},k)-\tilde{c}\geq 0 \\ \bar{\beta}(s,k) \\ \quad \forall\, s\in\mathbb{R}_+,\ k\in\mathbb{Z}_+ \text{ s.t. } \hat{\beta}(s+\hat{c},k)-\tilde{c}< 0 \end{cases} \tag{5.13}$$

Then $\beta(s,k)$ clearly gives an upper bound to $\hat{\beta}(s+\hat{c},k)-\tilde{c}$, but to see that $\beta\in\mathcal{KL}$, consider more closely the expression $\hat{\beta}(s+\hat{c},k)-\tilde{c}$. For constant k, $\hat{\beta}(s+\hat{c},k)-\tilde{c}$ is a $\mathcal{K}_\infty$ function minus a positive constant. Thus, the regions such that $\hat{\beta}(s+\hat{c},k)-\tilde{c}\geq 0$ and $\hat{\beta}(s+\hat{c},k)-\tilde{c}<0$ are described by intervals $s\in[r,\infty)$ and $s\in[0,r)$, respectively, for some $r\in\mathbb{R}_+$. Thus $\beta(0,k)=0$, and $\beta(s,k)$ is continuous and strictly increasing with respect to

s. A similar observation holds for constant s. Now, the regions such that $\hat{\beta}(s+\hat{c},k)-\tilde{c}\geq 0$ and $\hat{\beta}(s+\hat{c},k)-\tilde{c}<0$ are described by intervals $k\leq p$ and $k>p$, respectively, for some $p\in\mathbb{Z}_+$. Thus $\beta(s,k)$ is strictly decreasing with respect to k. Therefore, $\beta\in\mathcal{KL}$. □

Proof of Theorem 32. We denote id as the identity function, and the notation $\alpha_1\circ\alpha_2(\cdot)$ denotes $\alpha_1(\alpha_2(\cdot))$. Define the functions $\rho(\cdot)$ and $\hat{\alpha}_4(\cdot)$ to have the following properties: $\hat{\alpha}_4\in\mathcal{K}_\infty$, $\hat{\alpha}_4(s)\leq\alpha_4(s)\ \ \forall\ s$, $id-\hat{\alpha}_4(\cdot)\in\mathcal{K}_\infty$, $\rho(\cdot)\in\mathcal{K}_\infty$, and $id-\rho(\cdot)\in\mathcal{K}_\infty$. See Lemma B.1 of [35] for a proof that $\hat{\alpha}_4(\cdot)$ exists.

We now proceed by showing that β, γ, and c exist satisfying ISpS. Our proof follows along the lines of Lemma 3.5 in [35]. Define the constant $b:=\hat{\alpha}_4^{-1}\circ\rho^{-1}(\sigma(||\mathbf{w}||)+\bar{c}+c_2)$ with $\bar{c}$ defined in Lemma 33 and consider the set $D=\{x:V(x)\leq b\}$. If $x_k\in\mathcal{X}\cap D$ then we have from (5.7b), Lemma 33, and the definition of b that:

$$
\begin{aligned}
&V(k+1,\mathbf{w}_{k+1},x_0)\\
&\leq V(k,\mathbf{w}_k,x_0)-\alpha_3(|x_k|)+\sigma(||\mathbf{w}||)+c_2 && \text{(5.14a)}\\
&\leq V(k,\mathbf{w}_k,x_0)-\alpha_4(V(k,\mathbf{w}_k,x_0))\\
&\qquad +\bar{c}+\sigma(||\mathbf{w}||)+c_2 && \text{(5.14b)}\\
&\leq V(k,\mathbf{w}_k,x_0)-\hat{\alpha}_4\circ V(k,\mathbf{w}_k,x_0)\\
&\qquad +\bar{c}+\sigma(||\mathbf{w}||)+c_2 && \text{(5.14c)}\\
&=(id-\hat{\alpha}_4)\circ V(k,\mathbf{w}_k,x_0)+\bar{c}+\sigma(||\mathbf{w}||)+c_2 && \text{(5.14d)}\\
&\leq (id-\hat{\alpha}_4)\circ b+\bar{c}+\sigma(||\mathbf{w}||)+c_2 && \text{(5.14e)}\\
&=(id-\hat{\alpha}_4)\circ b+\rho\circ\hat{\alpha}_4(b) && \text{(5.14f)}\\
&=-(id-\rho)\circ\hat{\alpha}_4(b)+b && \text{(5.14g)}\\
&\leq b. && \text{(5.14h)}
\end{aligned}
$$

This holds for all $x_k\in D\cap\mathcal{X},\ \mathbf{w}\in\mathcal{W}$. Consequently, the set D is positive invariant. So,

set:

$$\gamma(||\mathbf{w}_k||) = \alpha_1^{-1} \circ \hat{\alpha}_4^{-1} \circ \rho^{-1}(\sigma(||\mathbf{w}||) + \bar{c} + c_2)$$
$$-\alpha_1^{-1} \circ \hat{\alpha}_4^{-1} \circ \rho^{-1}(\bar{c} + c_2) \tag{5.15}$$

and

$$c_3 = \alpha_1^{-1} \circ \hat{\alpha}_4^{-1} \circ \rho^{-1}(\bar{c} + c_2) \tag{5.16}$$

so that

$$\gamma(||\mathbf{w}_k||) + c_3 = \alpha_1^{-1}(b) \tag{5.17}$$

Note here that c_3 is a $\mathcal{K}_\infty$ function of $c_1 + c_2$, since $\bar{c}$ is a $\mathcal{K}_\infty$ function of c_1. Then, for all $x_{k_0} \in D$, we have:

$$\alpha_1(|x_k|) \leq V(k, \mathbf{w}_k, x_0) \leq b \;\; \forall\, k \geq k_0 \tag{5.18}$$
$$\Rightarrow \quad |x_k| \leq \gamma(||\mathbf{w}_k||) + c_3 \;\; \forall\, k \geq k_0 \tag{5.19}$$

Now consider $x_k \in \mathcal{X}$, $x_k \notin D$. Again, from (5.7b), Lemma 33, and the definition of b:

$$V(k+1, \mathbf{w}_{k+1}, x_0) - V(k, \mathbf{w}_k, x_0)$$
$$\leq -\alpha_3(|x_k|) + \sigma(||\mathbf{w}||) + c_2 \tag{5.20a}$$
$$\leq -\alpha_4(V(k, \mathbf{w}_k, x_0)) + \bar{c} + \sigma(||\mathbf{w}||) + c_2 \tag{5.20b}$$
$$\leq -\hat{\alpha}_4 \circ V(k, \mathbf{w}_k, x_0) + \bar{c} + \sigma(||\mathbf{w}||) + c_2 \tag{5.20c}$$
$$= -\hat{\alpha}_4 \circ V(k, \mathbf{w}_k, x_0) + \rho \circ \hat{\alpha}_4 \circ V(k, \mathbf{w}_k, x_0)$$
$$+\bar{c} + \sigma(||\mathbf{w}||) + c_2 - \rho \circ \hat{\alpha}_4 \circ V(k, \mathbf{w}_k, x_0) \tag{5.20d}$$
$$\leq -\hat{\alpha}_4 \circ V(k, \mathbf{w}_k, x_0) + \rho \circ \hat{\alpha}_4 \circ V(k, \mathbf{w}_k, x_0) \tag{5.20e}$$
$$= -(id - \rho) \circ \hat{\alpha}_4 \circ V(k, \mathbf{w}_k, x_0) \tag{5.20f}$$

$$\Rightarrow V(k+1, \mathbf{w}_{k+1}, x_0)$$
$$\leq (id - (id - \rho) \circ \hat{\alpha}_4) \circ V(k, \mathbf{w}_k, x_0) \tag{5.20g}$$
$$\forall\ x_k \notin D,\ x_k \in X,\ \mathbf{w} \in \mathcal{W}$$

Then by Lemma 4.3 of [93], there exists some $\hat{\beta} \in \mathcal{KL}$ such that:

$$V(k, \mathbf{w}_k, x_0) \leq \hat{\beta}(V(0, \mathbf{w}_0, x_0), k) \tag{5.21a}$$
$$\Rightarrow |x_k| \leq \alpha_1^{-1}(\hat{\beta}(\alpha_2(|x_0|) + c_1, k)) \tag{5.21b}$$
$$\forall\ x_k \notin D,\ x_k \in \mathcal{X},\ \mathbf{w} \in \mathcal{W}$$

and by Lemma 34, there exists some $\beta \in \mathcal{KL}$ and $c_4 \in \mathbb{R}_+$ such that:

$$|x_k| \leq \beta(|x_0|, k) + c_4 \tag{5.22}$$
$$\forall\ x_k \notin D,\ x_k \in \mathcal{X},\ \mathbf{w} \in \mathcal{W}$$

Note that, by Lemma 34, c_4 is a $\mathcal{K}_\infty$ function of c_1. Finally, add (5.22) and (5.19) together to see that

$$|x_k| \leq \beta(|x_0|, k) + \gamma(||\mathbf{w}||) + c_3 + c_4 \tag{5.23}$$
$$\forall\ \ x_0 \in \mathcal{X},\ \mathbf{w} \in \mathcal{W},\ k \in \mathbb{Z}_+$$

so ISpS is satisfied with $c = c_3 + c_4$ by Definition 12, and c is a $\mathcal{K}_\infty$ function of $c_1 + c_2$. □

As can be seen, the constants c_1, c_2 used in the Lyapunov function definition (5.7) relax the upper bound and the descent conditions of the traditional Lyapunov function used to enforce the more stringent ISS conditions. Consequently, we highlight that ISS is recovered for the special case in which $c_1 = c_2 = 0$.

5.4.2 Properties of eNMPC-sc

In this section we discuss properties of the eNMPC-sc formulation, leading up to our main robustness result. In particular, we will prove that the value function $V(k, \mathbf{w}_k, x_0)$ generated by the eNMPC-sc controller is a Lyapunov function satisfying the properties of Theorem 32 and thus the system under eNMPC-sc is ISpS.

Assumption 35. *(A) The set $\mathbb{W}$ is bounded (i.e., $||\mathbf{w}||$ is bounded) and contains zero in its interior. (B) There exists a solution to (5.6) with $z_N = 0 \; \forall \;\; x_0 \in \mathcal{X},\; \mathbf{w} \in \mathcal{W},\; k \in \mathbb{Z}_+$ if $w_{k-1} = 0$. (C) The penalty parameter ρ of (5.6) is chosen sufficiently large so that $\xi^{ss,L}$, $\xi^{ss,U}$, and ξ^S are zero at the solution of* (5.6) *$\forall \;\; x_0 \in \mathcal{X},\; \mathbf{w} \in \mathcal{W},\; k \in \mathbb{Z}_+$ if $w_{k-1} = 0$. (D) The functions $g_x(\cdot)$, $g_u(\cdot)$, $L^{tr}(\cdot,\cdot)$, $L^{ec}(\cdot,\cdot)$, and $f(\cdot,\cdot,\cdot)$ are twice continuously differentiable. (E) The set $\mathbb{U}$ is convex and compact. (F) The GSSOSC is always satisfied at the solution of* (5.6). *(G) There exists $\alpha_1 \in \mathcal{K}_\infty$ such that $L^{tr}(x,u) \geq \alpha_1(|x|)$ for all $x \in \mathbb{R}^{n_x},\; u \in \mathbb{U}^{n_u}$*

Note that Assumption 35G cannot be relaxed to strict dissipativity since using a rotated version of L^{tr} in (5.6g) is not necessarily equivalent, in contrast to the regularized case where stage costs are always considered in the objective and optimizing a dissipative stage cost is equivalent to optimizing its rotated counterpart.

Lemma 36. *Under Assumption 35, there exists a solution to (5.6) with $\xi^S = 0$ for all $k = 1 \dots K-1$, every $x_0 \in \mathcal{X}$, and every admissible $\mathbf{w}_k \in \mathcal{W}$ if $w_{k-1} = 0$.*

Proof. Consider the solution to (5.6) computed at $k-1$, $\{z_0^{k-1}, z_1^{k-1}, \dots, z_N^{k-1}, v_0^{k-1}, v_1^{k-1}, \dots, v_{N-1}^{k-1}\}$, and assume $w_{k-1} = 0$. Then the shifted solution $\{z_1^{k-1}, z_2^{k-1}, \dots, z_N^{k-1}, 0, v_1^{k-1}, v_2^{k-1}, \dots, v_{N-1}^{k-1}, 0\}$ provides a feasible solution to (5.6) solved at time k, since $x_k = z_1^{k-1}$. Furthermore, this solution is feasible with $\xi^S = 0$ since $L^{tr}(z_1^{k-1}, v_1^{k-1}) + L^{tr}(z_2^{k-1}, v_2^{k-1}) + \dots + L^{tr}(z_{N-1}^{k-1}, v_{N-1}^{k-1}) - \sum_{i \in \mathcal{N}} L^{tr}(z_i^{k-1}, v_i^{k-1}) = -L^{tr}(x_{k-1}, u_{k-1})$. $\square$

Remark 37. *Note that a penalty parameter ρ exists to satisfy Assumption 35 C when the MFCQ and GSSOSC are satisfied. Choosing ρ larger than the appropriate norm of the multipliers of the solution of problem (5.4) is sufficient to satisfy Assumption 35 C. Whether Assumption 35C holds can be assessed through off-line simulation of* (5.6)*, which includes checking for finite-time reachability of x_{ss}.*

Remark 38. *$\xi^S = 0$ is only required in the nominal case. In the case with uncertainty, ξ^S relates to $\sigma(|w_k|)$ in (5.7b); that is, $\sigma(|w_k|)$ gives an upper bound to ξ^S. Thus, ξ^S may be nonzero, but is bounded because $\sigma(|w_k|)$ and $||\mathbf{w}||$ are bounded.*

Remark 39. *Note that $x_k \in \mathbb{X}\ \forall\ k = 1 \dots K$ is only guaranteed if $x_0 \in \mathbb{X}$, $w_k = 0\ \forall\ k = 0 \dots K-1$, a solution always exists to (5.4), and ρ is chosen large enough to force the solutions to (5.4) and (5.6) to be equivalent.*

In order to show that the controller is ISpS, we first show that the Lyapunov function is uniformly continuous with respect to disturbances.

Lemma 40. *Under Assumption 35, the NLP (5.6) satisfies the MFCQ.*

Proof. The proof of Lemma 40 is nearly the same as that of Lemma 27, except with an additional constraint of the following form:

$$g(z_0, v_0, z_1.v_1, \dots, z_{N-1}, v_{N-1}, z_N) \leq 0 \tag{5.24}$$

with the linearization

$$G_z^J d_z + G_v^J d_v \leq 0 \tag{5.25}$$

and the matrices

$$G_z^J = \begin{bmatrix} G_z^{j_0} & G_z^{j_1} & \dots & G_z^{j_{N-1}} & G_z^{j_N} \end{bmatrix} \tag{5.26a}$$

$$G_v^J = \begin{bmatrix} G_v^{j_0} & G_v^{j_1} & \dots & G_v^{j_{N-1}} & 0 \end{bmatrix} \tag{5.26b}$$

and the relaxation at the optimum:

$$G_z^J d_z + G_v^J d_v - E_{J,s} d_{\xi,s} \leq 0, \quad d_{\xi,s} \geq 0 \tag{5.27}$$

which leads to

$$\nabla g_J^T = \begin{bmatrix} G_z^J & G_v^J & -E_{J,s} & 0 \\ 0 & 0 & -I & 0 \\ G_{x,z}^J & 0 & 0 & -E_J \\ 0 & 0 & 0 & -I \\ 0 & G_{u,v}^J & 0 & 0 \end{bmatrix} \tag{5.28}$$

in place of (3.7). Set the search direction $q^T = [d_z^T \mid d_v^T \mid d_{\xi,s}^T \mid d_\xi^T]$, and choose $d_{\xi,s}$ as follows:

$$E_{J,s} d_{\xi,s} > (G_v^J - G_z^J F_z^{-1} F_v) d_v^0 \tag{5.29}$$

and we see that $\nabla g_J^T q < 0$ and $\nabla c^T q = 0$ in Definition (19). Hence MFCQ is satisfied for system (5.4.2). □

Remark 41. *GSSOSC requires that the solution of the NLP satisfies the strong second order conditions for every Lagrange multiplier in the bounded set defined under MFCQ. If this does not hold, regularization to add positive curvature will be required. This can always be enforced by adding* $||\mathbf{y} - \mathbf{y}^*||_Y^2$ *to the objective of* (2.6) *after the KKT point* $\mathbf{y}^*$ *is found, with matrix* Y *sufficiently positive definite [92]. This ensures that* (5.6) *satisfies GSSOSC and does not change the solution* $\mathbf{y}^*$*. Note that the stabilizing constraint of eNMPC-sc can help induce positive curvature if the tracking stage cost is quadratic.*

5.4.3 ISpS of eNMPC-sc

We now prove our main result: that the dynamic system under the eNMPC-sc controller is ISpS.

Theorem 42. *If Assumptions 2 and 35 hold, there exists* $\alpha_1, \alpha_2, \alpha_3 \in \mathcal{K}_\infty$, $\sigma \in \mathcal{K}$, *and* $c_1, c_2 \in \mathbb{R}_+$ *such that* $V(k, \mathbf{w}_k, x_0)$ *satisfies* (5.7)*, and the system under eNMPC-sc is ISpS with respect to* $c = \alpha_c(\hat{u})$*, for some* $\alpha_c \in \mathcal{K}_\infty$ *for all* $x_0 \in \mathcal{X}, \mathbf{w} \in \mathcal{W}, k \in \mathbb{Z}_+$.

Proof. We assume that L^{tr} has a $\mathcal{K}_\infty$ lower bound, so that $\alpha_1(|x|) \leq L^{tr}(x, u)$, which gives a lower bound for the sum. Second, since we assume that (5.6g) holds with $\xi^S = 0$ in the nominal case, we have that $\alpha_3(|x|) = \delta\, \alpha_1(|x|)$ in (5.7). To show the upper bound of V, we must assume uniform continuity of the stage cost $L^{tr}(\cdot, \cdot)$ and of the nonlinear system $f(\cdot)$. This ensures that $L^{tr}(x, u) \leq \sigma_L(|x| + |u|)$ and $f(x, u) \leq \sigma_f(|x| + |u|)$ hold for $\sigma_L(\cdot), \sigma_f(\cdot) \in \mathcal{K}$. This allows us to establish an upper bound of the constrained sum from (5.6g) of the form:

$$
\begin{aligned}
&\sum_{i \in \mathcal{N}} L^{tr}(z_i, v_i) \\
&\leq \sigma_L(|x_k| + \hat{u}) + \sum_{i=1}^{N-1} L^{tr}(z_i, v_i) && \text{(5.30a)} \\
&\leq \sigma_L(|x_k| + \hat{u}) + \sigma_L(\sigma_f(|x_k| + \hat{u}) + \hat{u}) && \text{(5.30b)} \\
&\qquad + \sum_{i=2}^{N-1} L^{tr}(z_i, v_i) && \text{(5.30c)} \\
&\leq \sigma_L(|x_k| + \hat{u}) + \sigma_L(\sigma_f(|x_k| + \hat{u}) + \hat{u}) \\
&\qquad + \sigma_L(\sigma_f(\sigma_f(|x_k| + \hat{u}) + \hat{u}) + \hat{u}) \\
&\qquad + \sum_{i=3}^{N-1} L^{tr}(z_i, v_i) && \text{(5.30d)} \\
&=: \alpha(|x_k| + \hat{u}) && \text{(5.30e)}
\end{aligned}
$$

for some $\alpha \in \mathcal{K}_\infty$. We then have that (5.7a) holds with $\alpha_2(|x_k|) := \alpha(|x_k| + \hat{u}) - \alpha(\hat{u})$ and $c_1 := \alpha(\hat{u})$.

Next, by Assumption 35C, ρ is chosen large enough such that (5.6g) satisfies $\xi^S = 0$ in the nominal case. Then, since (5.6) satisfies MFCQ by Lemma 27, and by Assumption 35F the GSSOSC holds, we have from Lemma 26:

$$V(k+1, \mathbf{w}_{k+1}, x_0) - V(k, \mathbf{w}_k, x_0) =$$

$$V(k+1, \mathbf{w}_{k+1}, x_0) - V(k+1, (w_0, \ldots, w_{k-1}, 0), x_0)$$

$$+V(k+1, (w_0, \ldots, w_{k-1}, 0), x_0) - V(k, \mathbf{w}_k, x_0)$$

$$\leq -\alpha_3(|x_k|) + \sigma_V(|w_k|)$$

Consequently, (5.7) is satisfied and the system is ISpS with $c_1 = \alpha(\hat{u})$, where $\alpha \in \mathcal{K}_\infty$, and $c_2 = 0$. Furthermore, from the proof of Theorem 32 we have that c is a $\mathcal{K}_\infty$ function of c_1. □

Remark 43. *It is important to highlight that there exists an upper bound on c, used in the definition of ISpS, which depends on the bound $\hat{u}$.. From the proof of Theorem 32, it is clear that the constant c used in the definition of ISpS is a $\mathcal{K}_\infty$ function of c_1 which is in turn a $\mathcal{K}_\infty$ function of $\hat{u} = \max_{u \in \mathbb{U}} |u|$. Consequently, c is a $\mathcal{K}_\infty$ function of $\hat{u}$.*

5.4.4 Observations on the Nominal Case

The constant $c_1 = \alpha(\hat{u})$ (and associated c) used in the proof of Theorem 42 play a critical role in the theoretical properties of the eNMPC-sc controller and is tightly connected to weak controllability (see Assumption 1 in [48]). To see the implications of this, we make the following observations. First note that, since $c_2 = 0$, eNMPC-sc becomes ISS if $c_1 = 0$ holds (which implies that $c = 0$ holds as well). This is important because, whenever $c_1 = 0$, we have that asymptotic stability holds in the nominal case, and ISS holds in the case with

uncertainty. In general, however, we have that $c_1 > 0$ (and thus $c > 0$) holds and thus eNMPC-sc is only ISpS and not necessarily asymptotically stable in the nominal case.

The upper bound condition of the cost function (5.30d) directly relates the constant c_1 to violation of weak controllability. In particular, $c_1 > 0$ implies that the implicit control law $\mathbf{u}(x_k)$ may not satisfy $\mathbf{u}(0) = 0$, as is required for weak controllability, which can be advantageous in terms of economic performance. If controller (5.6), satisfies Definition 31 with $\omega = 0$ (a non-typical case), then weak controllability can be obtained, since uniform continuity of the solution also holds. Otherwise, we can still show the following nominal result.

Assumption 44. *(A)* $w_k = 0 \quad \forall\ k \in \mathbb{Z}_+$ *(B) There exists a solution to* (5.6) *with* $z_N = 0$ $\forall\ x_0 \in \mathcal{X}$. *(C) The penalty parameter* ρ *of* (5.6) *is chosen sufficiently large so as to force* $\xi^{ss,L}$, $\xi^{ss,U}$, *and* ξ^S *to zero at the solution of* (5.6) $\forall \quad k \in \mathbb{Z}_+$ *(C) The functions* $g_x(\cdot)$, $g_u(\cdot)$, $L^{tr}(\cdot,\cdot)$, $L^{ec}(\cdot,\cdot)$, *and* $f(\cdot,\cdot,\cdot)$ *are twice continuously differentiable. (E) The set* $\mathbb{U}$ *is convex and compact. (D) There exists* $\alpha_1 \in \mathcal{K}_\infty$ *such that* $L^{tr}(x,u) \geq \alpha_1(|x|)$ *for all* $x \in \mathbb{R}^{n_x},\ u \in \mathbb{U}^{n_u}$

Theorem 45. *If Assumption 44 holds, then the system under eNMPC-sc is attractive for all* $x_0 \in \mathcal{X}$.

Proof. Take the infinite sum of (5.7b) with $\sigma(|w_k|) = 0$ (true with no uncertainty) and $c_2 = 0$ (true for eNMPC-sc in general):

$$\sum_{k=0}^{\infty} \alpha_3(x_k) \leq \sum_{k=0}^{\infty} \left(V(k, \mathbf{w}_k, x_0) - V(k+1, \mathbf{w}_{k+1}, x_0)\right) \tag{5.31a}$$

$$= V(0, \mathbf{w}_0, x_0) \leq \alpha_2(|x_0|) + c_1. \tag{5.31b}$$

□

Remark 46. *In this work we have exclusively used an endpoint equality constraint. This terminal constraint is only important to show recursive feasibility in Lemma 36. To that end, another termi-*

nal cost and/or terminal region could also be employed (as will be discussed in Section 5.6, but we use the endpoint constraint here for simplicity.

5.5 Case Studies

5.5.1 Nonlinear CSTR

For our first example we consider a nonlinear continuously stirred tank reactor (CSTR) from [48]:

$$\frac{dc_A}{dt} = \frac{q}{V}(c_{Af} - c_A) - kc_A \tag{5.32a}$$

$$\frac{dc_B}{dt} = \frac{q}{V}(-c_B) + kc_A \tag{5.32b}$$

where c_A and c_B denote the concentrations of components A and B, respectively, in mol/l. The manipulated input is q in l/min, the reactor volume is $V = 10\ l$, the rate constant is $k = 1.2\ l/(mol \cdot min)$, and $c_{Af} = 1\ mol/l$ is the feed concentration. In addition, we set variable bounds as $10 \leq q \leq 20$ and $0.45 \leq c_B \leq 1$ which are softened with slack variables that are penalized in the objective function in the NLP. The economic stage cost is:

$$L^{ec}(c_A, c_B, q) = -q\left(2c_B - \frac{1}{2}\right) \tag{5.33}$$

The steady state used for the tracking objective is $c_A^* = 0.5$, $c_B^* = 0.5$, $q^* = 12$, so $L_{ss}^{ec} = -6$. We compare the performance of eNMPC-sc with a regularized economic NMPC controller. Regularization weights for the latter are calculated in [1] and are $w_A = 1.01$, $w_B = 0.01$, and $w_q = 1.01$ (assuming $\omega = 1$), so the tracking stage cost is:

$$L^{tr}(c_A, c_B, q) = 1.01c_A^2 + .5c_B^2 + 12q^2 \tag{5.34}$$

We discretize the system using three point Radau collocation and a finite element length of 1 min. The penalty parameter is chosen as $\rho = 10^8$. We use condition $c_A^0 = .1$, $c_B^0 = 1$. We implement the problem in AMPL [94] and solve the NLPs with IPOPT [64].

First we consider the effect of δ in (5.6g) on the performance of eNMPC-sc, using a horizon of $N = 100$. To investigate this, we first simulate forward for 5 time steps, then solve the NLP at the resulting initial condition. This case is repeated for several δ values. The existence of an economically optimal periodic orbit causes eNMPC-sc to become oscillitory, as shown in Figures 5.1 and 5.2. Results for this are shown in Table 5.1. The sum of predicted costs shows a monotonic relationship with δ.

Table 5.1: CSTR example, comparison of solutions with varying δ, constant $N = 100$ and x_k

δ	$\sum_{i \in \mathcal{N}} L^{ec}(z_i, v_i) - L^{ec}_{ss}$
.99	-28.0709
.9	-28.4348
.7	-28.461
.5	-28.4872
.3	-28.5134
.1	-28.5396
.01	-28.5514

Economic results for the case without uncertainty are shown in the left column of Table 5.2. Economic results for the case with additive state uncertainty w_k (with standard deviation of 0.01 and zero mean) are shown in the right column of Table 5.2. We use the same realization of the uncertainty in every case. Both with and without uncertainty, we consider the tracking case (3.1), the economic case (5.2), the regularization case $eNMPC-reg$ (5.3) with different fractions of the sufficient weight, and eNMPC-sc (5.6) with different values of δ (inequality constraints are softened in each formulation with uncertainty). A

short simulation length of $K = 9$ is chosen so that we can focus on the dynamics that occur before the set-point is reached.

Table 5.2: CSTR example with $N = 100$, comparing the accumulated cost $\sum_{k=0}^{K} L^{ec}(x_k, u_k) - L^{ec}_{ss}$

Case	w/o uncertainty	w/ uncertainty
Tracking	-14.0177	-12.689
eNMPC-reg 100 %	-14.3527	-13.0301
75%	-14.4694	-13.1488
50%	-14.7109	-13.3944
25%	-15.5087	-14.2052
Average	-14.7604	-13.4446
eNMPC-sc $\delta = 0.99$	-20.8853	-19.3943
0 .9	-20.8774	-19.3459
0 .7	-20.9073	-19.3292
0.5	-20.9122	-19.3692
0.3	-20.9106	-19.3529
0.1	-20.9116	-19.389
0.01	-20.9168	-19.4038
Average	-20.9030	-19.3692
Purely economic	-21.7259	-20.2366

Similar trends are seen both with and without uncertainty. The cases with regularization (5.3) have similar cost to the tracking case (3.1), and the cases with a stabilizing constraint (5.6) have similar cost to the economic case (5.2). Costs roughly decrease with the regu-

larization weight and with δ, although this relationship is not perfectly monotonic. Even though we expect that total predicted costs to be monotonic with δ, the sum of implemented costs does not need to be, due to potential local solutions and a finite horizon in (5.6).

Finally we examine the dynamic behaviors for select cases. We show the eNMPC-sc case with $\delta = 0.99$, with and without uncertainty in Figures 5.1 and 5.2, respectively. We include two different horizon lengths. We note that this system has the property that maximum economic performance is obtained under a periodic orbit [48], which explains the oscillatory behavior. The proposed eNMPC-sc controller allows the system to explore that orbit to gain economic performance but the stabilizing constraint eventually forces it to converge to the equilibrium point. We note that the system converges to the equilibrium point in the nominal case and to a neighborhood of the equilibrium point in the robust case. However, the speed and manner of convergence is not guaranteed. Note that convergence is much faster for the shorter horizon, as (5.6g) is more constraining in this case. Also, for the case where $\delta = 0.01$ (not shown in figures), convergence takes about 12,000 time steps.

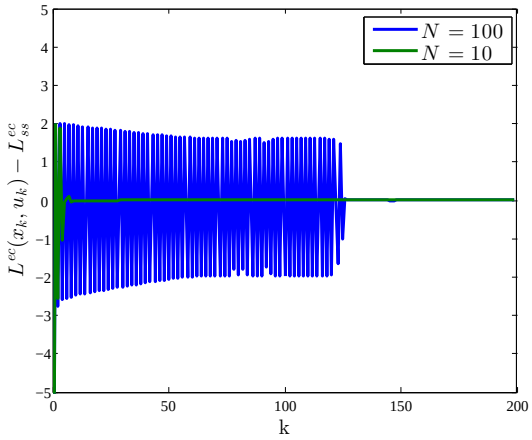

Figure 5.1: CSTR, eNMPC-sc with $\delta = 0.99$, no uncertainty

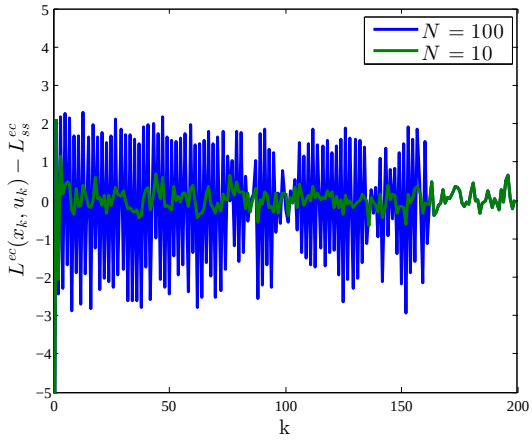

Figure 5.2: CSTR, eNMPC-sc with $\delta = 0.99$ and uncertainty

The stabilizing constraint used in eNMPC-sc has demonstrated a clear economic benefit for this example. Again, note that this constraint is easy to implement, unlike the regularization weights, which require offline calculations and are overly conservative. Also note that the economic performance is generally poorer with uncertainty, which commonly occurs in eNMPC. Nevertheless, the eNMPC-sc provides clear benefits here as well.

5.5.2 Large-Scale Distillation System

As a larger computational example, we again consider the distillation system from Section 4.3.3 with model shown in equations (4.19)-(4.26). We use a finite element length of 1 min and $N = 25$. Each NLP (5.6) has $120,000$ variables, $108,000$ equality constraints, and $14,000$ inequality constraints. The models are implemented in AMPL and solved with IPOPT.

Finding sufficient regularization weights in this case is much more cumbersome due to the size of the system. Here, the Hessian of the steady state problem must be found at many points in the state space. We refer to the regularized case using weights obtained

from the Gershgorin Circle theorem as the 100% regularization instance and we relaxed this instance by using smaller percentages. The Gershgorin weights are reported and compared in [1]. We highlight that, in order to rigorously enforce strict dissipativity, the Hessian must be checked at every possible point of operation in the state space, a difficult task for a problem of this size and complexity. We also define L^{tr} such that these weights are on the diagonals of matrices Q and R and $L^{tr}(x,u) = x^T Q x + u^T R u$.

We first compare solution times for the specific cases that eNMPC-sc (5.6) is implemented with $\delta = 0.01$ and of eNMPC-reg (5.3) with 100% of the Gershgorin weight. The eNMPC-sc problems can be solved in approximately 271 seconds and 188 IPOPT iterations, while eNMPC-reg averages 83 seconds and 70 iterations. This clearly illustrates that regularization is beneficial for computational performance but sacrifices economic performance.

A comparison of accumulated stage costs over ten time steps ($\sum_{k=0}^{K} L^{ec}(x_k, u_k) - L^{ec}_{ss}$) from the same initial condition for various cases is shown in the left column of Table 5.3. Again, we choose a short simulation length of $K = 9$ to emphasize dynamic performance. The penalty parameter is chosen as $\rho = 10^4$. The steady state cost, L^{ec}_{ss}, is -0.223.

Table 5.3: Distillation example, $\sum_{k=0}^{K} \left(L^{ec}(x_k, u_k) - L_{ss}^{ec}\right)$

Case	nominal	w/ uncertainty
Tracking	-20.903	-20.736
eNMPC-reg 100 %	-22.665	-21.662
75%	-22.675	-21.599
50%	-22.676	-21.511
25%	-22.658	-21.361
Average	-22.668	-21.534
eNMPC-sc, $\delta = 0.99$	-25.876	-24.283
0.9	-28.933	-24.162
0.7	-28.406	-24.947
0.5	-29.701	-24.234
0.3	-27.481	-25.199
0.1	-29.453	-25.656
0.01	-29.693	-24.039
Average	-28.506	-24.646
Economic	-27.081	-24.479

From the nominal results, it is apparent that eNMPC-sc provides economic benefit over regularized formulation eNMPC-reg, but the accumulated cost is again not monotonic with δ, due to a short horizon and local solutions. It is also interesting that reducing the regularization weight (by a given percentage) does little to improve performance.

We also consider the cases with uncertainty w_k in the feed flow rate and composition in (4.23). We use additive uncertainty with values of w_k sampled from a normal distribution. The disturbance w_k has zero mean and standard deviation 0.1 for the feed flow rate and

0.01 for the mole fractions of A and B. These results are shown in the right column of Table 5.3, and eNMPC-sc (5.6) again shows a clearly improved economic performance over eNMPC-reg (5.3). However, economic performance is decreased due to the presence of disturbances.

5.6 eNMPC-sc with Terminal Constraints

We also note that the economic NMPC formulation shown in Section 5.3 can be extended to a formulation with terminal constraints, using the quasi-infinite horizon framework shown here. Then, the NLP solved online becomes:

$$\min_{v_i} \quad \sum_{i=0}^{N-1} L^{ec}(z_i, v_i) \tag{5.35a}$$

$$\text{s.t.} \;\; z_{i+1} = f(z_i, v_i) \;\; \forall\, i = 0 \dots N-1 \tag{5.35b}$$

$$z_0 = x_k \tag{5.35c}$$

$$z_i \in \mathbb{X},\; v_i \in \mathbb{U} \;\; \forall\, i \in 0 \dots N-1 \tag{5.35d}$$

$$z_N \in \mathcal{X}_f \tag{5.35e}$$

$$\sum_{i=0}^{N-1} L^{tr}(z_i, v_i) + \psi(z_N) - V(k-1, \mathbf{w}_{k-1}, x_0) \leq -\delta\, L^{tr}(x_{k-1}, u_{k-1}) \tag{5.35f}$$

where $\delta \in (0, 1]$ is a scalar parameter. After the NLP is solved, we inject the control law $u(x_k) = v_0$ into the system and set

$$V(k, \mathbf{w}_k, x_0) := \sum_{i=0}^{N-1} L^{tr}(z_i^k, v_i^k) + \psi(z_N^k), \tag{5.36}$$

where z_i^k, v_i^k is the solution of (5.4) at time k. We thus note that $V(k-1, \mathbf{w}_{k-1}, x_0)$ is the value function at time $k-1$.

We can also extend the robust reformulation (5.6) of (5.4) to the case with terminal constraints:

$$\min_{v_i} \quad \sum_{i=0}^{N-1} L^{ec}(z_i, v_i) + \rho \left(\sum_{i=0}^{N-1} \xi_i^x + \xi^S + \xi^N \right) \tag{5.37a}$$

$$\text{s.t.} \;\; z_{i+1} = f(z_i, v_i) \;\; \forall\, i = 0 \dots N-1 \tag{5.37b}$$

$$z_0 = x_k \tag{5.37c}$$

$$g_x(z_i) \leq \xi_i^x \;\; \forall\, i = 0 \dots N-1 \tag{5.37d}$$

$$g_u(v_i) \leq 0 \;\; \forall\, i = 0 \dots N-1 \tag{5.37e}$$

$$|z_N| \leq c_f + \xi^N \tag{5.37f}$$

$$\sum_{i=0}^{N-1} L^{tr}(z_i, v_i) - V(k-1, \mathbf{w}_{k-1}, x_0) \leq -\delta\, L^{tr}(x_{k-1}, u_{k-1}) + \xi^S \tag{5.37g}$$

$$\xi_i^x, \xi^S, \xi^N \geq 0 \tag{5.37h}$$

where ξ_i^x, ξ^S, ξ^N are slack variables and $\rho \in \mathbb{R}_+$ is a penalty parameter. For this formulation, we replace Assumption 35 with Assumption 47.

Assumption 47. *(A) The set $\mathbb{W}$ is bounded (i.e., $||\mathbf{w}||$ is bounded) and contains zero in its interior. (B) There exists a solution to (5.37) with $z_N \in \mathcal{X}_f \;\forall\;\; x_0 \in \mathcal{X},\; \mathbf{w} \in \mathcal{W},\; k \in \mathbb{Z}_+$ if $w_{k-1} = 0$. (C) The penalty parameter ρ of (5.37) is chosen sufficiently large so that ξ^N and ξ^S are zero at the solution of* (5.6) $\forall\;\; x_0 \in \mathcal{X},\; \mathbf{w} \in \mathcal{W},\; k \in \mathbb{Z}_+$ *if $w_{k-1} = 0$. (D) The functions $g_x(\cdot)$, $g_u(\cdot)$, $L^{tr}(\cdot,\cdot)$, $L^{ec}(\cdot,\cdot)$, and $f(\cdot,\cdot,\cdot)$ are twice continuously differentiable. (E) The set $\mathbb{U}$ is convex and*

compact. (F) The GSSOSC is always satisfied at the solution of (5.37). *(G) There exists* $\alpha_1 \in \mathcal{K}_\infty$ *such that* $L^{tr}(x,u) \geq \alpha_1(|x|)$ *for all* $x \in \mathbb{R}^{n_x},\ u \in \mathbb{U}^{n_u}$

Then, formulation (5.37) is subject to the same analysis shown in Section 5.4.1, with the additional modification that recursive feasibility (Lemma 36) relies on the properties of the terminal controller.

Furthermore, we note that the terminal regions constructed via (4.16) also fulfill the assumptions for economic NMPC with terminal constraints and stability shown via the dissipativity property shown in [95].

5.6.1 Distillation Example

As a larger computational example, we again consider the distillation system from Section 4.3.3. We use a finite element length of 1 min and $N = 25$. We repeat the simulation conditions introduced in Section 4.5.2, considering a sequence of setpoint changes both with and without noise in the feed flow and composition. The setpoints and terminal conditions introduced in Section 4.5.1 are used again here, with parameter values shown in Table 4.7. We compare the tracking and economic performances of economic NMPC, eNMPC-sc with two different values of the tuning parameter δ, economic NMPC with a regularized objective, and tracking NMPC. These formulations are the same as discussed previously in Section 5.5.2, except with the addition of terminal constraints (a terminal cost $\psi(z_N)$ and terminal constraint $z_N \in \mathcal{X}_f$) in all cases.

The tracking performances are shown in Figure 5.3 for the nominal case, and Figure 5.4 for the case with uncertainty. First note that the performance of tracking and regularized NMPC are nearly identical, since the regularization case is utilizing sufficiently large weights to guarantee stability. Next, note that the purely economic case is not stable. Finally, eNMPC is attractive, but not necessarily stable, i.e. it converges to the steady state,

even if convergence is slow. Higher values of the parameter δ tend to induce faster convergence. Note that recursive feasibility is not guaranteed if $\delta > 1$, but the attractivity property holds if the problem is always feasible.

Economic performances are compared in Table 5.4, specifically the cost relative to steady state summed over the simulation time, $\sum_{k=0}^{K} (L^{ec}(x_k, u_k) - L_{ss}^{ec})$. As can be seen, the same trends hold regardless of the presence of uncertainty, although the uncertain case tends to have worse performance overall. The purely economic case has the best performance, although convergence to the steady state is never guaranteed. The tracking and regularized cases have the worst performance, as they are forced to converge to the steady state relatively aggressively. The cases with a stabilizing constraint have intermediate economic performance, while still guaranteeing convergence to the steady state in the nominal case.

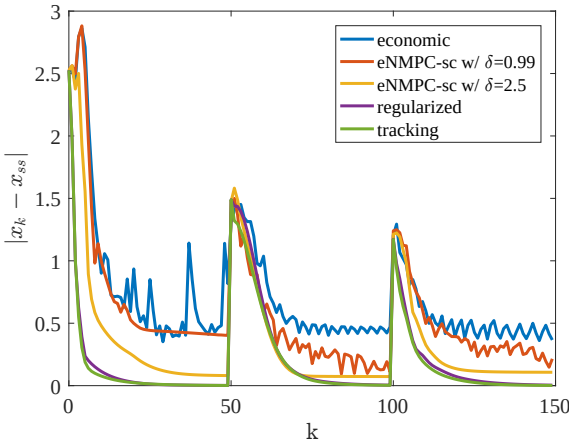

Figure 5.3: Distillation with terminal constraints, nominal case

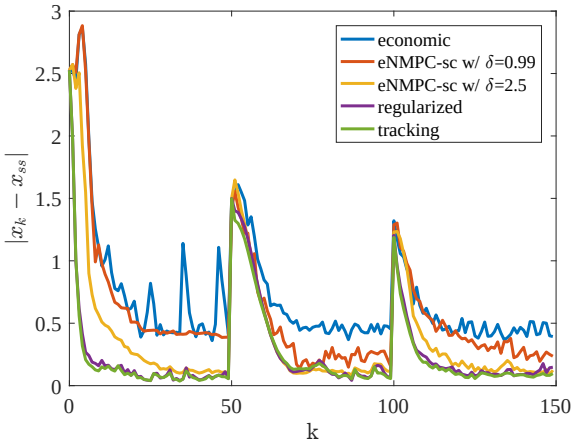

Figure 5.4: Distillation with terminal constraint, w/ noise in feed

5.7 Conclusions

We have established robustness properties for an economic NMPC controller that trades off convergence rate and economic performance, but does not require strict dissipativity

Table 5.4: Distillation example with changing steady states, $\sum_{k=0}^{K} (L^{ec}(x_k, u_k) - L_{ss}^{ec})$

Case	Nominal	w/ uncertainty
Economic	-16.06	-15.87
eNMPC-sc w/ $\delta = 0.99$	-15.93	-15.29
eNMPC-sc w/ $\delta = 2.5$	-15.91	-15.23
Regularized	-15.66	-14.90
Tracking	-15.67	-15.07

with respect to stage costs used in the objective. In particular, we show that this controller is input-to-state practically stable under reasonable assumptions. Computational studies show significantly improved economic performance compared to existing regularization approaches. Finally, we have shown an extension to allow for the inclusion of terminal conditions that removes the need for a restrictive endpoint constraint.

Chapter 6

Adaptive Horizon NMPC

6.1 Introduction

We now consider another major issue in NMPC design, which is the selection of horizon length. In particular, we note a significant trade-off in this choice. The longer the horizon length, the larger the computational burden of the NLP that is solved online. In this case, control actions may be delayed, leading to degradation in control performance. The shorter the horizon, the smaller the region of the state space from which the terminal region is N-reachable. In this case, the problem solved online may become infeasible. Moreover, we recognize that this trade-off can vary with the state of the system. Thus, it is desirable to have a method for updating horizon lengths online.

One method for updating horizon lengths is known as variable horizon MPC [96, 97]. Here, the horizon length is treated as a decision variable in the optimization problem. However, in the nonlinear case, this leads to solving a mixed-integer nonlinear program (MINLP) online, which is currently impractical for large systems with significant nonlinearities. Furthermore, auto-tuning of the time horizon in the context of adaptive control has been discussed in [98].

Another approach is what we refer to as adaptive horizon NMPC (AH-NMPC), where the prediction horizon is updated online based on some rule. A special case of this approach is shrinking horizon NMPC [99], but in the more general case we allow for an expanding horizon as well as changes in the horizon of multiple step lengths. The methodol-

ogy shown in [100] is also similar, except that our method does not necessitate knowledge of the required horizon length at a given time point. Instead, we propose a new method by which horizon lengths may be chosen in real time based on the current state. Regardless of how the finite horizon length varies from timepoint to timepoint, the terminal conditions serve to approximate the infinite horizon problem. To that end, we show a modified form of the terminal conditions calculated in Chapter 5 that apply to the cases of both increasing and decreasing horizons.

We also propose a method that utilizes sensitivity updates from sIPOPT [101] in order to choose a sufficient horizon length in real time. We show that, under reasonable assumptions, AH-NMPC is Input-to-State Practically Stable (ISpS). Finally, we demonstrate our methods on a quad-tank example and a large-scale distillation example.

6.2 Quasi-Infinite Adaptive Horizon NMPC (QIAH-NMPC)

6.2.1 Terminal Region Construction

For the case of adaptive horizons, we slightly modify the terminal region construction shown in Section 4.2.1. Essentially, the method is the same, except that $\rho_x = \rho_u = 0$, so that the stage costs of the LQR are not increased relative to the stage costs of the NMPC, as the conceptual goal is to accurately approximate the objective function of the infinite horizon problem. In this case, in place of (4.14) we have:

$$\psi(x_{k+1}) - \psi(x_k) \tag{6.1a}$$

$$= x_{k+1}^T P x_{k+1} - x_k^T P x_k \tag{6.1b}$$

$$= (A_K x_k + \bar{\phi}(x_k))^T P (A_K x_k + \bar{\phi}(x_k)) - x_k^T P x_k \tag{6.1c}$$

$$= x_k^T(A_K^T P A_K - P)x_k + 2x_k^T A_K^T P\bar{\phi}(x_k) + \bar{\phi}(x_k)^T P\bar{\phi}(x_k) \tag{6.1d}$$

$$= -x_k^T W x_k + 2x_k^T A_K^T P\bar{\phi}(x_k) + \bar{\phi}(x_k)^T P\bar{\phi}(x_k) \tag{6.1e}$$

$$= -x_k^T W x_k + 2x_k^T A_K^T P\bar{\phi}(x_k) + \bar{\phi}(x_k)^T P\bar{\phi}(x_k) \tag{6.1f}$$

$$\leq -\lambda_W^{min}|x_k|^2 + 2\hat{\sigma}\frac{\lambda_W^{max}}{1-\hat{\sigma}^2}M|x_k|^{q+1} + \frac{\lambda_W^{max}}{1-\hat{\sigma}^2}M^2|x_k|^{2q} \quad \forall\, x_k \in \mathcal{X}_f \tag{6.1g}$$

and the terminal region becomes

$$\begin{aligned} |x| &\leq c_f \\ &:= \left(\frac{-\hat{\sigma}\Lambda_P + \sqrt{(\hat{\sigma}\Lambda_P)^2 + \lambda_W^{min}\Lambda_P}}{\Lambda_P M}\right)^{\frac{1}{q-1}} \end{aligned} \tag{6.2}$$

Thus, the descent property $\psi(x_{k+1}) - \psi(x_k) \leq -x^T W x$ under evolution of the nonlinear dynamics $x_{k+1} = f(x_k, u_k)$ is no longer enforced, but rather $\psi(x_{k+1}) - \psi(x_k) \leq -\alpha(|x_k|)$ for some $\alpha \in \mathcal{K}_\infty$. Now, $\psi(x)$ is no longer a strict upper bound of the infinite horizon cost inside of the terminal region, but rather an approximation. This is done to enable the results in Lemmas 49 and 50.

6.2.2 Sensitivity Calculations

Here we briefly describe the NLP sensitivity calculations that will be used in the next section. For sensitivity of the NLP solution, we note that problem (3.1) is parametric in the initial condition x_k, which here will be treated as parameter p, and the (3.1) can be written as:

$$\min_{\mathbf{x}}\ F(\mathbf{x}, p),\ s.t.\ c(\mathbf{x}, p) = 0,\ g(\mathbf{x}, p) + y = 0, y \geq 0 \tag{6.3}$$

where $\mathbf{x}$ is the vector of all variables in (3.1), and y are slack variables. With interior-point NLP solvers, inequality constraints of problem (6.3) are handled *implicitly* by adding barrier terms to the objective function:

$$\min \quad F(\mathbf{x}, p) - \mu \sum_{j=1}^{n_y} \ln(y^{(j)}), \tag{6.4a}$$

$$s.t. \quad c(\mathbf{x}, p) = 0,\ g(\mathbf{x}, p) + y = 0 \tag{6.4b}$$

where $y^{(j)}$ denotes the j^{th} component of vector y. Solving (6.4) for the sequence of $\mu^l \to 0$, with $l = 0, 1, 2, \ldots, \infty$, leads to solution of (6.3). As discussed in [92], convergence of solutions of (6.4) to (6.3) has been proved under mild second order conditions (GSSOSC) and constraint qualifications (MFCQ).

For a given barrier parameter value μ, IPOPT ([64]) solves the KKT conditions of barrier problems (6.4) directly, with an exact Newton method. At the ith Newton iteration, the search direction is computed by linearization of these conditions, with the so-called KKT matrix given by:

$$\mathbf{K}^i = \begin{bmatrix} \mathbf{H}_i & 0 & \mathbf{A^c}_i & \mathbf{A^g}_i \\ \mathbf{A^c}_i{}^T & 0 & 0 & 0 \\ \mathbf{A^g}_i{}^T & I & 0 & 0 \\ 0 & \mathbf{V}_i & 0 & \mathbf{Y}_i \end{bmatrix} \tag{6.5}$$

where $\mathbf{A^c}_i := \nabla c(\mathbf{x}_i, p)$, $\mathbf{A^g}_i := \nabla g(\mathbf{x}_i, p)$ and $\mathbf{H}_i \in \Re^{n \times n}$ is the Hessian of the Lagrange function. After solving a sequence of barrier problems for $\mu \to 0$, the solver returns the primal-dual solution vector $s^{*,T}(p) = [\mathbf{x}^{*,T}\, y^{*,T}, \lambda^{*,T}\, \nu^{*,T}]$ for problem (6.3).

For sensitivity of the NLP solution, we note that problem (6.3) is parametric in the data p and the optimal primal and dual variables can be treated as implicit functions of p. For a *sufficiently small* μ^l, the KKT conditions of the barrier problem (6.4) can be expressed as the equations $\varphi(s^*(p), p) = 0$. To compute approximate neighboring solutions around an already available nominal solution $s^*(p_0)$, we apply the implicit function theorem to $\varphi(s^*(p), p) = 0$ and obtain:

$$\mathbf{K}^*(p_0) \frac{\partial s^*}{\partial p} = - \left. \frac{\partial \varphi(s(p), p)}{\partial p} \right|_{s^*(p_0), p_0} \tag{6.6}$$

where $\mathbf{K}^*(p_0)$ is the KKT matrix (6.5) evaluated at $s^*(p_0)$, and first-order estimates of neighboring solutions are obtained from:

$$s^*(p) = s^*(p_0) + \frac{\partial s^*}{\partial p}(p - p_0) + O(|p - p_0|^2) \tag{6.7}$$

$$\tilde{s}(p) = s^*(p_0) + \frac{\partial s^*}{\partial p}(p - p_0) \tag{6.8}$$

where $\tilde{s}(p)$ is an approximate solution of $s^*(p)$. This solution is implemented automatically by sIPOPT, which we leverage in the following section. See [92] and [101] for more details on the sensitivity calculations.

6.2.3 Adaptive Horizon Algorithm

An algorithm for choosing N based on sensitivity calculations is shown in Figure 6.1. The first step is to determine N_s, a safety factor chosen through simulation, and N_{max}, a sufficiently long horizon length that guarantees feasibility of (3.1) and serves as an initialization for N. We note that N_s also serves as a minimum horizon length. Then, at each time point k, solve the NMPC problem $\mathcal{P}(x_k)$ (3.1). Next, solve the sensitivity problem to obtain the prediction using the successor state x_{k+1} as a parametric perturbation. We denote this sensitivity problem as $\mathcal{P}_s(x_{k+1})$, which is calculated as in (6.8) by considering $\mathcal{P}(x_k)$ (3.1) as being parametric in the initial condition:

$$\tilde{s}(x_{k+1}) = s^*(x_k) + \frac{\partial s^*(x_k)}{\partial x_k}(x_{k+1} - x_k) \tag{6.9}$$

where $s^*(x_k)$ is the optimal primal and dual solution of $\mathcal{P}(x_k)$ (3.1) calculated at time k and $\tilde{s}(x_{k+1})$ is a linearized approximation of $s^*(x_{k+1})$ given by $\mathcal{P}_s(x_{k+1})$ (6.9).

If the state profile from $\mathcal{P}_s(x_{k+1})$ reaches the terminal region in N_k time steps, then we determine S_T, the time step at which the state enters the terminal region. We then set $N_{k+1} = S_T + N_s$, $k = k + 1$ and proceed to the next NMPC problem. If the state profile

from $\mathcal{P}_s(x_{k+1})$ does not reach the terminal region in N_k steps, then we set $N_{k+1} = N_{max}$ and $k = k + 1$, and proceed to the next NMPC problem. In this fashion, the horizon length is chosen based on a sensitivity prediction plus a safety factor, and N_{max} is chosen as a default in case the terminal region is not reached in N_k steps.

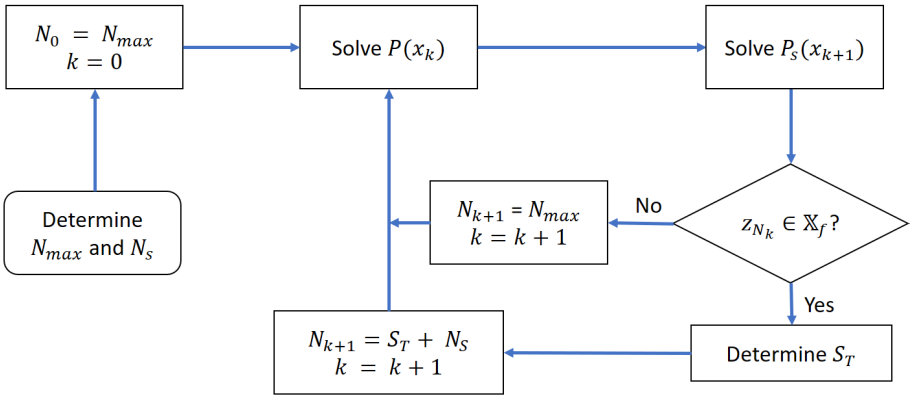

Figure 6.1: Algorithm to Determine N_k

Algorithm 48. *Horizon Adaption*

1: *Determine* N_{max}, N_s

2: $k := 0$, $N_0 := N_{max}$

3: *Solve NMPC problem* $P(x_k)$ *with horizon* N_k *and obtain* $x_{k+1} = f(x_k, u_k)$.

4: *Use* (6.8) *to solve the sensitivity problem* $P_s(x_{k+1})$ *as an approximation of* $P(x_{k+1})$ *with horizon* N_k. *Obtain* z_N *from solution of* $P_s(x_{k+1})$.

5: ***if*** $z_N \in \mathcal{X}_f$ ***then***

6: *Determine* S_T, *step at which* $\mathcal{X}_f$ *is reached*

7: $N_{k+1} := S_T + N_s$

8: ***else if*** $z_N \notin \mathcal{X}_f$ ***then***

9: $N_{k+1} := N_{max}$

10: ***end if***

11: $k := k + 1$

12: *go to Step 3*

We include only one dynamic optimization problem and one sensitivity calculation at each iteration for the sake of practical online implementation. With this method, we note that the chosen horizon length is not the minimum required to reach the terminal region, but rather the number of time steps for the optimum tracking objective. Although this approach may lead to slightly increased computational costs, it is reasonable to expect better tracking performance than the minimum horizon length for reachability.

6.3 Properties of QIAH-NMPC

First we establish relationships between the linear and nonlinear systems in $\mathcal{X}_f$. Consider the cost of the LQR control evaluated for (3.1):

$$V_N^K(x) = \sum_{i=0}^{N-1} L(z_i, -Kz_i) + \psi(z_N) \tag{6.10a}$$

$$\text{where } z_N = 0,\ z_{i+1} = Az_i + Bv_i + \phi(z_i, v_i)\ \ \forall\, i = 0 \dots N-1 \tag{6.10b}$$

Lemma 49. *There exists* $\alpha_{NL} \in \mathcal{K}_\infty$ *such that* $|V_N^K(x) - \psi(x)| \leq \alpha_{NL}(|x|)\ \ \forall x \in \mathcal{X}_f,\ N \in \mathcal{N}$.

Proof. First define the state trajectory according to LQR control and linearized dynamics, $z_{i+1}^L = A_K z_i^L\ \forall\, i = 0 \dots \infty$, and the state trajectory according to LQR control and nonlinear dynamics, $z_{i+1}^{NL} = A_K z_i^{NL} + \bar{\phi}_K(z_i^{NL})\ \forall\ i = 0 \dots \infty$, both with initial condition $x \in \mathcal{X}_f$. The nonlinear trajectory is bounded by $|z_{i+1}^{NL}| \leq ||A_K||\,|z_i^{NL}| + M|z_i^{NL}|^q \leq C|z_i^{NL}|$ where $C := ||A_K|| + Mc_f^{q-1}$. Then for state trajectory bounds under linear or nonlinear dynamics

we have:

$$|z_i^L| \leq ||A_K||^i |x| \tag{6.11a}$$

$$|z_i^{NL}| \leq C^i |x| \tag{6.11b}$$

Define the function $L_K(x) := L(x, -Kx)$, then we have:

$$|V_N^K(x) - \psi(x)| = \left| \sum_{i=0}^{N-1} L_K(z_i^{NL}) + \psi(z_N^{NL}) - \psi(x) \right| \tag{6.12a}$$

$$= \left| \sum_{i=0}^{N-1} \left[L_K(z_i^{NL}) - L_K(z_i^L) \right] + \psi(z_N^{NL}) - \psi(z_N^L) \right| \tag{6.12b}$$

$$\leq \sum_{i=0}^{N-1} \left[L_K(z_i^{NL}) + L_K(z_i^L) \right] + \psi(z_N^{NL}) + \psi(z_N^L) \tag{6.12c}$$

$$\leq \sum_{i=0}^{N-1} \left[\alpha_U(|z_i^{NL}|) + \alpha_U(|z_i^L|) \right]$$

$$+ \alpha_{U,\psi}(|z_N^{NL}|) + \alpha_{U,\psi}(|z_N^L|) \tag{6.12d}$$

$$\leq \sum_{i=0}^{N-1} \left[\alpha_U(C^i|x|) + \alpha_U(||A_K||^i |x|) \right]$$

$$+ \alpha_{U,\psi}(C^N|x||) + \alpha_{U,\psi}(||A_K||^N |x|) \tag{6.12e}$$

$$=: \alpha_{NL}(|x|) \tag{6.12f}$$

□

where (6.12b) follows from the identity $\psi(x) = \sum_{i=0}^{N-1} L_K(z_i^L) + \psi(z_N^L)$, (6.12d) follows from Assumption 22(A), and (6.12e) follows from (6.11). Although Lemma 49 only states existence, α_{NL} could be estimated from a sampling of simulations under LQR control.

Lemma 50. *There exists $\alpha_V \in \mathcal{K}_\infty$ such that $|\psi(x) - V_N(x)| \leq \alpha_V(|x|) \;\; \forall\, x \in \mathcal{X}_f,\; N \in \mathcal{N}$*

Proof. Consider the following parameterized problem:

$$V_N^\eta(x, \eta) = \min \sum_{i=0}^{N-1} \left(L(z_i, v_i) + \rho \eta \epsilon_i \right) + \psi(z_N) \tag{6.13a}$$

$$s.t.\ z_{i+1} = Az_i + Bv_i + \gamma_i \ \ \forall\, i = 0 \dots N-1 \tag{6.13b}$$

$$|\gamma_i - \phi(z_i, v_i)| \leq \epsilon_i,\ \epsilon_i \geq 0 \ \ \forall\, i = 0 \dots N-1 \tag{6.13c}$$

$$|\gamma_i| \leq \eta \ \ \forall\, i = 0 \dots N-1 \tag{6.13d}$$

$$z_0 = x \tag{6.13e}$$

where $\eta, \rho > 0$. We use (6.13) to relate problem (3.1) and problem (4.2) via Lemma 50.

Note from (4.2) that $V_N^\eta(x, 0) = \psi(x)$. Also, from weak controllability there exists some $\eta = \alpha_\eta(|x|)$ such that $V_N^\eta(x, \alpha_\eta(|x|)) = V_N(x)$ from (3.1) when ρ is chosen sufficiently large so that $\epsilon_i = 0$. Thus, (6.13) is parameterized in the evolution of the nonlinearities of the system. Furthermore, it can be shown that the solution of (6.13) satisfies the Mangasarian-Fromovitz Constraint Qualification (MFCQ) [84], since any control v_i is feasible. Then $V_N^\eta(x, \eta)$ is uniformly continuous in η, and there exists $\alpha_g \in \mathcal{K}_\infty$ such that $|V_N^\eta(x, \eta) - V_N^\eta(x, 0)| \leq \alpha_g(\eta)$. Thus, $|\psi(x) - V_N(x)| = |V_N^\eta(x, 0) - V_N^\eta(x, \alpha_\eta(x))| \leq \alpha_g(\alpha_\eta(|x|)) =: \alpha_V(|x|)$. Therefore, Lemma 50 holds. $\square$

Although Lemma 50 only states existence, α_V could be estimated from a sampling of open loop problems (3.1). Note that the necessity of the existence of α_V and α_{NL} is the reason that $\psi(x)$ is chosen to approximate $V_\infty(x)$ rather than give it a strict upper bound as in [67] and [68]. If the stage costs in (4.2) were increased so as to enforce $\psi(x) \geq V_\infty(x)$, then Lemmas 49 and 50 may not hold.

6.3.1 Asymptotic Stability of QIAH-NMPC

We next consider the stability of (2.2) under control according to (3.1) with terminal conditions described in Section 4.2, and a horizon length that is updated adaptively and assumed to be feasible. For now, we assume no plant model mismatch, i.e., $w_k = 0 \ \ \forall\, k \in \mathbb{I}_+$. Define the bounded set of acceptable horizon lengths $\mathcal{N} = \{N | N_s \leq N \leq N_{max},\ N \in \mathbb{I}_+\}$,

and the subset of horizon lengths that define feasible problems (3.1) at time k that we denote as $\mathcal{N}_k \subset \mathcal{N}$. Furthermore, define some process (e.g. Figure 6.1) that determines horizon lengths $H : \mathbb{R}^n \times \mathcal{N} \times \mathbb{R}^n \to \mathcal{N}$ so that $N_{k+1} = H(x_k, N_k, x_{k+1}) \in \mathcal{N}_{k+1}$.

Assumption 51. *Problem* (3.1) *at time k is always feasible with $N_k = N_{max}$. Furthermore, if problem* (3.1) *at time k with x_k and N_k is feasible, then so is problem* (3.1) *solved at time $k+1$ with x_{k+1} and $N_{k+1} = H(x_k, N_k, x_{k+1})$. That is, $H(x_k, N_k, x_{k+1}) \in \mathcal{N}_{k+1} \;\; \forall x_k, x_{k+1} \in \mathcal{X}, \; N_k \in \mathcal{N}_k$.*

Note that, for our particular case, Assumption 51 is enforced by Algorithm 48 and sIPOPT. However, for the sake of the proceeding theoretical results, we consider any H that provides feasible horizon lengths.

Assumption 52. *There exists a value of the parameter N_s such that the solution of* (3.1) *with horizon $N_k \geq N_s$ satisfies*

$$\alpha_L(|x_k|) - \alpha_{NL}(|z_{N_k|_k}|) \geq \alpha_3(|x_k|) \text{ if } N_{k+1} \geq N_k \tag{6.14a}$$

$$\alpha_L(|x_k|) - \alpha_V(|z_{N_{k+1}+1|_k}|) \geq \alpha_3(|x_k|) \text{ if } N_{k+1} < N_k \tag{6.14b}$$

when $w_k = 0$ for some $\alpha_3 \in \mathcal{K}_\infty$, where $N_{k+1} = H(x_k, N_k, x_{k+1})$, α_L satisfies Assumption 22(A), and α_{NL}, α_V satisfy Lemmas 49 and 50, respectively.

Essentially, this condition means that costs due to nonlinear effects in the terminal region must be small compared to the stage cost of the initial condition, and therefore (3.1) is a good approximation of the infinite horizon problem. Note that, in the case of a lengthening horizon ($N_{k+1} > N_k$), choosing $\psi(x) \geq V_\infty(x) \;\; \forall \; x \in \mathcal{X}_f$ (as in [67] and [68]) would also suffice. However, we instead employ Lemma 52 so that the horizon may be lengthened or shortened freely.

Condition (6.14) may need to be checked through simulation and enforced by selection of N_s. We recognize that a value of N_s that rigorously guarantees (6.14) may be difficult

or impossible to find. However, in the case of our examples, it is straightforward to find a value that leads to satisfactory simulation results.

We now show that AH-NMPC is asymptotically stable.

Theorem 53. *Under Assumptions 2, 22, 51, and 6.14, there exist* $\alpha_1, \alpha_1, \alpha_3 \in \mathcal{K}_\infty$ *with* $w_k = 0 \ \forall \ k \in \mathbb{I}_+$ *such that:*

$$\alpha_1(|x_k|) \leq V_{N_k}(x_k) \leq \alpha_2(|x_k|) \tag{6.15a}$$

$$V_{H(x_k,N_k,x_{k+1})}(x_{k+1}) - V_{N_k}(x_k) \leq -\alpha_3(|x_k|) \tag{6.15b}$$

$$\forall \ x_k \in \mathcal{X}, \ N_k \in \mathcal{N}_k$$

and asymptotic stability holds.

Proof. The inequalities (6.15a) are satisfied by the form of the objective function and weak controllability. The descent inequality (6.15b) is not as simple in the case of a variable horizon length. We consider two cases in which the horizon increases or decreases.

Increasing horizon, $\mathbf{N_{k+1} \geq N_k}$

In the case of an increasing horizon we define the initialization for (3.1) solved at time $k+1$ as the following:

$$\hat{v}_{i|k+1} = \begin{cases} v_{i+1|k} \ \forall \ i = 0 \dots N_k - 2 \\ -Kz_i \ \forall \ i = N_k - 1 \dots N_{k+1} - 1 \end{cases} \tag{6.16}$$

$$\hat{z}_{0|k+1} = z_{1|k} \tag{6.17a}$$

$$\hat{z}_{i+1|k+1} = f(\hat{z}_{i|k}, \hat{v}_{i|k}) \ \forall \ i = 0 \dots N_{k+1} \tag{6.17b}$$

with the value function $\hat{V}_{N_{k+1}}(x_{k+1})$. Then the descent inequality of the Lyapunov function is given as follows:

$$
\begin{aligned}
& V_{N_{k+1}}(x_{k+1}) - V_{N_k}(x_k) && \text{(6.18a)}\\
& \leq \hat{V}_{N_{k+1}}(x_{k+1}) - V_{N_k}(x_k) && \text{(6.18b)}\\
& = \sum_{i=0}^{N_{k+1}-1} L(\hat{z}_{i|k+1}, \hat{v}_{i|k+1}) + \psi(\hat{z}_{N_{k+1}|k+1}) \\
& - \sum_{i=0}^{N_k-1} L(z_{i|k}, v_{i|k}) - \psi(z_{N_k|k}) && \text{(6.18c)}\\
& = -L(x_k, u_k) \\
& + \sum_{i=0}^{N_k-2} \big(L(\hat{z}_{i|k+1}, \hat{v}_{i|k+1}) - L(z_{i+1|k}, v_{i+1|k})\big) \\
& + \sum_{i=N_k-1}^{N_{k+1}-1} L(\hat{z}_{i|k+1}, \hat{v}_{i|k+1}) + \psi(\hat{z}_{N_{k+1}|k+1}) - \psi(z_{N_k|k}) && \text{(6.18d)}\\
& = -L(x_k, u_k) + \sum_{i=N_k-1}^{N_{k+1}-1} L(\hat{z}_{i|k+1}, \hat{v}_{i|k+1}) \\
& + \psi(\hat{z}_{N_{k+1}|k+1}) - \psi(z_{N_k|k}) && \text{(6.18e)}\\
& = -L(x_k, u_k) + V^K_{N_{k+1-N_k+1}}(z_{N_k|k}) - \psi(z_{N_k|k}) && \text{(6.18f)}\\
& \leq -\alpha_L(|x_k|) + \alpha_{NL}(|z_{N_k|k}|) && \text{(6.18g)}\\
& \leq -\alpha_3(|x_k|) && \text{(6.18h)}
\end{aligned}
$$

where (6.18g) follows from Lemma 49 and (6.18h) follows from (6.14a).

Decreasing horizon, $\mathbf{N_{k+1} < N_k}$

In the case of a decreasing horizon we define the initialization for (3.1) solved at time

$k+1$ as the following:

$$\hat{v}_{i|k+1} = v_{i+1|k} \; \forall \; i = 0 \dots N_{k+1} - 1, \tag{6.19}$$

again with the state initialization given by (6.17) and the value function denoted as $\hat{V}_{N_{k+1}}(x_{k+1})$. Then the descent inequality of the Lyapunov function is given as follows:

$$V_{N_{k+1}}(x_{k+1}) - V_{N_k}(x_k) \tag{6.20a}$$

$$\leq \hat{V}_{N_{k+1}}(x_{k+1}) - V_{N_k}(x_k) \tag{6.20b}$$

$$= \sum_{i=0}^{N_{k+1}-1} L(\hat{z}_{i|k+1}, \hat{v}_{i|k+1}) + \psi(\hat{z}_{N_{k+1}|k+1})$$

$$- \sum_{i=0}^{N_k-1} L(z_{i|k}, v_{i|k}) - \psi(z_{N_k|k}) \tag{6.20c}$$

$$= -L(x_k, u_k) + \sum_{i=0}^{N_{k+1}-1} \big(L(\hat{z}_{i|k+1}, \hat{v}_{i|k+1}) - L(z_{i+1|k}, v_{i+1|k})\big)$$

$$+ \psi(\hat{z}_{N_{k+1}|k+1}) - \sum_{i=N_{k+1}+1}^{N_k-1} L(z_{i|k}, v_{i|k}) - \psi(z_{N_k|k}) \tag{6.20d}$$

$$= -L(x_k, u_k) + \psi(\hat{z}_{N_{k+1}|k+1})$$

$$- \sum_{i=N_{k+1}+1}^{N_k-1} L(z_{i|k}, v_{i|k}) - \psi(z_{N_k|k}) \tag{6.20e}$$

$$= -L(x_k, u_k) + \psi(z_{N_{k+1}+1|k})$$

$$- V_{N_k - N_{k+1}-1}(z_{N_{k+1}+1|k}) \tag{6.20f}$$

$$\leq -\alpha_L(|x_k|) + \alpha_V(|z_{N_{k+1}+1|k}|) \tag{6.20g}$$

$$\leq -\alpha_3(|x_k|) \tag{6.20h}$$

where we use $\hat{z}_{N_{k+1}|k+1} = z_{N_{k+1}+1|k}$ in (6.20f), (6.20g) follows from Lemma 50, and (6.20h) follows from (6.14b).

Thus $V_N(x)$ satisfies (6.15), and QIAH-NMPC is asymptotically stable. $\square$.

6.3.2 Robust Stability

We now relax the assumption that $w_k = 0 \quad \forall \; k \in \mathbb{I}_+$, and instead assume that w_k is bounded. Consider a robust reformulation of (3.1):

$$V_N^r(x) = \min \sum_{i=0}^{N-1} L(z_i, v_i) + \psi(z_N) + \rho\epsilon_f \tag{6.21a}$$

$$s.t.\ z_{i+1} = Az_i + Bv_i + \phi(z_i, v_i) \;\; \forall\, i = 0 \dots N-1 \tag{6.21b}$$

$$v_i \in \mathbb{U} \;\; \forall\, i = 0 \dots N-1 \tag{6.21c}$$

$$z_0 = x \tag{6.21d}$$

$$|z_N| \leq c_f + \epsilon_f, \epsilon_f \geq 0 \tag{6.21e}$$

Assumption 54. *(A) The parameter ρ is chosen large enough so as to force the solution of $V_N^r(x)$* (6.21) *to that of $V_N(x)$* (3.1) *$\forall\; x \in \mathcal{X}, N \in \mathcal{N}_k$. (B)* (6.21) *satisfies the General Strong Second Order Sufficient Condition (GSSOSC)*

Note that GSSOSC is easily enforced by choosing $L(z_i, v_i) = z_i^T Q z_i + v_i^T R v_i$ with Q and R large enough.

Lemma 55. *Under Assumption 54, the robust reformulation* (6.21) *satisfies the Mangasarian-Fromowitz Constraint Qualification and the optimal value function $V_N^r(x)$ of* (6.21) *is uniformly continuous.*

See [92] for proof of Lemma 55.

Remark 56. *Note that a penalty parameter ρ exists to satisfy Assumption 54 when the MFCQ and GSSOSC are satisfied. Choosing ρ larger than the appropriate norm of the multipliers of the solution of problem* (3.1) *is sufficient to satisfy Assumption 54. Furthermore, it is typically possible to conservatively overestimate a sufficient value for ρ without significantly affecting the performance of the NMPC.*

Lemma 57. *There exists $c \in \mathbb{R}_+$ such that $|V_\infty(x_k) - V_N(x_k)| \leq c \ \ \forall\ N \in \mathcal{N}_k,\ x \in \mathcal{X}$.*

Proof. Consider a parameterized problem similar to that used to (6.13):

$$V^\eta_{N,\infty}(x,\eta) = \min \sum_{i=0}^{\infty} L(z_i, v_i) + \rho\eta \sum_{i=N}^{\infty} \epsilon_i \tag{6.22a}$$

$$s.t.\ z_{i+1} = f(z_i, v_i) \ \ \forall i = 0 \dots N-1 \tag{6.22b}$$

$$z_{i+1} = Az_i + Bv_i + \gamma_i \ \ \forall\ i = N \dots \infty \tag{6.22c}$$

$$|\gamma_i - \phi(z_i, v_i)| \leq \epsilon_i,\ \epsilon_i \geq 0 \ \ \forall\ i = N \dots \infty \tag{6.22d}$$

$$|\gamma_i| \leq \eta \ \ \forall\ i = N \dots \infty \tag{6.22e}$$

$$z_0 = x \tag{6.22f}$$

where $\rho > 0$ is chosen sufficiently large. Note that $V^\eta_{N,\infty}(x,0) = V_N(x)$ and $V^\eta_{N,\infty}(x, \alpha_\eta(|x|)) = V_\infty(x)$ for some $\alpha_\eta \in \mathcal{K}_\infty$ large enough. Furthermore, since (6.22) satisfies MFCQ, $V^\eta_{N,\infty}(x,\eta)$ is uniformly continuous in η, and there exists some $\alpha_\infty \in \mathcal{K}_\infty$ such that $|V_\infty(x) - V_N(x)| \leq \alpha_\infty(|x|)$. Thus, c exists since $\mathcal{X}$ is bounded, and we can see that the size of c depends on α_η, which bounds the nonlinear effects in the terminal region. □

Again, although Lemma 57 only states existence, c could be estimated from a sampling of open loop problems (3.1) in the terminal region.

Theorem 58. *Under Assumptions 2, 22, 51, 52, and 54, adaptive horizon NMPC with control u_k determined by* (6.21) *is input-to-state practically stable (ISpS) for all $x_0 \in \mathcal{X}$ with constant $c := 2c_r$ from Lemma 57.*

Proof. Define the true successor horizon length $N_{k+1} := H(x_k, N_k, f(x_k, u_k, w_k)$, and the successor horizon length in the case of no plant-model mismatch, $N'_{k+1} := H(x_k, N_k, f(x_k, u_k, 0))$. Then we have:

$$
\begin{aligned}
& V^r_{N_{k+1}}(x_{k+1}) - V^r_{N_k}(x_k) && \text{(6.23a)}\\
& = V^r_{N_{k+1}}(f_p(x_k, u_k, w_k)) - V_\infty(f_p(x_k, u_k, w_k)) \\
& + V_\infty(f_p(x_k, u_k, w_k)) - V_\infty(f_p(x_k, u_k, 0)) \\
& + V_\infty(f_p(x_k, u_k, 0)) - V^r_{N'_{k+1}}(f_p(x_k, u_k, 0)) \\
& + V^r_{N'_{k+1}}(f_p(x_k, u_k, 0)) - V^r_{N_k}(x_k) && \text{(6.23b)}\\
& \leq |V^r_{N_{k+1}}(f_p(x_k, u_k, w_k)) - V_\infty(f_p(x_k, u_k, w_k))| \\
& + |V_\infty(f_p(x_k, u_k, w_k)) - V_\infty(f_p(x_k, u_k, 0))| \\
& + |V_\infty(f_p(x_k, u_k, 0)) - V^r_{N'_{k+1}}(f_p(x_k, u_k, 0))| \\
& + V^r_{N'_{k+1}}(f_p(x_k, u_k, 0)) - V^r_{N_k}(x_k) && \text{(6.23c)}\\
& \leq -\alpha_3(|x_k|) + \sigma(|\mathbf{w}|) + c && \text{(6.23d)}
\end{aligned}
$$

where (6.23b) follows from addition and subtraction of $V^r_{N'_{k+1}}(f_p(x_k, u_k, 0)) + V_\infty(f_p(x_k, u_k, w_k)) + V_\infty(f_p(x_k, u_k, 0))$, and (6.23d) follows from Lemma 57, Assumption 1, and Theorem 53. Thus $V^r_{N_k}(x_k)$ satisfies Definition 5.7, and (2.1) is ISpS by Theorem 11.

6.4 Reformulation for State Constraints

Thus far, we have ignored state constraints other than the terminal constraint for simplicity of presentation. Since the examples considered in this work include state constraints, we may reformulate as in [92], where these constraints are softened with an auxiliary variable penalized in the objective, and the problem solved online becomes (6.24):

$$V_N^r(x) = \min \sum_{i=0}^{N-1} L(z_i, v_i) + \psi(z_N)$$
$$+\rho \left(\sum_{i=0}^{N-1} \left(\epsilon_i^{up} + \epsilon_i^{lo} \right) + \epsilon_f \right) \tag{6.24a}$$

$$s.t.\ z_{i+1} = Az_i + Bv_i + \phi(z_i, v_i)\ \ \forall\, i = 0 \dots N-1 \tag{6.24b}$$

$$z_i \leq z^{up} + \epsilon_i^{up}\ \ \forall\, i = 0 \dots N-1 \tag{6.24c}$$

$$z_i \geq z^{lo} - \epsilon_i^{lo}\ \ \forall\, i = 0 \dots N-1 \tag{6.24d}$$

$$v_i \in \mathbb{U}\ \ \forall\, i = 0 \dots N-1 \tag{6.24e}$$

$$z_0 = x \tag{6.24f}$$

$$|z_N| \leq c_f + \epsilon_f \tag{6.24g}$$

$$\epsilon_i^{up}, \epsilon_i^{lo}, \epsilon_f \geq 0 \tag{6.24h}$$

Although this formulation does not guarantee constraint satisfaction in the closed loop, it does satisfy the Mangasarian-Fromovitz Constraint Qualification, and the continuity property in Lemma 55 is preserved, as shown in [92].

6.5 Quad Tank Example

We consider the experimental quad tank system from [3] described by the following equations, ignoring state constraints for this work:

$$\dot{x}_1 = -\frac{a_1}{A_1}\sqrt{2gx_1} + \frac{a_3}{A_1}\sqrt{2gx_3} + \frac{\gamma_1}{A_1}u_1 \tag{6.25a}$$

$$\dot{x}_2 = -\frac{a_2}{A_2}\sqrt{2gx_2} + \frac{a_4}{A_2}\sqrt{2gx_4} + \frac{\gamma_2}{A_2}u_2 \tag{6.25b}$$

$$\dot{x}_3 = -\frac{a_3}{A_3}\sqrt{2gx_3} + \frac{(1-\gamma_2)}{A_3}u_2 \tag{6.25c}$$

$$\dot{x}_4 = -\frac{a_4}{A_4}\sqrt{2gx_4} + \frac{(1-\gamma_1)}{A_4}u_1 \tag{6.25d}$$

$$-43.4 \leq u_1 \leq 16.6 \tag{6.25e}$$

$$-35.4 \leq u_2 \leq 24.6 \tag{6.25f}$$

$$x \geq 0 \tag{6.25g}$$

$$x_{ss} = [14, 14, 14.2, 21.3]^T \tag{6.25h}$$

The plant schematic is shown in Figure 6.2. The valve parameters are held constant at $\gamma_1 = \gamma_2 = 0.4$. We discretize the system with sampling time $h = 10$.

6.5.1 Terminal Region Calculations

The LQR parameters are shown in Table 6.1. We then use these parameters to define the LQR, which is then used to simulate the system and find the upper bound for ϕ. This is done by simulating one step forward from many initial conditions and subtracting the linear part of the system. The results for 10,000 such simulations are shown in Figure 6.3, and the bound parameters are shown in Table 6.1. The terminal region is then found from (6.2). In this case the terminal region is given by $|z_N| \leq c_f = 28.1$, and we confirm that the control constraints are satisfied for $u = -Kx$ in this region. This region has a volume $\frac{1}{2}\pi^2 c_f^4 = 3.15 \times 10^6$, which is significantly larger than the region of volume 3×10^4 given in [3] using the method of [44]. We attribute the improvement in our method to a more accurate bound on nonlinearities (4.3), although the original calculation was done for a continuous time system and is therefore not a direct comparison.

Table 6.1: Example parameters and results

	h	Q	R	M	q	c_f
Quad tank	10	$1.5I_4$	I_2	0.005	2.1	28.3

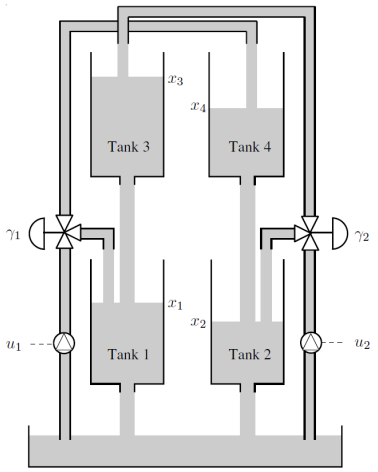

Figure 6.2: Quad Tank Schematic [3]

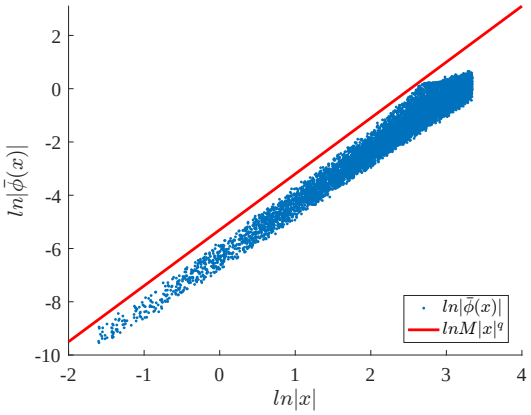

Figure 6.3: Quad Tank, nonlinearity bound

6.5.2 Nominal Results

We have implemented both standard and adaptive horizon NMPC for (6.25) using IPOPT on an Intel i7-4770 3.4 GHz CPU. For standard NMPC, we set $N = 25$, and for AH-NMPC we set $N_{max} = 25, N_s = 5$. Note that N_s was chosen through simulation trial and error to ensure that (6.14) holds. Also, sIPOPT is used with the initial condition as the sensitivity parameter p for updated NMPC calculations. However, because our computed terminal region is so large, we artificially reduce it to $|z_N| \leq 1$ in order to more adequately test the adaptive horizon algorithm. Also, in order to simulate a disturbance for which the sensitivity prediction is infeasible, we set the states to large predefined values at $k = 0, 50, 100$. The norm of the state trajectories over time is shown in Figure 6.4. The tracking behaviors

Table 6.2: Predefined state values

k	x_1	x_2	x_3	x_4
0	40	40	0	0
50	40	0	40	0
100	40	0	0	40

of standard NMPC and AH-NMPC are nearly identical.

The difference between the two methods is in the horizon lengths and solve times, shown in Figures 6.6 and 6.7, respectively. The standard NMPC case has a constant horizon length and a higher average solve time. For the adaptive horizon case, under normal process operation, the horizon is updated according to the sensitivity predictions. The horizon length tends to decrease as the system approaches the steady state, leading to faster average solution times. In the case of constant horizon NMPC, the average solve time is $0.0115s$, while the average solve time in the case of AH-NMPC is $0.0062s$, which shows a decrease of 46%. However, when the sensitivity prediction is infeasible ($z_N \notin \mathcal{X}_f$) due to a large disturbance, the algorithm detects this and defaults to $N_k = N_{max}$, which guarantees feasibility of (3.1) for all $x_k \in \mathcal{X}$. Thus, the horizon can be updated adaptively under normal conditions, allowing for faster average solve times, but still retains robustness in the case of large disturbances.

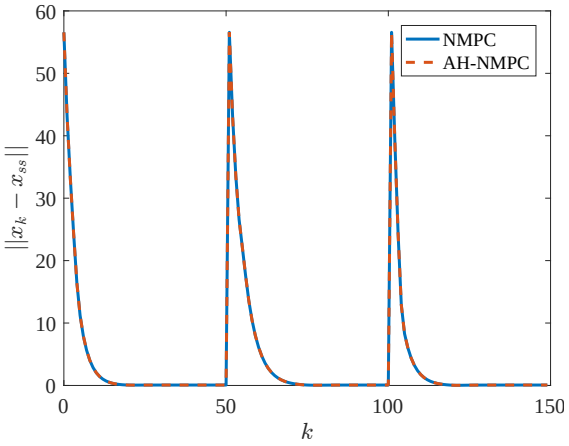

Figure 6.4: Nominal quad tank, norm of states

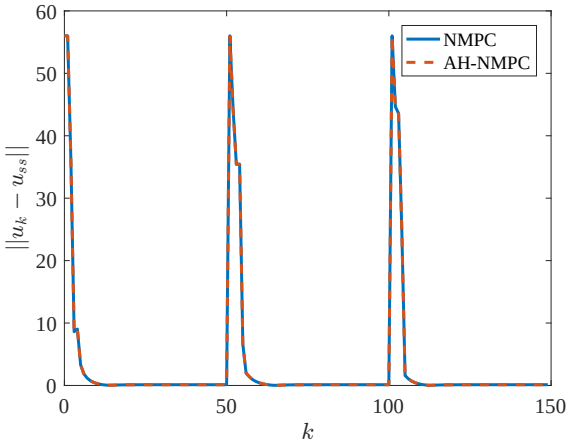

Figure 6.5: Nominal quad tank, norm of controls

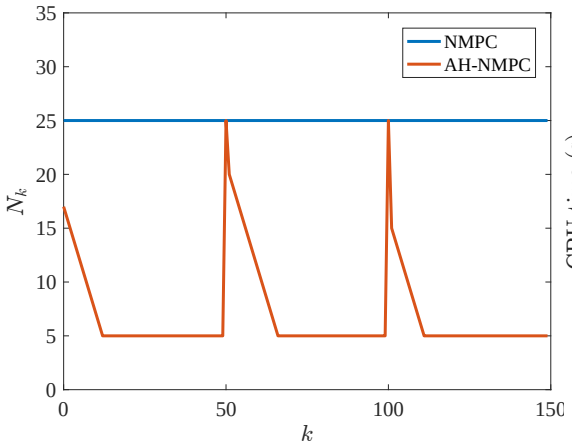

Figure 6.6: Nominal quad tank, Horizon Lengths

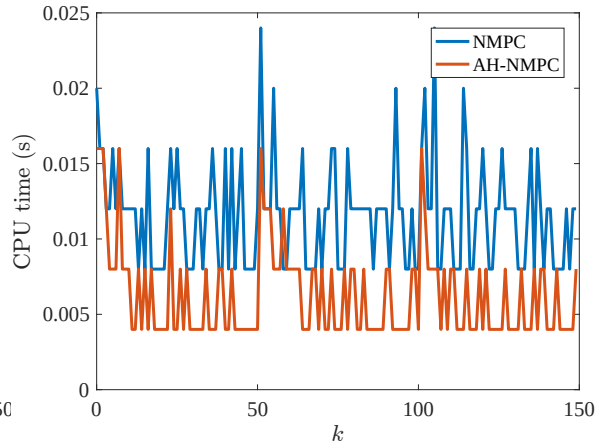

Figure 6.7: Nominal quad tank, Solution time (CPU s)

6.5.3 Results with Uncertainty

Next we repeat the same simulation, but with additive state noise for each state with mean of zero and variance of 1. The results show similar trends in this case, while retaining robustness with noise. Results are shown in Figures 6.8 - 6.11. As can be seen, Algorithm

48 successfully determines feasible horizon lengths even in the case of a noisy process.

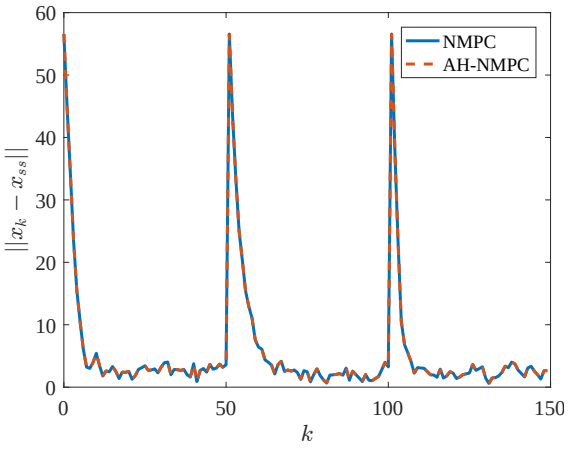

Figure 6.8: Quad tank w/ noise, Norm of states

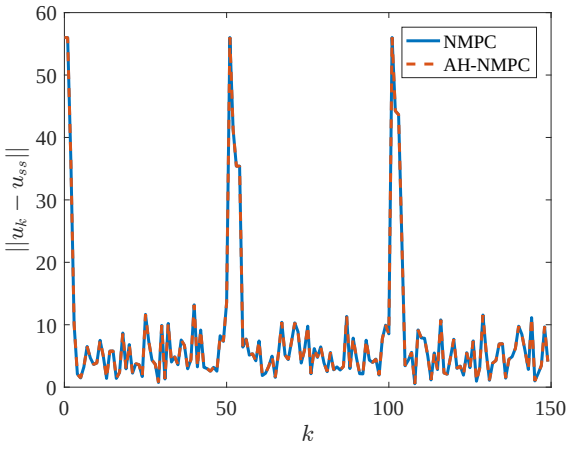

Figure 6.9: Quad tank w/ noise, Norm of controls

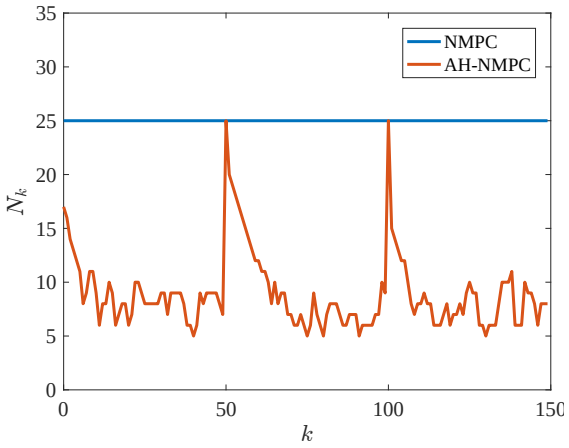

Figure 6.10: Quad tank w/ noise, Horizon Lengths

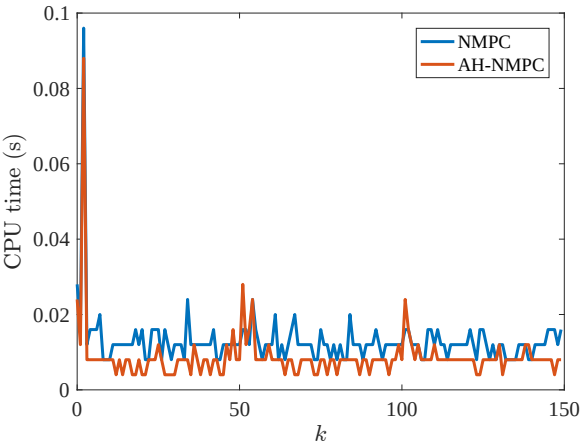

Figure 6.11: Quad tank w/ noise, Solution time (CPU s)

The summed tracking costs for each case are summarized in Table 6.3. These results again show that NMPC and AH-NMPC are nearly identical in terms of tracking performance. The average computational time in this case is $0.0129s$ for NMPC and $0.0087s$ for AH-NMPC, which shows a 33% decrease. Thus, the computational benefits of a shorter

Table 6.3: Quad tank summed tracking costs $\sum_{k=0}^{K-1} x_k^T Q x_k + u_k^T R u_k$

	Nominal	w/ noise
NMPC	$5.468 \cdot 10^4$	$5.9644 \cdot 10^4$
AH-NMPC	$5.468 \cdot 10^4$	$5.9645 \cdot 10^4$

horizon are obtained when possible, without loss of robustness (since all problems are feasible) or significant degradation of tracking performance.

6.6 Distillation Example

As a larger computational example, we again consider the distillation system from Section 4.3.3 with model shown in equations (4.19)-(4.26).

We discretize the DAE system using three point Radau collocation, and we use a finite element length of 1 min. The problem size, however, is variable. For standard NMPC we set $N = 25$, and each NLP has 120,000 variables and constraints. For AH-NMPC we set $N_{max} = 25, N_s = 5$, and each NLP varies from 120,000 to 24,000 variables and constraints. Note that N_s was chosen through simulation trial and error to ensure Assumption 6.14. This leads to large differences in solve time, as will be shown. The models are implemented in AMPL and solved with IPOPT on an Intel i7-4770 3.4 GHz CPU. Also, sIPOPT is used with the initial condition as the sensitivity parameter for updated NMPC calculations.

6.6.1 Terminal Region Calculations

We simulate multiple setpoint transitions, with setpoints calculated from the economic steady state problem for differing nominal feed compositions. The nonlinearity bound,

Table 6.4: Terminal Region Results

Setpt #	Feed Comp	$\sigma_{A_K}^{max}$	λ_W^{max}	λ_W^{min}	c_f	c_u
1	0.4,0.2,0.4	0.9096	24.6187	10	0.43	0.41
2	0.4,0.4,0.2	0.9137	27.9409	10	0.36	0.37
3	0.2,0.4,0.4	0.898	24.3761	10	0.51	0.38

terminal cost, and terminal region must then be calculated for each setpoint at minimum economic cost. This is the cost of feed and energy to the reboilers minus the cost of the products, $L^{ec} = p_F \cdot F_1 + pV(V_{\bar{B},1} + V_{\bar{B},2}) - p_A \cdot D_1 - p_B \cdot D_2 - p_C \cdot B_2$, where $p_F = \$1/mol$ is the price of feed, p_i for $i = A, B, C$ is the price of component i with $p_A = \$1/mol$, $p_B = \$2/mol$, and $p_C = \$1/mol$, $p_V = \$0.008/mol$ is the price per mole vaporized in the reboilers, and the indices represent the first or second column.

For the cost matrices of the LQR (and for NMPC) we use $Q = 10I_{246}$ and $R = I_8$, and the terminal region is calculated as in (6.2). The nonlinear bound is found to be the same in all three cases, with $q = 1.8$ and $M = 0.0743$ and the nonlinearity bound data being nearly identical to that shown in Figure 4.10 in Section 4.3.3. The differences are in the LQR control computed from the linearization at each setpoint, and the region which satisfies control constraints $|z_N| \leq c_u$, where c_u is chosen to be the largest value that ensures ensure $-Kz_N \in \mathbb{U}$. For this example, we only consider the lower bounds of zero for each control. A summary of the terminal region calculations for each setpoint for different feed compositions is shown in Table 6.4.

6.6.2 Nominal Results

First we consider a nominal simulation (i.e., no noise). Setpoints are changed at $k = 50$ and $k = 100$, and have the order corresponding to feed compositions shown in Table 6.4. In Figure 6.12, the distance to the setpoint $|x_k - x_{ss}|$ is plotted over time, for both the standard NMPC and adaptive horizon NMPC cases, with the terminal region plotted for reference. As seen, the tracking performances are nearly the same. This can also be seen in Figure 6.13, where the control deviation $|u_k - u_{ss}|$ is plotted over time for both cases.

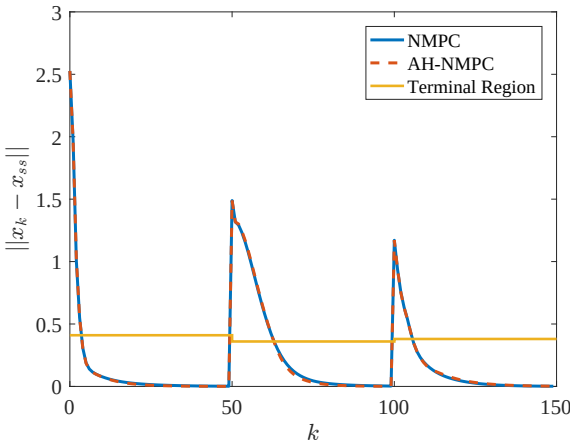

Figure 6.12: Nominal distillation, Norm of states

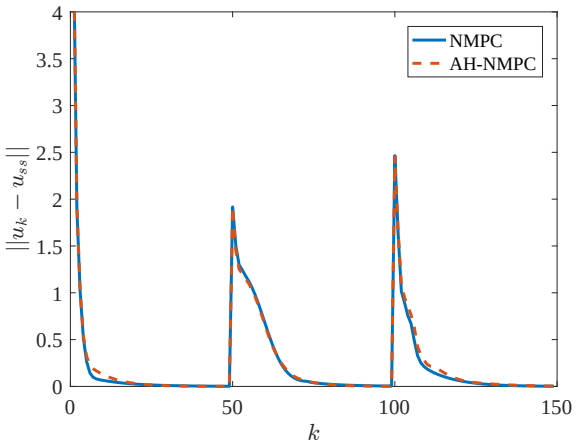

Figure 6.13: Nominal distillation, Norm of controls

The horizon lengths for each problem solved are shown in Figure 6.14. Standard NMPC has a constant horizon length of $N = 25$ for the entire simulation. However, adaptive horizon NMPC utilizes a horizon length that changes with time accord to predictions from sIPOPT. The initial horizon length N_0 is set to $N_{max} = 25$, and then the horizon is allowed to adapt over time. At times $k = 50$ and $k = 100$, the horizon lengths are also set to $N_k = 25$ since the sensitivity prediction is infeasible, as per Algorithm 48. As seen in the figure, the horizons shorten over time as the setpoint is approached, until the lower bound of $N_s = 5$ is reached. This leads to a large difference in solve times, which is shown in

Figure 6.15. The standard NMPC has an average solve time of $103.7s$, and this does not change much with the initial condition. However, AH-NMPC only has long solution times at the beginning of transitions, with a worst-case time of $129.6s$. However, the average solve time is $17.4s$. Solution times are much faster when the system is near the setpoint, because the horizon length and, therefore, the size of the NLP, is smaller.

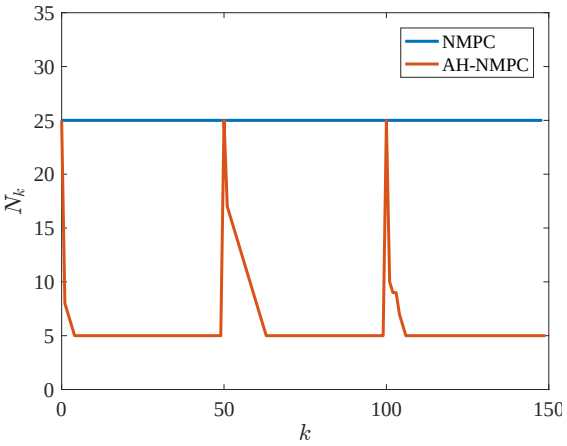

Figure 6.14: Nominal distillation, Horizon Lengths

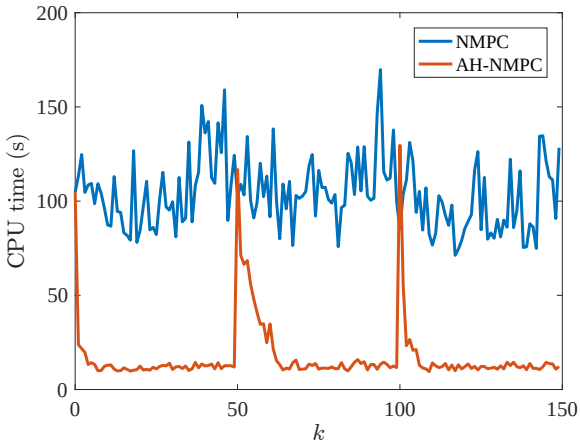

Figure 6.15: Nominal distillation, Solution time (CPU s)

6.6.3 Results with Uncertainty

Next, we repeat the same simulations, but with normally distributed uncertainty in the feed flow F with standard deviation 1.41 and composition z_F with standard deviation 0.03. The norms of the state and control actions over time are shown in Figures 6.16 and 6.17, respectively. The behaviors of AH-NMPC and NMPC are very similar here, although the difference is larger than in the nominal case. The horizon lengths are shown in Figure 6.18 and are nearly the same as in the nominal case, showing that $N_s = 5$ provides a reasonable degree of robustness, as every problem is feasible. The solve times are shown in Figure 6.19, and a significant improvement in solve time is seen here as well. The average solve time for NMPC is $97.3s$, while the average solve time for AH-NMPC is $16.5s$. The results

here show roughly the same behaviors as in the nominal case, but with additional noise in the trajectory, as is expected from ISpS.

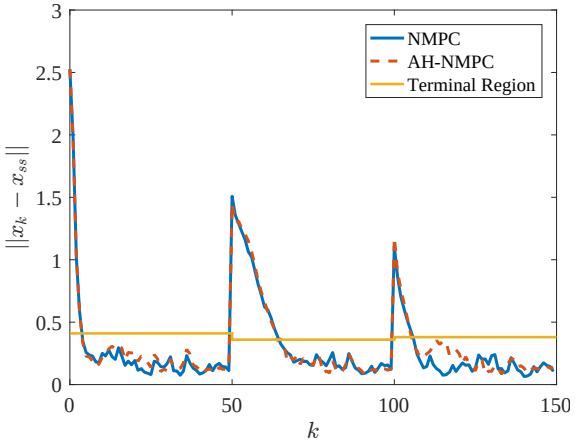

Figure 6.16: Distillation w/ noise, Norm of states

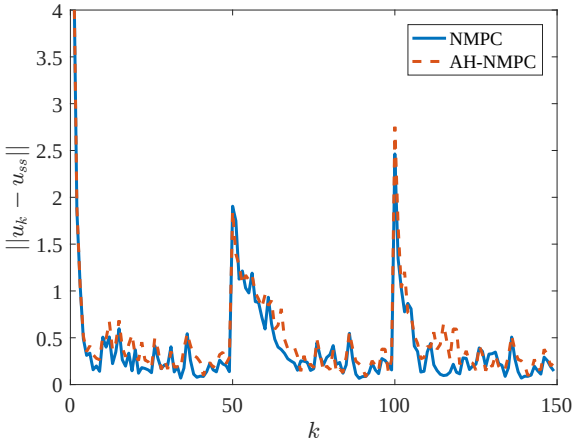

Figure 6.17: Distillation w/ noise, Norm of controls

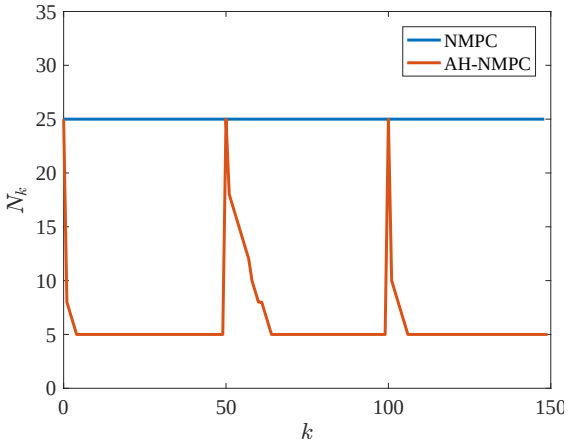

Figure 6.18: Distillation w/ noise, Horizon Lengths

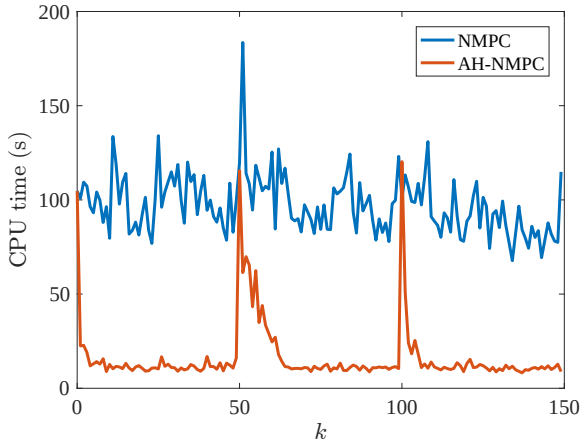

Figure 6.19: Distillation w/ noise, Solution time (CPU s)

The summed tracking costs for each case are summarized in Table 6.5. Again, these results show that NMPC and AH-NMPC are nearly identical in terms of tracking performance.

Table 6.5: Distillation summed tracking costs $\sum_{k=0}^{K-1} x_k^T Q x_k + u_k^T R u_k$

	Nominal	w/ noise
NMPC	148.86	170.70
AH-NMPC	149.06	183.51

6.7 Conclusions

This chapter has presented an online method for updating prediction horizon lengths adaptively, via a framework that retains stability properties of the NMPC under assumptions of the approximation of the infinite horizon NMPC problem. Furthermore, we show robust stability properties via reformulation of the NLP. Finally, we demonstrate significant performance improvements on two computational examples. Simulation results reveal that the proposed approach is able to achieve significant reduction in the average computation time without loss in performance compared to fixed horizon NMPC, while retaining robustness and feasibility of the optimization problems solved online. Possible future extensions to this work will be discussed in the conclusion of this thesis.

Chapter 7

Conclusions

7.1 Summary and Contributions

This thesis has examined all components of the NMPC problem and proposed practical improvements with theoretical justification that focus on extending the applicability of NMPC to larger and more complex systems. Further, control theory and optimization theory are integrated such that they may work together in order to further the technology of NMPC.

Chapter 1 gives the background and context of process control in the chemical industry. The state-of-the-art in model predictive control is discussed, and challenges to the technology are explained. Chapter 2 presents the basic formulations and results for NMPC. Further, the basics of Lyapunov stability theory and nonlinear programming properties that will be leveraged later are defined.

In Chapter 3, robustness issues caused by state-dependent constraints are addressed via robust reformulations of the NLP solved online. This may apply to path constraints, terminal constraints, or Lyapunov stabilizing constraints. Although constraint satisfaction is not guaranteed with a robust reformulation, this method is significantly easier to implement than other forms of robust NMPC in the literature. The robustness of the NMPC is proved by connecting the properties of the NLP solved online to the continuity of the Lyapunov function. This framework is shown to be easily applied even in the case of more specialized NMPC formulations shown later in the thesis. Further, a method for calculating

predictive bounds on robustness that can apply to large systems is shown. This method is based on finding bounds on comparison functions used to prove ISS via simulations, and this is demonstrated on two computational examples from the literature. The major contributions of this chapter are listed as follows:

- Proposed a framework for reformulating NMPC in order to ensure robustness
- Analyzed the NLP properties of terminal region / terminal cost tracking NMPC with a robust reformulation
- Proposed a method for calculating predictive robustness bounds for NMPC
- Applied robustness bound calculations to two examples

In Chapter 4, a scalable method of calculating terminal regions and costs for NMPC stabilization is shown. This method is based on the quasi-infinite horizon framework in which terminal conditions are designed to approximate the infinite horizon problem. The extension that allows for application to large systems concerns a method for bounding the nonlinear effects of the system via a method utilizing simulations under LQR control. This allows terminal regions and costs to be accurately calculated for larger systems than previously possible, and this eliminates the restrictiveness of endpoint constrains for these systems, while still ensuring the stability properties afford by conditions that are much more difficult to check. Further, a method is shown for updating terminal conditions online in the case of changing steady states. Terminal condition calculations are demonstrated on examples from the literature, and simulation results are also shown. The major contributions of this chapter are listed as follows:

- Proposed a method for bounding nonlinear system effects that allows calculation of terminal conditions for large-scale systems
- Proposed a procedure for updating terminal conditions online that retains stability properties

- Demonstrated terminal region calculations on three examples from literature, including a large-scale distillation system
- Showed through simulations that terminal condition calculations may allow for NMPC applications with shorter horizons

In Chapter 5, economic objective functions are addressed via a stabilizing constraint that ensures stability properties and is easily scalable. This formulation is contrasted with formulations involving objective regularization to ensure stability. The computational burden and conservativeness of the regularization-based approach is avoided, and a connection is drawn to multi-objective optimization in order to provide the intuition of the stabilizing constraint. A robust reformulation is applied to this problem, and softening the stabilizing constraint is justified. Constraint qualification of the NLP with a robust reformulation is proved, and both nominal and robust stability properties are analyzed. Furthermore, and extension is proposed to allow for eNMPC-sc with terminal regions and costs. The performance of this controller is demonstrated on two process examples from the literature. The major contributions of this chapter are listed as follows:

- Proposed an economic NMPC formulation with a stabilizing constraint (eNMPC-sc)
- Proved attractivity in eNMPC-sc in the nominal case
- Analyzed the NLP properties of a robust reformulation of eNMPC-sc
- Proved ISpS of eNMPC-sc with a robust reformulation
- Proposed an extension to allow for the inclusion of terminal regions and costs
- Demonstrated eNMPC-sc on a CSTR and a large-scale distillation system

In Chapter 6, a method for adapting horizon lengths online is detailed. By this approach, it is possible to have both the benefit of fast NMPC solutions with short horizons when possible and the robustness of long horizons when necessary. Terminal regions are found to

apply for the case of changing horizons, and we propose a method for updating horizon lengths online via sIPOPT. This is done by analyzing the behavior of the sensitivity based solutions in order to find a horizon length that is sufficient for reachability. We analyze the nominal behavior of this problem, as well as the properties of the robust reformulation under uncertainty. The theoretical results rely on proving fundamental relationships between the LQR, finite horizon, and infinite horizon problems. Computational results are shown for two examples from the literature. Furthermore, a direct extension to this project will be proposed in the following section. The major contributions of this chapter are listed as follows:

- Proposed a framework for allowing NMPC horizon lengths to adapt online called adaptive horizon NMPC (AH-NMPC)
- Proposed a modification to previously shown terminal condition construction that allows application to changing horizon lengths
- Proposed a method for finding sufficient horizon lengths online based on NLP sensitivity calculations
- Proved nominal stability of AH-NMPC
- Proved ISpS of AH-NMPC with a robust reformulation
- Demonstrated AH-NMPC on a quad tank system and a large-scale distillation system, both of which show robustness and significant reduction in computational time

The summation of this work represents a concerted effort to provide better strategies for implementing NMPC so that the benefits of nonlinear dynamic optimization may be obtained in more real-world applications.

7.2 Recommendations for Future Work

Here we discuss recommendations for future work in this area. The first is a direct extension to the results of this thesis, and the second is a more general direction for the field to take that represents a significant departure from previous work.

7.2.1 FASt-NMPC

The main immediate and obvious extension to the work in this thesis would be to fully integrate the adaptive horizon developments of Chapter 6 with advanced-step NMPC (asNMPC) [27] and advanced-multi-step NMPC (amsNMPC) [26]. In asNMPC, a sensitivity update is found at time k for the NLP solve begun at time $k-1$ so that a near-optimal control can be implemented without delay. In amsNMPC, this concept is generalized so that a given NLP may take several time steps to solve. In the serial case, multiple sensitivity solutions based on the same NLP will be implemented across multiple time steps. In the parallel case, multiple NLPs are solved in parallel on multiple processors. Integration with adaptive horizons could take the form of a controller that automatically switches between NMPC, asNMPC, and amsNMPC , as horizon lengths adapt and solve times change. We term this as flexible-advanced-step NMPC, or FASt-NMPC. Under this framework, the NMPC scheme will change based on the solve time of the current problem and user-defined bounds on control action delay and number of problems to be solved in background. A simple example of this would be to alternate between NMPC and asNMPC based on a threshold for solve time. If the NMPC solve time is less than the threshold, then implement the NMPC solution. If the NMPC solve time exceeds the threshold, then implement the advanced-step solution. In this fashion, the exact NLP solutions are used when they are fast enough, and advanced-step solutions are implemented when the NLP solve

is too slow. This could be further extended to include transitions to amsNMPC if the NLP solve time exceeds a full time step. This would allow for near-optimal solutions with a bounded control action delay for systems of arbitrary size. The stability analysis in this case becomes very complex, but, conceptually speaking, FASt-NMPC should inherit the stability properties of amsNMPC in the worst case.

7.2.2 Terminal Conditions for MPC with discrete variables

Another important direction for MPC research is that of problems with discrete variables, including scheduling problems [85, 102] or process control problems with discrete actuators [103, 104]. This represents a major generalization of MPC theory, and could lead to applications to many more types of problems, including those at significantly longer time scales. However, there are significant difficulties in this pursuit. Particularly, the concept of terminal conditions is much less clear in this context. In principle, the analysis in this case would roughly follow that shown in Chapter 5, however, LQR does not apply to the case with discrete variables unless heavy assumptions are made. Furthermore, the concept of a steady-state may not even apply to the case of a scheduling problem. Therefore, defining more general terminal constraints for these types of problems will require investigating deep connections between control theory and scheduling or supply chain optimization theory. It is likely that any developments in this area will be very case-dependent, with particular results for systems that admit a periodic steady-state, or systems that admit certain heuristic policies that are positive invariant for some region of the state space. Even if results in this vein are found to hold in the nominal case, the robustness of such a controller is not clear. In particular, the continuity properties that are typically leveraged to show robust stability properties do not hold in the case with discrete variables. The typical procedure for showing robust stability employed in this thesis only holds for problems

with discrete variables if it can be assumed that the discrete variables are held constant inside of the robustly positive invariant region defined by the stability property, which is a large assumption that somewhat requires putting the cart before the horse. If this assumption does not hold, then entirely new avenues for showing robust stability will be required.

Bibliography

[1] X. Yang, *Advanced-multi-step and Economically Oriented Nonlinear Model Predictive Control*. PhD thesis, Carnegie Mellon University, 2015.

[2] R. Leer, "Self-optimizing control structures for active constraint regions of a sequence of distillation columns," Master's thesis, Norweign University of Science and Technology, 2012.

[3] T. Raff, S. Huber, Z. Nagy, and F. Allgöwer, "Nonlinear model predictive control of a four tank system: An experimental stability study," *Proceedings of the 2006 IEEE International Conference on Control Applications*, pp. 237–242, 2006.

[4] N. H. Lappas and C. E. Gounaris, "Multi-stage adjustable robust optimization for process scheduling under uncertainty," *AICHE Journal*, vol. 62, no. 5, pp. 1646–1667, 2016.

[5] T. Marlin and A. Hrymak, "Real-time operations optimization of continuous processes," *AICHE Symposium Series CPC-V*, vol. 93, pp. 156–164, 1997.

[6] T. Binder, L. Blank, H. G. Bock, R. Bulirsch, W. Dahmen, M. Diehl, T. Kronseder, W. Marquardt, J. P. Schlöder, and O. von Stryk, "Introduction to model based optimization of chemical processes on moving horizons," in *Online Optimization of Large Scale Systems* (M. Grötschel, S. O. Krumke, and J. Rambau, eds.), pp. 295–339, Springer Berlin Heidelberg, 2001.

[7] C. Cutler and B. Ramaker, "Dynamic matrix control - a computer control algorithm," in *86th AICHE Nation Meeting*, 1979.

[8] S. J. Julier and J. K. Uhlmann, "New extension of the kalman filter to nonlinear systems," *Proceedings of SPIE - The International Society for Optical Engineering*, vol. 3068, pp. 182–193, 1997.

[9] E. Wan and R. Van Der Merwe, "The unscented kalman filter for nonlinear estimation," *Adaptive Systems for Signal Processing, Communications, and Control Symposium*, pp. 153–158, 2000.

[10] V. M. Zavala, C. D. Laird, and L. T. Biegler, "A fast moving horizon estimation algorithm based on nonlinear programming sensitivity," *Journal of Process Control*, vol. 18, no. 9, pp. 876 – 884, 2008.

[11] B. Nicholson, R. Lopez-Negrete, and L. T. Biegler, "On-line state estimation of nonlinear dynamic systems with gross errors," *Computers and Chemical Engineering*, vol. 70, pp. 149–159, 2014.

[12] K. V. Pontes, I. J. Wolf, M. Embiruu, and W. Marquardt, "Dynamic real-time optimization of industrial polymerization processes with fast dynamics," *Industrial & Engineering Chemistry Research*, vol. 54, no. 47, pp. 11881–11893, 2015.

[13] J. Rawlings, D. Angeli, and C. Bates, "Fundamentals of economic model predictive control," in *Decision and Control (CDC), 2012 IEEE 51st Annual Conference on*, pp. 3851–3861, Dec 2012.

[14] I. Grossmann, M. Erdirik-Dogan, and R. Karuppiah, "Overview of planning and scheduling for enterprise-wide optimization of process industries," *Automatisierungstechnik*, vol. 56, no. 2, pp. 64–79, 2008.

[15] J. Busch, J. Oldenburg, M. Santos, A. Cruse, and W. Marquardt, "Dynamic predictive scheduling of operational strategies for continuous processes using mixed-logic dynamic optimization," *Computers and Chemical Engineering*, vol. 31, no. 5, pp. 574–587, 2007.

[16] S. Terrazas-Moreno, A. Flores-Tlacuahuac, and I. Grossmann, "Simultaneous cyclic scheduling and optimal control of polymerization reactors," *AICHE Journal*, vol. 53, no. 9, pp. 2301–2315, 2007.

[17] R. H. Nystrm, I. Harjunkoski, and A. Kroll, "Production optimization for continuously operated processes with optimal operation and scheduling of multiple units," *Computers and Chemical Engineering*, vol. 30, no. 3, pp. 392–406, 2006.

[18] R. Kalman, "Contributions to the theory of optimal control," *Automatica*, vol. 5, pp. 102–119, 1960.

[19] S. Qin and T. Bagdwell, "A survey of industrial model predictive control technology," *Control Engineering Practice*, vol. 1, pp. 733–764, 2003.

[20] J. Rawlings and D. Mayne, *Model Predictive Control: Theory and Design*. Madison, WI: Nob Hill Publishing, 2009.

[21] R. D. Bartusiak, "NLMPC: A platform for optimal control of feed- or product-flexible manufacturing," in *Assessment and Future Directions of Nonlinear Model Predictive Control* (R. Findeisen, F. Allgöwer, and L. T. Biegler, eds.), pp. 367–381, Springer Berlin Heidelberg, 2007.

[22] J. Richalet, "Industrial applications of model based predictive control," *Automatica*, vol. 29, no. 5, pp. 1251 – 1274, 1993.

[23] L. Grüne and J. Pannek, *Nonlinear Model Predictive Control: Theory and Algorithms*. London: Springer, 2011.

[24] S. J. Qin and T. A. Badgwell, "An overview of nonlinear model predictive control applications," in *Nonlinear Model Predictive Control* (F. Allgöwer and A. Zheng, eds.), pp. 369–392, Birkhäuser Basel, 2000.

[25] G. Pannocchia, J. Rawlings, and S. Wright, "Conditions under which suboptimal nonlinear MPC is inherently robust," *Systems & Control Letters*, vol. 60, pp. 747–755, 2011.

[26] X. Yang and L. Biegler, "Advanced-multi-step nonlinear model predictive control," *Journal of Process Control*, vol. 23, no. 8, pp. 1116 – 1128, 2013.

[27] V. M. Zavala and L. Biegler, "The advanced-step NMPC controller: Optimality, stability, and robustness," *Automatica*, vol. 45, pp. 86–93, 2009.

[28] U. Ascher and L. Petzold, *Computer methods for ordinary differential equations and differential-algebraic equations*. SIAM, 1998.

[29] L. Biegler, *Nonlinear Programming: Concepts, Algorithms, and Applications to Chemical Processes*. SIAM, 2010.

[30] L. T. Biegler, A. M. Cervantes, and A. Wchter, "Advances in simultaneous strategies for dynamic process optimization," *Chemical Engineering Science*, vol. 57, no. 4, pp. 575–593, 2002.

[31] A. M. Lyapunov, "The general problem of the stability of motion," *International Journal of Control*, vol. 55, no. 3, pp. 531–534, 1992.

[32] S. Sastry, *Nonlinear Systems Analysis, Stability, and Control*. Springer New York, 1999.

[33] H. K. Khalil, *Nonlinear systems*. Prentice Hall, 3rd ed. ed., 2002.

[34] E. Sontag, "Smooth stabilization implies coprime factorization," *IEEE Transactions on Automatic Control*, vol. 34, pp. 435–443, Apr 1989.

[35] Z. Jiang and Y. Wang, "Input-to-state stability for discrete-time nonlinear systems," *Automatica*, vol. 37, no. 6, pp. 857–869, 2001.

[36] D. Limon, T. Alamo, D. Raimondo, D. Peña, J. Bravo, A. Ferramosca, and E. Camacho, "Input-to-state stability: A unifying framework for robust model predictive control," in *Nonlinear Model Predictive Control: Towards New Challenging Applications* (L. Magni, D. Raimondo, and F. Allgöwer, eds.), Berlin: Springer, 2009.

[37] J. Nocedal and S. Wright, *Numerical Optimization*. New York, NY: Springer, 2 ed., 2009.

[38] A. Fiacco, *Introduction to Sensitivity and Stability Analysis in Nonlinear Programming*. Academic Press, New York, 1983.

[39] J. Gauvin, "A necessary and sufficient regularity condition to have bounded multipliers in nonconvex programming," *Mathematical Programming*, vol. 12, pp. 136–138, 1977.

[40] R. Janin, "Directional derivative of the marginal function in nonlinear programming," in *Sensitivity, Stability and Parametric Analysis* (A. Fiacco, ed.), vol. 21 of *Mathematical Programming Studies*, pp. 110–126, Springer Berlin Heidelberg, 1984.

[41] D. Ralph and S. Dempe, "Directional derivatives of the solution of a parameteric nonlinear program," *Mathematical Programming*, vol. 70, pp. 159–172, 1995.

[42] S. Keerthi and E. Gilbert, "Optimal infinite-horizon feedback laws for a general class of constrained discrete-time systems: Stability and moving-horizon approximations," *Journal of Optimization Theory and Applications*, vol. 57, no. 2, pp. 265–293, 1988.

[43] L. Grüne, "Economic receding horizon control without terminal constraints," *Automatica*, vol. 49, pp. 725–734, 2013.

[44] H. Chen and F. Allgöwer, "A quasi-infinite horizon nonlinear model predictive control scheme with guaranteed stability," *Automatica*, vol. 34, no. 10, pp. 1205–1217, 1998.

[45] M. G. R. R. Bitmead and V. Wertz, "Adaptive optimal control: The thinking man's gpc," *Automatica*, vol. 29, no. 3, pp. 798–800, 1993.

[46] H. Michalska and D. Q. Mayne, "Robust receding horizon control of constrained nonlinear systems," *IEEE Transactions on Automatic Control*, vol. 38, no. 11, pp. 1623–1633, 1993.

[47] P. O. M. Scokaert, D. Q. Mayne, and J. B. Rawlings, "Suboptimal model predictive control (feasibility implies stability)," *IEEE Transactions on Automatic Control*, vol. 44, no. 3, pp. 648–654, 1999.

[48] M. Diehl, R. Amrit, and J. Rawlings, "A Lyapunov function for economic optimizing model predictive control," *IEEE Transactions on Automatic Control*, vol. 56, no. 3, pp. 703–707, 2011.

[49] V. Zavala and A. Flores-Tlacuahuac, "Stability of multiobjective predictive control: A utopia-tracking approach," *Automatica*, vol. 48, no. 10, pp. 2627–2632, 2012.

[50] C. Rao, J. Rawlings, and J. Lee, "Constrained linear state estimation - a moving horizon approach," *Automatica*, vol. 37, no. 10, pp. 1619–1628, 2001.

[51] G. Grimm, M. Messina, S. Tuna, and A. Teel, "Examples when nonlinear model predictive control is nonrobust," *Automatica*, vol. 40, pp. 1729–1738, 2004.

[52] D. Mayne, M. Seron, and S. Rakovic, "Robust model predictive control of constrained linear systems with bounded and state-independent uncertainties," *Automatica*, vol. 41, no. 2, pp. 219–224, 2005.

[53] D. Mayne, E. Kerrigan, E. van Wyk, and P. Falugi, "Tube-based robust nonlinear model predictive control," *International Journal of Robust and Nonlinear Control*, vol. 21, pp. 1341–1353, 2011.

[54] D. Mayne, "Control of constrained dynamic systems," *European Journal of Control*, vol. 7, pp. 87–99, 2001.

[55] D. Limon, T. Alamo, F. Salas, and E. Camacho, "Input to state stability of min-max mpc controllers for nonlinear systems with bounded uncertainties," *Automatica*, vol. 42, pp. 797–803, 2006.

[56] E. Visser, B. Srinivasan, S. Palanki, and D. Bonvin, "A feedback-based implementation scheme for batch process optimization," *Journal of Process Control*, vol. 10, pp. 399–410, 2000.

[57] J. Shi, L. Biegler, I. Hamdan, and J. Wassick, "Optimization of grade transitions in polyethylene solution polymerization process under uncertainty," *Computers and Chemical Engineering*, vol. 95, pp. 260–279, 2016.

[58] G. Grimm, M. Messina, S. Tuna, and A. Teel, "Nominally robust model predictive

control with state constraints," *IEEE Transactions on Automatic Control*, vol. 52, no. 10, pp. 1856–1870, 2007.

[59] S. Lucia, T. Finkler, and S. Engell, "Multi-stage nonlinear model predictive control applied to a semi-batch polymerization reactor under uncertainty," *Journal of Process Control*, vol. 23, pp. 1306–1319, 2013.

[60] N. Patel and J. Rawlings, "Model predictive control for optimal zone tracking," in *AICHE National Meeting*, 2016.

[61] A. Shapiro, "Sensitivity analysis of nonlinear programs and differentiability properties of metric projections," *SIAM Journal on Control and Optimization*, vol. 26, pp. 628–645, 1988.

[62] R. Huang, L. Biegler, and E. Harinath, "Robust stability of economically oriented infinite horizon NMPC that include cyclic processes," *Journal of Process Control*, vol. 22, pp. 51–59, 2011.

[63] R. Huang, E. Harinath, and L. Biegler, "Lyapunov stability of economically oriented NMPC for cyclic processes," *Journal of Process Control*, vol. 21, pp. 501–509, 2011.

[64] A. Wächter and L. Biegler, "On the implementation of an interior-point filter line-search algorithm for large-scale nonlinear programming," *Math. Program.*, vol. 106, no. A, pp. 25–57, 2006.

[65] W.-H. Chen, J. O'Reilly, and D. J. Ballance, "On the terminal region of model predictive control for non-linear systems with input/state constraints," *International Journal of Adaptive Control and Signal Processing*, vol. 17, no. 3, pp. 195–207, 2003.

[66] C. Rajhans, S. Patwardhan, and H. Pillai, "Two alternate approaches for characteri-

zation of the terminal region for continuous time quasi-infinite horizon nmpc," *12th IEEE Conference on Control & Automation*, pp. 98–103, 2016.

[67] D. Limon, *Control predictivo de sistemas no lineales con restricciones: estabilidad y robustez*. PhD thesis, Universidad de Sevilla, 2002.

[68] C. Rajhans, S. Patwardhan, and H. Pillai, "Discrete time formulation of quasi infinite horizon nonlinear model predictive control scheme with guaranteed stability," *IFAC World Congress*, p. WeA04.8, 2017.

[69] G. Hicks and W. Ray, "Approximation methods for optimal control synthesis.," *The Canadian Journal of Chemical Engineering*, vol. 49, no. 4, pp. 522–528, 2013.

[70] R. Huang, S. C. Patwardhan, and L. T. Biegler, "Robust stability of nonlinear model predictive control based on extended kalman filter," *Journal of Process Control*, vol. 22, no. 1, pp. 82 – 89, 2012.

[71] S. Skogestad, "Dynamcis and control of distillation columns: A tutorial introduction," *Trans IChemE*, vol. 75, no. A, pp. 539–562, 1997.

[72] R. Huang, L. Biegler, and S. Patwardhan, "Fast offset-free nonlinear model predictive control based on moving horizon estimation," *Industrial & Engineering Chemistry Research*, vol. 49, no. 17, pp. 7882–7890, 2010.

[73] G. Pannocchia and E. Kerrigan, "Offsetfree receding horizon control of constrained linear systems," *AIChE Journal*, vol. 51, no. 12, pp. 3134–3146, 2005.

[74] R. Huang, S. C. Patwardhan, and L. T. Biegler, "Adaptive quasi-infinite horizon nmpc of a continuous fermenter," *IFAC Proceedings Volumes*, vol. 43, no. 5, pp. 619 – 624, 2010.

[75] M. Müller, D. Angeli, and F. Allgöwer, "On necessity and robustness of dissipativity in economic model predictive control," *IEEE Transactions on Automatic Control*, vol. 60, no. 6, pp. 1671–1676, 2015.

[76] T. Faulwasser and D. Bonvin, "On the design of economic nmpc based on approximate turnpikes," in *54th IEEE Conference on Decision and Control*, pp. 4964–4970, 2015.

[77] T. Faulwasser, M. Korda, C. Jones, and D. Bonvin, "On turnpike and dissipativity properties of continuous-time optimal control problems," *Automatica*, vol. 81, pp. 297–304, 2017.

[78] L. Grüne and M. Stieler, "A lyapunov function for economic mpc without terminal conditions," in *53rd IEEE Conference on Decision and Control*, pp. 2740–2745, 2014.

[79] L. Grüne and M. Müller, "On the relation between strict dissipativity and turnpike properties," *Systems & Control Letters*, vol. 90, pp. 45–53, 2016.

[80] V. Zavala and L. Biegler, "Optimization-based strategies for the operation of low-density polyethylene tubular reactors: nonlinear model predictive control," *Computers & Chemical Engineering*, vol. 33, no. 10, pp. 1735–1746, 2009.

[81] R. Huang, V. Zavala, and L. Biegler, "Advanced step nonlinear model predictive control for air separation units," *Journal of Process Control*, vol. 19, no. 4, pp. 678–685, 2009.

[82] H. Tian, Q. Lu, R. Gopaluni, V. Zavala, and J. Olson, "Economic nonlinear model predictive control for mechanical pulping processes," in *American Control Conference (ACC), 2016*, pp. 1796–1801, American Automatic Control Council (AACC), 2016.

[83] E. Harinath, L. Biegler, and G. Dumont, "Control and optimization strategies for

thermo-mechanical pulping processes: Nonlinear model predictive control," *Journal of Process Control*, vol. 21, pp. 519–528, 2011.

[84] J. Jäschke, X. Yang, and L. Biegler, "Fast economic model predictive control based on NLP-sensitivities," *Journal of Process Control*, vol. 24, pp. 1260–1272, 2014.

[85] K. Subramanian, J. Rawlings, and C. Maravelias, "Economic model predictive control for inventory management in supply chains," *Computers & Chemical Engineering*, vol. 64, pp. 71–80, 2014.

[86] R. Huang, L. Biegler, and E. Harinath, "Robust stability of economically oriented infinite horizon nmpc that include cyclic processes," *Journal of Process Control*, vol. 22, pp. 51–59, 2012.

[87] L. Biegler, X. Yang, and G. Fischer, "Advances in sensitivity-based nonlinear model predictive control and dynamic real-time optimization," *Journal of Process Control*, vol. 30, pp. 104–116, 2015.

[88] V. M. Zavala, "A multiobjective optimization perspective on the stability of economic MPC," *9th International Symposium on Advanced Control of Chemical Processes*, pp. 975–981, 2015.

[89] M. Heidarinejad, J. Liu, and P. Christofides, "Economic model predictive control of nonlinear process systems using Lyapunov techniques," *AICHE Journal*, vol. 58, no. 3, pp. 855–870, 2012.

[90] T. Badgwell, "A robust model predictive control algorithm for stable nonlinear plants," in *Preprints of the 1997 International Symposium on Advanced Control of Chemical Processes*, 1997.

[91] J. Maree and L. Imsland, "Combined economic and regulatory predictive control," *Automatica*, vol. 37, no. 6, pp. 857–869, 2001.

[92] X. Yang, D. Griffith, and L. Biegler, "Nonlinear programming properties for stable and robust NMPC," *IFAC-PapersOnLine*, vol. 48, pp. 388–397, 2015.

[93] Z. Jiang and Y. Wang, "A converse Lyapunov theorem for discrete-time systems with disturbances," *Systems & Control Letters*, vol. 45, pp. 49–58, 2002.

[94] R. Fourer, D. Gay, and B. Kernighan, *AMPL, A Modeling Language for Mathematical Programming*. USA: Duxbury, 2 ed., 2003.

[95] R. Amirit, J. Rawlings, and D. Angeli, "Economic optimization using model predictive control with a terminal cost," *Annual Reviews in Control*, vol. 35, pp. 178–186, 2011.

[96] P. Scokaert and D. Mayne, "Min-max feedback model predictive control for constrained linear systems," *IEEE Transactions on Automatic Control*, vol. 43, no. 8, pp. 1136–1142, 1998.

[97] R. Shekhar, *Variable horizon model predictive control: robustness and optimality*. PhD thesis, University of Cambridge, 2012.

[98] B. E. Ydstie, "Auto tuning of the time horizon," *IFAC Proceedings Volumes*, vol. 20, no. 2, pp. 391 – 395, 1987.

[99] J. Eaton and J. Rawlings, "Feedback control of chemical processes using on-line optimization techniques," *Computers & Chemical Engineering*, vol. 60, no. 6, pp. 1671–1676, 2015.

[100] M. Kögel and R. Findeisen, "Stability of nmpc with cyclic horizons," *IFAC Proceedings Volumes*, vol. 46, no. 23, pp. 809 – 814, 2013. 9th IFAC Symposium on Nonlinear Control Systems.

[101] H. Pirnay, R. López-Negrete, and L. Biegler, "Optimal sensitivity based on Ipopt," *Math. Prog. Comp.*, vol. 4, pp. 307–331, 2012.

[102] Y. Nie, L. Biegler, C. Villa, and J. Wassick, "Discrete time formulation for the integration of scheduling and dynamic optimization," *Industrial & Engineering Chemistry Research*, vol. 54, no. 16, pp. 4303–4315, 2015.

[103] J. B. Rawlings, N. R. Patel, M. J. Risbeck, C. T. Maravelias, M. J. Wenzel, and R. D. Turney, "Economic mpc and real-time decision making with application to large-scale hvac energy systems," *Computers & Chemical Engineering*, 2017.

[104] J. B. Rawlings and M. J. Risbeck, "Model predictive control with discrete actuators: Theory and application," *Automatica*, vol. 78, pp. 258 – 265, 2017.